Science of Climate Change

Volume 3.1
2023

https://scienceofclimatechange.org

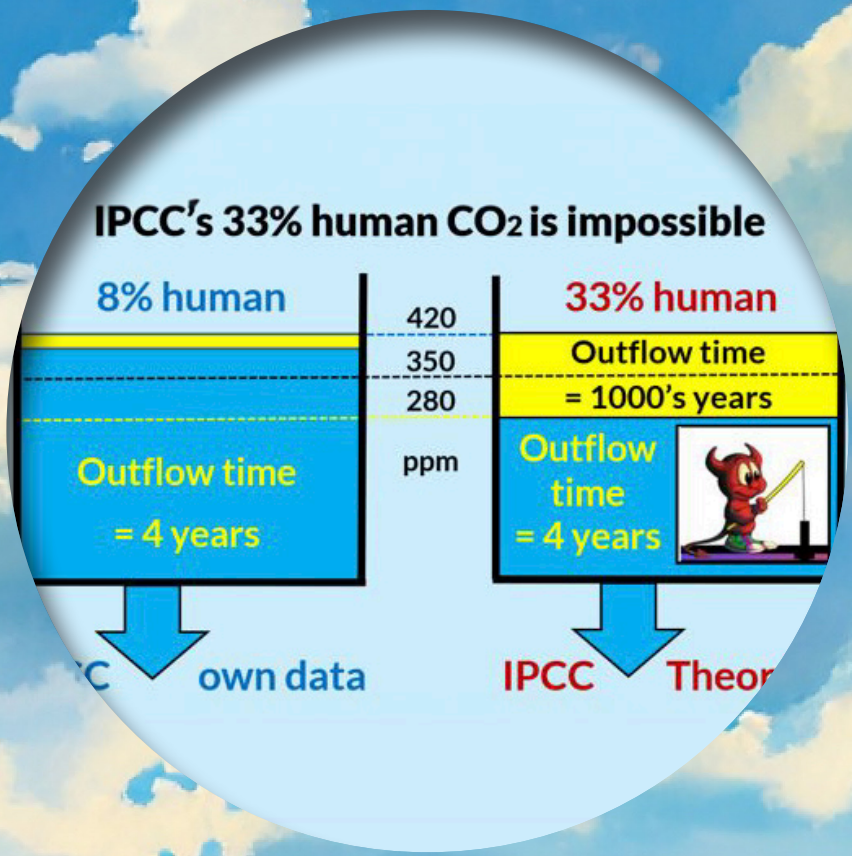

Published by: Klimarealistene (Org. no. 995 314 592)

ISSN 2703-9080 (print) ISNN 2703-9072 (online)

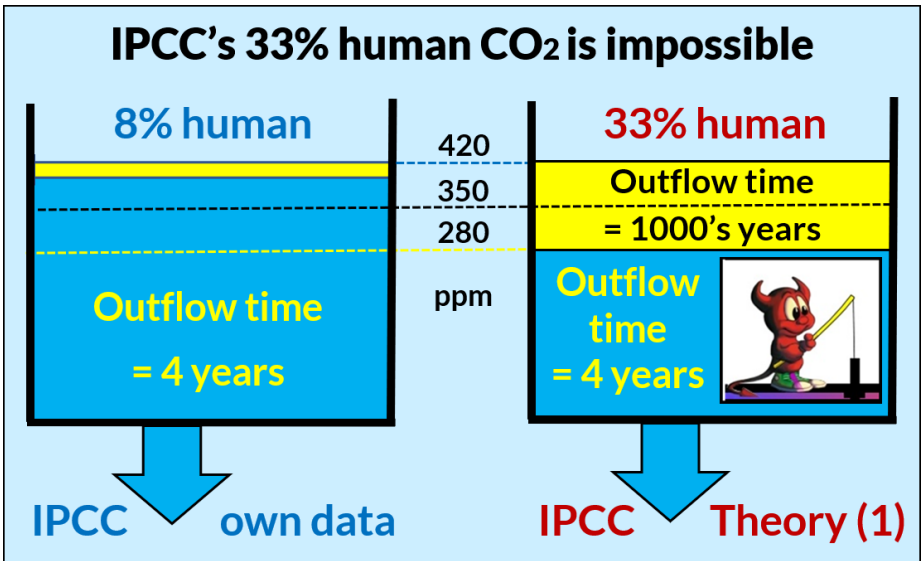

IPCC's true human carbon cycle that says human carbon is 8% of the carbon increase.
IPCC's Theory (1) that says human carbon is 33% of the carbon increase.

From an article by Edwin X Berry: *Nature Controls the CO2 increase.*

Figure 11, page 83

SCIENCE OF CLIMATE CHANGE

Volume 3.1

March 2023

ISSN 2703-9072

Klimarealistene, P.O. Box 33, 3901 Porsgrunn, Norway

Table of Content

Editorial

With this issue of we start our 3rd year for this journal. Our goal is to produce quarterly issues. The challenge is to get scientific acceptable articles which generate enough interest to maintain a flow of good science.

In this issue Martin Hovland finishes his triology on the termination of the last ice age and the dramatic climate change in southwestern Norway which made the way for human settlers. John Parmentola follow up by calculating the time of termination of the Holocene warm period by Celestial mechanics. His model gives 500 years left of the recent warm period before the return to the ne next ice age.

An article by David Andrew defending the majority view that all atmospheric CO_2 increase since the start of the industrial revolution is a consequence of human use of fossil energy sources, created responses from Hermann Harde and Edwin X Berry who defended their research showing that the increase is created by Nature itself due to the warm equatorial oceans. According to Berry this is the first time an open discussion of this question takes place in a scientific journal. The debate terminates for now with two shorter contributions by Ferdinand Engelbeen and Herman Harde.

Finallay Jonas Rosén and Sten Kaijser develop an analytical response function for the carbon cycle between atmosphere and sea. They claim that this is a better representation of the physics in the presently used "sum of exponentials" used in the Bern Carbon Cycle model.

We are pleased to realize one of our goals which is to provide a scientific debate. This is what brings science forward. We welcome contributors to a lively debate in future issues.

Good reading

Jan-Erik Solheim
Editor

The Editorial Board consists of Stein Storlie Bergsmark, Ole Henrik Ellestad, Rögnvaldur Hannesson, Martin Hovland, Ole Humlum, Gunnar Juliusson, Olav Martin Kvalheim and Jan-Erik Solheim.

A digital version of this volume can be found here: https://doi.org/10.53234/SCC202308/17

The Holocene climate change story: Witnessed from Sola, Norway. Part III.

Martin Torvald Hovland

Independent Researcher

Sola, Norway

Correspondence to mthovland@gmail.com

Vol. 3.1 (2023)

pp. 1-8

Abstract

Towards the end of the Weichsel ice age came a period with warmer climate referred to as the Late Glacial Interstadial (c.14,670 to 12,900 years BP), when the great inland ice started to retreat. This retreat was interrupted by a new period of cold climate - The Younger Dryas (YD) (c. 12,900 to 11,700 years BP). This period represented the last part of the Pleistocene epoch and preceded the current Holocene epoch. YD was characterized by a very cold climate, and the glaciers expanded and advanced towards what is termed the Ra-line; a terminal moraine ridge that developed along the coasts of Norway, but not as far south as Sola. The first humans probably arrived at Sola just after YD. The first neolithic tools found in Rogaland/Sola are dated between 11,000 and 9,800 years BP.

Keywords

Younger Dryas (YD), Rapid cooling, Younger Dryas Boundary (YDB), glacial advance, Esmark Moraine, Vassryggen, Holocene, sea level, Doggerland, human arrival Sola

Submitted 01-12-2022, Accepted 16-12-2022. https://doi.org/10.53234/scc202301/10

1. Introduction

The municipality of Sola (58° 55’ N, 5° 40’ E; see Part 1, Fig. 1) located in Rogaland County, coastal Norway has a long and rich history of archaeological finds that date back to when Norway was first populated, soon after the Weichselian glaciation, which was followed by a warmer climate that continued until about 12,900 years BP, when a new climatic cooling took place - the Younger Dryas (YD) period.

In this 3rd installment, I begin with an updated description of the mysterious YD cold spell, and the subsequent transition to continued warming and down-melting and retreat of the ice sheet in Norway. This is a dramatic and defining period when hunter/gatherers came to Sola and the nearby ice border and glaciers inland. They probably crossed over on winter ice, from the exposed land to the south-west, only about 180 km away, as central parts of the North Sea were exposed due to the retreat of Weichselian glaciers, and the sea level was about 40 m lower than at present (Fig. 1).

2. 14,670 to 12,900 years BP: - From warmth to bitter cold

At 14,670 years BP the global warming that started about 19,000 years ago, continued, with relatively rapid melting of the enormous ice sheets covering Scandinavia and parts of North America. The municipality of Sola was from now on, free of ice, and the cold Weichselian ice age was apparently finished. At Sola there was a tundra landscape and vegetation consisting of herbs, grass, and heather (Andersen and Borns, 1994) To our knowledge, there were no human beings roaming around, even if the conditions would probably have been perfect for hunter/gatherers.

Because of the high melt-rate of the ice sheets, the sea-level crept upwards, until 12,900 years ago

when the sea-level was about 40 m lower than at present. From 14,670 BP the warming rate was estimated to be as much as 1 °C per century (Andersen and Borns, 1994). This was called the Bölling – Alleröd period, named after a type-location in Sjælland, Denmark, where climatic conditions have been interpreted by pollen analyses. According to Andersen and Borns (1994), this warming was the start of the so-called Windmere Interstadial, which also includes the Bölling and Alleröd periods: "*The beetle-fauna record from Britain indicates that both Bölling and Alleröd were the warmest, pre-YD period*." (Andersen and Borns, 1994).

The reconstructed geography/ecology during this special period from Alleröd to YD is shown in Fig. 1 (by Andersen and Borns, 1994).

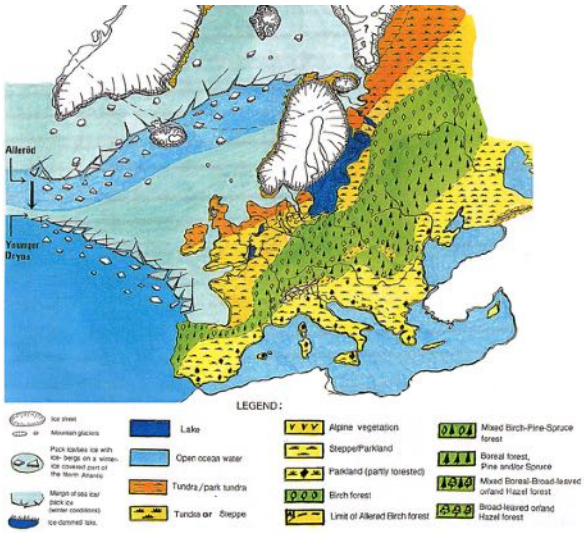

Figure 1: Illustration from Andersen and Borns (1994). Their figure caption reads:

"Europe and parts of the Arctic, 14,000 – 11,600 years ago, including the YD period. A considerable lowering of the temperature in early Younger Dryas time resulted in an expansion of the tundra, a small expansion of the ice sheet, and a considerable expansion of the pack-ice on the Atlantic Ocean. The map shows the approximate limits of the winter ice cover during the Alleröd (13,900 – 12,900 years ago) and the YD (12,900 – 11,700) periods. The Fennoscandian Ice Sheet was only slightly smaller, and the northern European forest-zone boundaries lay slightly further to the north during the Alleröd than during the YD period. The Baltic Ice Lake was ice covered during much of the year. Information about the glacial conditions in northernmost Russia is conflicting." (Andersen and Borns, 1994). (The present author has adjusted some of the timeframes provided, as the 1994-ages were not as precise as the present ones). Please note the two fresh-water lakes in the middle of the North Sea ('Doggerland'), and the 180 km wide 'Norwegian Trench' sea-strait, hugging the coastline of southern Norway. This is probably where the pioneering humans crossed to hunt and settle just after the YD-cold spell.

2.1 ***Full glaciation in only few years: - What really happened during the Younger Dryas?***

It is reckoned that the transition from global warming to deep-freeze (glaciation) took less than 50 years, to kick in, and start (Alley, 2000). Again, Scandinavia and North America were thrown into full glacial mode, with several degree temperature drop in the northern hemisphere. Also, the monsoon winds over Asia altered. The Scandinavian ice sheet grew in all directions and deposited a terminal moraine called the Younge Dryas moraine. This period lasted for ~1,200 years (the equivalent of 40 human generations), from 12,900 to 11,700 years BP. Thereafter the climate went back to 'normal' (e.g., continued warming) during a period of only a couple of hundred years (Mangerud, 2021).

The results from GISP2 have been used by several workers to construct a proxy temperature curve for the transition period between Weichselian and Holocene periods, as shown in Fig. 2.

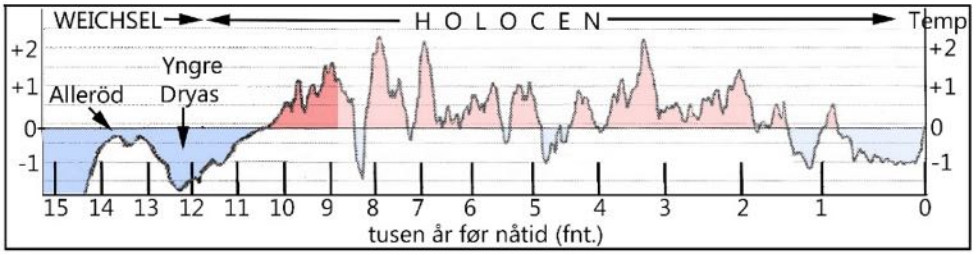

Figure 2: An approximated Weichsel glaciation to the Holocene interglacial temperature curve. It especially illustrates the Alleröd stadial (to the left) and YD periods in relation to each-other, and the following Holocene period. (Based on Gisp2, e.g., www.joannenova.com.au; https://climatechange.umaine.edu/gisp2/data/alley1.html; Wrightstone, 2017).

The mystery of what really caused the YD-event continues today. We know that during the long pre-YD warming period, the Atlantic Drift Current (The Gulfstream) had established itself running north of Scotland, over towards SW Norway, before running north along the coast of mid- and northern-Norway. It has been speculated that the YD-event occurred because this current abruptly changed its course to a route south of England and re-established the 'glaciation route' that went directly from the Gulf of Mexico to Portugal, and from there turning southwards. This could account for why the cooling started so abruptly. One of the species that indicates this, is the *Mytilus edulis* bivalve, an indicator species for the 'Gulfstream'. It suddenly died out during the YD-period along the entire Norwegian coast (Mangerud, 2021).

Several YD-explanations have been scientifically discussed. The most realistic ones are: 1) an asteroid impact in North America; 2) A sudden flow of meltwater from the draining of Lake Agazzis, an enormous lake that formed in NE America (this is unlikely because there are other indications that the lake drained much later, at around 8,200 BP); 3) That thick sea ice formed in arctic waters just before YD, melted and, thus, formed a 'barrier' of low-salinity water to dampen the Gulfstream, and hinder its migration northwards. However, none of these scenarios have been possible to model numerically yet.

Perhaps the most likely theory has to do with asteroid impacts. In 2007, Firestone et al. (2007), proposed that a cosmic impact event occurred around 12,800 years ago. It resulted in numerous so-called 'airbursts', which refers to a collision of a cosmic body within the Earth's atmosphere, after which numerous smaller fragments strike ground forming transient surface craters (Moore et al., 2020). This event is proposed to have created the Younger Dryas boundary layer (YDB), which contains peak abundances of magnetic spherules, melt-glass, carbon spherules, glasslike carbon, charcoal, platinum, iridium, nickel, cobalt, and nanodiamonds at about 40 locations in North America and Europe, including from the location with the highest density of these anomalies: Abu Hureyra (AH), Syria (Moore et al., 2020).

Further investigations at Abu Hureyra showed that this place may have been at the very epicentre of the cosmic impact. Thus, the YDB hypothesis "*posits multiple*

airburst/impacts across at least four continents. These are proposed to have resulted from a one of a series of short-period, active comets known to break up frequently and to shed dozens to thousands of fragments that are 10 to 1000 m in diameter, each capable of producing catastrophic airburst/impacts, …" "*An encounter with such a million-km-wide debris cluster would be thousands of times more probable than a collision with a 100-km-wide comet or a 10-km asteroid. The YDB hypothesis proposes this mechanism to account for the impact at Abu Hureyra and coeval impacts across > 14,000 km of the Northern and Southern Hemispheres*." (Moore et al., 2020).

In the present author's opinion, this 'Atomic Winter' scenario seems to be the most likely one that could explain how the Earth can suddenly be thrown into brutal cooling with rapid glaciation, such as was the case during the YD. It is likely that the atmosphere would have become very turbid by the numerous large impacts and mid-air collisions. There would probably be formation of a long-lasting sun shield in the stratosphere. Hopefully, future numerical modelling may be able to confirm or denounce this interesting theory.

Figure 3 by Fjeldskaar & Amatov (2018) shows a comparison of the southwestern Scandinavian glaciation ice thickness before and immediately after the Younger Dryas cold-spell.

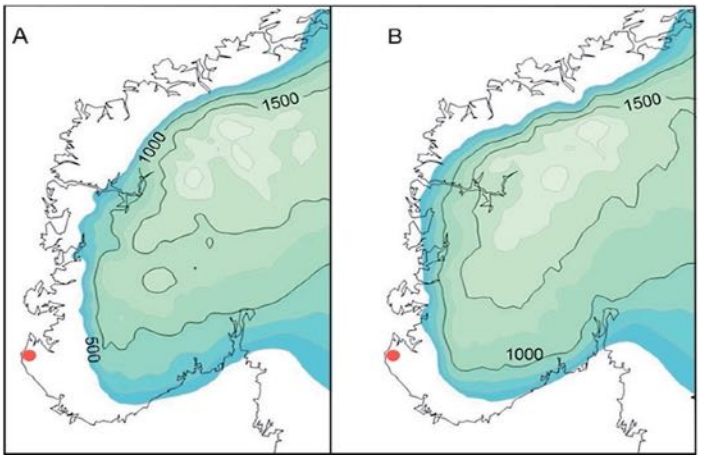

Figure 3: The readvance of the ice during the YD. A) the ice distribution and thickness at 13,000 BP. B) The situation at 11,600 BP. The location of Sola is marked with a red dot (modified from Fjeldskaar & Amatov, 2018).

It is reckoned that the conditions at Sola during the 1,200 year long YD-period was like that of the current west coast of Greenland. The dating of an intact ice bear skeleton (Fig. 5), found in 1976 on the island of Finnøy, north of Sola to 11,000 yBP, proves that there were large terrestrial mammals near Sola, and therefore that there was plenty of fish, birds, and seals, etc.

3. The period immediately after the YD

According to Alley (2000), "*The ice cores show that the end of the Younger Dryas interval involved: 5-10°C warming and a doubling of snow accumulation in central Greenland; a large drop in wind-blown materials, indicating reduced wind speed and other changes in distant source regions or between source regions and Greenland; and a large increase in methane, indicating expansion of global wetlands, probably including those of the tropics. Most of these changes occurred in less than a few decades, and possibly in less than a few years*." And, because we still do not know what triggered the Younger

Dryas rapid climate change, Alley concludes with the following: "*Recurrence of a larger Younger Dryas type event is not impossible, and this possibility merits careful study*." (Alley, 2000).

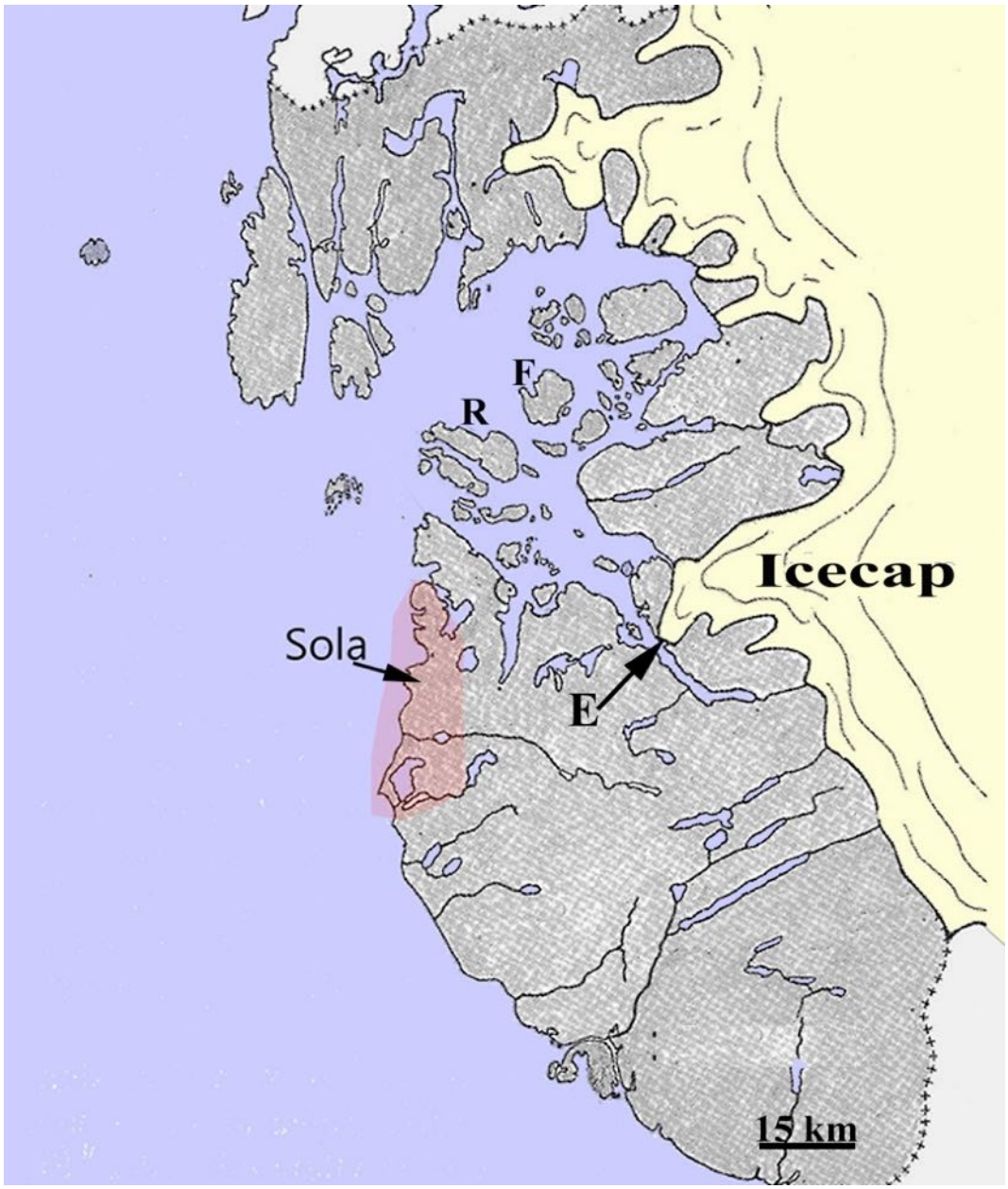

Figure 4: A detailed map of the position of the ice sheet, located inland from Sola, at around 11,300, about 300 years post YD. Notice how the ice-edge covers the deepest fjords, such as the great Lysefjord and Vindafjord 30 – 50 kilometres east and north of Sola. The 'E' denotes the Esmark Moraine, mentioned in the text. R and F on the map shows island locations with the earliest archaeological finds near Sola (R=Rennesøy; F=Finnøy). Note the numerous mountain lakes in the south-east of the map. This is near Gjesdal, with early reindeer hunting remnants found (Source: Simonsen and Lye, 1978).

The terminal moraine ('Vassryggen') formed by the YD glacial expansion, in the municipality of Forsand, near the Lysefjord, is quite a landmark (Fig. 3). This very end moraine is called the 'Esmark moraine' (E, in Fig. 3), as it was here, that the "ice-age concept" originated. It was Professor Jens Esmark who first postulated, around 1810 that glaciers in Norway once must have filled the valleys in Norway right down to the sea level. And it was this very terminal moraine, 'Vassryggen' that provided the necessary clues to him,

as it must have been constructed by a large, massive glacier, he reckoned.

3.1 Towards the Holocene Thermal Maximum (HTM) period

Finally, the climate changed to one of warming. And, it continued, and the Holocene period starts, at ~11,700 y PB.

The first archaeological finds of human operations (stone axes, fishing hooks, neolithic arrowheads, etc.) in Rogaland County, were dated between 11,000 and 9,800 years BP. These finds stem from several islands, including the island of Rennesøy (G on the map, Fig. 3), about 40 km north of Sola, not far from the beach at that time (Lillehammer, 2003).

These people were evidently not alone, as there are numerous finds including some from the ice-free mountains just 40 kilometres east of Sola (Fig. 3). Thus, there were finds of reindeer hunting at 600 m elevation in Gjesdal, only about 10 km from the snout of the glacier ice at that time.

4. Humans arrive Sola and roam all over Rogaland County

In the Preboreal period, starting around 11,000 yr BP, the temperature increased by around 1 degree per century. Over only few generations, the mean annual air temperature went from around 10 °C to 14 degrees. The sea level was still lower than at present, and there was still an opportunity to cross, either on winter ice or by boat (in summer) from the Doggerland to the beaches of Sola. Because of the improving climatic conditions, the landscape turned into one of bushes and trees, with open birch forests inland from the coastline.

The boats that the pioneers to Sola probably arrived in, must have been light-weight, skin-clad, large kayak-types, known from historic and modern Greenland (where they are known as 'Konebåt'). In the largest boats, there would be room for three to four people (Lillehammer, 1988). When the glaciers continued to melt, the sea level gradually rose, and "the window of opportunity" for arriving Sola in boats, started to dwindle. The sea would gradually overflow the newcomer's first shelters near the coast, and they had to move to higher ground.

The pioneers must have been a well experienced group of hunter/gatherers and probably made some return trips to collect family members when they found promising grounds for their future. The combination of west- and south-facing slopes, a wide beach and low-lying land with the sea, with plenty of inlets and islands, with the mountain terrain and glaciers in the east, made everything look very promising for future settlement.

Figure 5: A complete ice bear skeleton dated at 11,000 years BP, was found on the island of Finnøy, about 40 km north of Sola. (Photo courtesy of Terje Tveit, Arkeologisk Museum, Universitetet i Stavanger).

The second stage of settlement would probably consist of family groups that moved

around and found some food here and there. "*They would meet up with each other and exchange knowledge, goods, food, and materials. Ultimately, they would also mingle, and, not least, find a new spouse or husband.*" (Lillehammer, 1988).

There are numerous neolithic finds, all over Rogaland County, that suggest this pattern of population, during the pioneering interval, before more permanent settlements were established (Lillehammer, 1988). The temperature was a couple of degrees lower than at present, and they sheltered beneath large rocks, mountain hollows, coastal grottoes, like the well-known 'Vistehola', in Randaberg municipality, just north-west of Stavanger City.

Excavations of Vistehola exposed a one-metre-thick culture layer, where the dweller's menu was documented. They had a healthy menu consisting of small land- and sea-mammals, many types of fish and birds. Small, fine tools were also found among the food remnants, such as fishhooks, net-sinkers, arrowheads, scrapers, and spearheads (Bang-Andersen, 1995). The settling of southern Scandinavia had started.

Funding

Nil

Reviewer: Ole Humlum

Acknowledgements

The review and advice given by Håkon Rueslåtten is greatly appreciated. The author also thanks Ole Humlum for his review and advice.

References

Alley, R.B., 2000. The Younger Dryas cold interval as viewed from central Greenland. J. Quaternary Science Reviews 19, 213-226.

Andersen, B.G. and Borns Jr., H.W. (1994) The Ice Age World. *Scandinavian University Press (Universitetsforlaget, Oslo)*. ISBN 82-00-21810-4, 208 pp.

Bang-Andersen, S., 1995. Den tidligste bosetningen i Sørvest-Norge i nytt lys. Arkeologiske skrfiter #8, 65-77.

Firestone, R.B., et al., 2007. Evidence for an extraterrestrial impact 12,900 years ago, that contributed to the megafaunal extinctions and the Younger Dryas cooling. Proc. Nat. Acad. Sci. 104, 16016-16021.

Fjeldskaar, W., Amatov, A., 2018. Younger Dryas transgression in western Norway: a modelling approach. Norwegian J. Geol. 98 (1), 127-139. Doi: 10.17850/ngj98-1-08.

Lillehammer, A., 1988. Dei eldste spor etter menneske, Frá haug ok heiðni, 1988.

Mangerud, J. (2021) En uventet klimakatastrofe under siste istid. (In Norwegian). https://forskersonen.no/geofag-geokjemi-istiden/en-uventet-klimakatastrofe-under-siste-istid/1882907

Moore, A.M.T., Kennett, J.P., Napier, W.M., et al., 2020. Evidence of cosmic impact at Abu Hureyra, Syria at the Younger Dryas onset (~12.8 ka): High-temperature melting at >2200 °C. Nature research. Scientific Reports. https://doi.org/10.1038/s41598-020-60867-w

Simonsen, A., Lye, K.A. 1978. Korleis Jæren vart til. In: Birkeland, T. et al., 1978. Jærboka Naturmiljøet. Norsk Oikos A/S, 21-30. ISBN 82-7096-055-1.

Vorren, T. O., Mangerud, J. (2006) Istider kommer og går. In: Ramberg, I.B., Bryhni, I. and Nøttvedt, A. eds. *Landet blir til*. Norsk Geologisk Forening, pp. 482-515. ISBN 978-92-92344-31-6. (In Norwegian).

Wrightstone, 2017. Published by Silver Crown Productions, LLC, 2017
ISBN 10: 1545614105ISBN 13: 9781545614105

Celestial Mechanics and Estimating the Termination of the Holocene Warm Period

Correspondence to
johnparmentola@gmail.com

Vol. 3.1 (2023)

pp. 9-32

John A. Parmentola

The RAND Corporation, Santa Monica, CA 90401 USA

Abstract

This paper addresses several issues concerning Milankovitch Theory and its relationship to paleoclimate data over the last 800,000 years. The approach taken treats the insolation as it is physically, a time-dependent wave. A parameter free model, based solely on the earth's celestial motions and the sun's rays, is presented that partitions the precession index (the precession modulated by the eccentricity) wave and the obliquity wave contributions to the percentage change between successive mean-daily-insolation minima and maxima at 65N latitude during the summer solstice. The model predictions indicate that the precession index contribution dominates such insolation changes and correlates with the occurrences of interglacial and glacial periods and temperature trends over the last 800,000 years. The predictions also indicate that all interglacial terminations over this period occur in the same manner through synchronized constructive interference of the precession index and obliquity waves. Similarly, all interglacial inceptions coincide with synchronized constructive interference of the precession index and obliquity waves, except for the timing of two inceptions, Marine Isotope Stage (MIS) 18d and 13c. These specific timing discrepancies are associated with deep ice cores, which have also been noted by Parrenin et al. through a comparison of Lisiecki and Raymo benthic δ^{18}O and EPICA Dome C (EDC) ice core datasets. Finally, the model enables the classification of interglacial periods into two distinct types based on wave interference that approximately accounts for their different durations. This classification strongly suggests that the current warm period, MIS 1, is very similar to MIS 19c that occurred about 787,000 years ago. When extended into the future, the repetitive wave pattern deduced from the model also enables an estimate for the Holocene warm period termination of 500 years from present.

Keywords: Milanovich cycles; insolation wave; daily-insolation minima and maxima, glacial and interglacial periods; temperature trends last 800 000 years; model predictions.

Submitted: 27-12-2022, Accepted 01-02-2023. https://doi.org/10.53234/SCC202301/11

1. Introduction

Since Milutin Milankovitch's seminal papers (Milankovitch, 1998) concerning the occurrence of ice ages, numerous papers have supported (Hays et al., 1976; Imbrie, 1982; Imbrie et al., 1986; Zachos et al., 2001; Gradstein et al., 2005; Huybers et al., 2011; Roe, 2006) and challenged (Wunsch, 2004; Berger, 2012) his hypothesis that changes in insolation at northern latitudes during the summer solstice is the likely cause of ice sheet changes associated with ice age occurrences. In its most basic form, Milankovitch Theory is a set of insolation conditions on the earth's climate system that have been shown to correlate with features in paleoclimate data.

A substantial number of papers have connected eccentricity, precession, and obliquity cyclical behaviors to features in the paleoclimate data (Lisiecki et al., 2005; Lisiecki, 2010). For example, these celestial parameters, as well as the insolation, exhibit specific characteristic frequencies that are also found in spectral analyses of paleoclimate data over the Pleistocene (Meyers et al., 2008). However, this approach does not completely account for interglacial and glacial durations and the timing of the prominent temperature excursions in paleoclimate data, such as those exhibited in EDC ice core data and other datasets (NCEI, 2007; Jouzel, 2013).

In this paper, the insolation is described physically as a time-dependent wave. It is analogous to an AM radio wave. Its wave-like nature is produced by the "beating" of the earth's celestial motions on the solar irradiance (about 1,368 W/m^2) resulting in its complex time-dependent distribution over the earth's surface. Each of the three celestial motions, precession, eccentricity, and obliquity, contributes a wave component to the insolation. Like ordinary waves, they can produce a beat-like structure through constructive and destructive interference. This description begs several questions. How large in magnitude is each of these wave components, and how do they interfere? Does the interference manifest itself in the paleoclimate data, and if so, how? Does the description of the insolation as a wave and its components have any predictive power for determining the reoccurrence and duration of interglacial and glacial periods? The objective of this paper is to answer these questions.

The results presented are described in temporal space as opposed to typical frequency space analyses for two reasons. First, paleoclimate data is commonly represented as a time series. The goal of this paper is to present a model that accounts for the features in the data as a function of time. Second, the three basic celestial parameters, the precession, eccentricity, and obliquity, are all quasiperiodic functions of time. They have no fixed period as can be seen from the following graphs of their half-cycles,

F*igure 1: Precession half-cycle durations during the period -843,900 years to +54,200 (IMCCE, 2018).*

for the precession, and

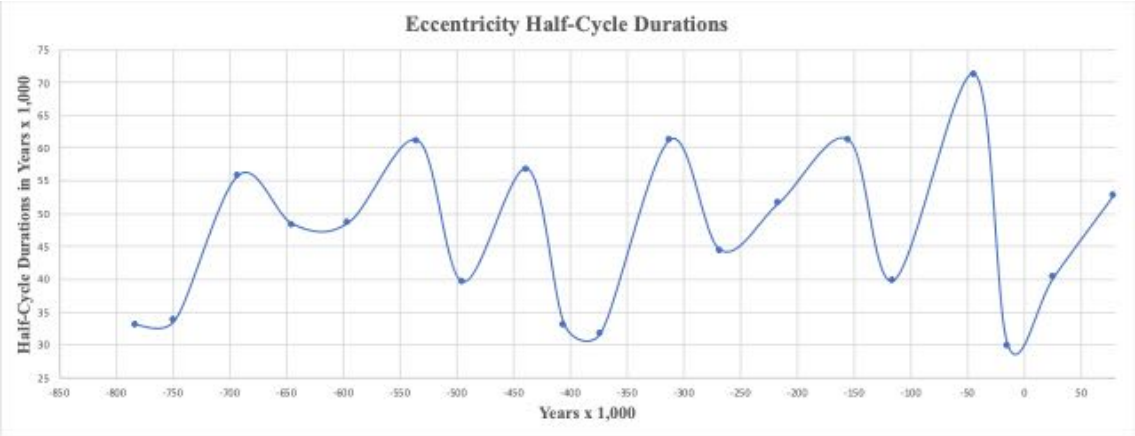

Figure 2: Eccentricity half-cycle durations during the period -815,000 to +79,000 years (IMCCE, 2018).

for the eccentricity, and

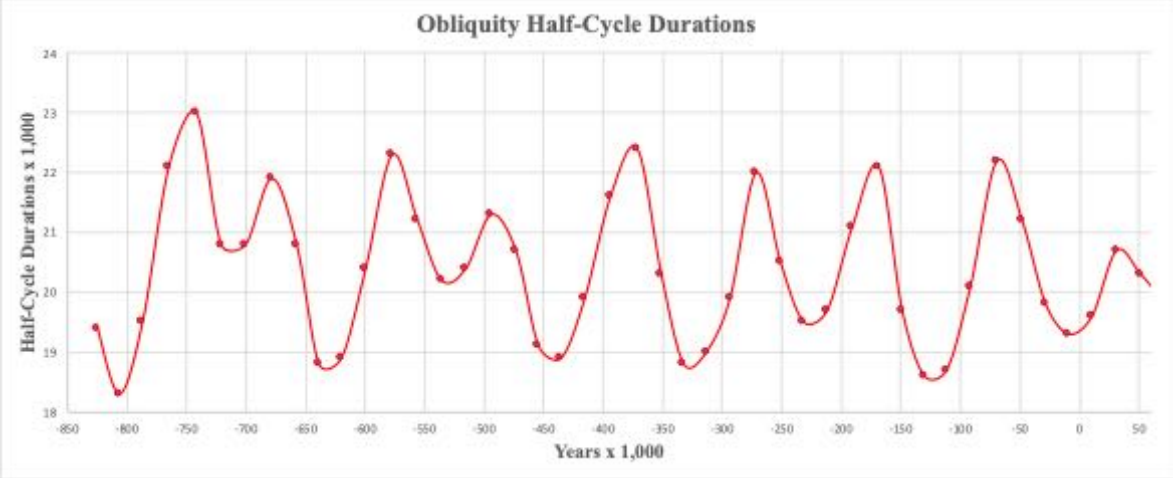

Figure 3: Obliquity half-cycle durations during the period -844,700 years to +51,100 years (IMCCE, 2018).

for the obliquity.

The shortest cycle of the three celestial parameters is that of the precession, which, over the last 800,000 years, on average, has been about 21,000 years. That of the obliquity has been about 41,000 years and the eccentricity about 94,000 years. However, the variation in these cycles and their half-cycles is quite large. For example, precession half-cycles vary from 7,000 to 15,000 years, the obliquity half-cycles from 18,000 to 23,000 years, and the eccentricity half-cycles from 30,000 to 70,000 years. In terms of timescales, the precession sets the scale for the time-dependent behavior of the insolation. As will be demonstrated through a time series comparison, the quasiperiodic nature of these parameters plays an essential role in the timing of wave interferences and prominent features in the paleoclimate data.

In terms of physical effects, the obliquity primarily affects the angular distribution of the insolation over the earth. In a half-cycle, it shifts the sun's rays south to north and vice versa by about 2.4 degrees in latitude or roughly 267 km. This shift changes the angle the sun's rays make with the vertical at

each illuminated point on the earth's surface resulting in a comparatively small overall effect on the insolation amplitude.

The most significant effect on the insolation amplitude comes from the combination of the precession and eccentricity, the precession index (sometimes referred to as the climate precession.) It is defined as the precession modulated by the eccentricity and physically accounts for insolation minima and maxima. For example, when the earth is at perihelion (the closest distance to the sun), and the earth's axis points toward the sun, the insolation approaches a maximum for the northern hemisphere. Fast forward about 11,000 years, an average precession half-cycle, the earth's axis points toward the sun at aphelion (the farthest distance from the sun) the insolation approaches a minimum for the northern hemisphere. The change from maximum to minimum and vice versa can be quite significant (more than 100 W/m^2) at northern latitudes during the summer solstice and is driven by changes in the eccentricity over a precession half-cycle. This qualitative analysis suggests that the insolation can be approximated by the effects produced by just two parameters, the precession index, and the obliquity at insolation maxima and minima.

Over the last 800,000 years, the insolation has transitioned from maxima to minima and vice versa a total of 74 times. These transitions range in percentage from about +28% to -19% with half-cycle durations (the average is about 11,000 years) that range from 4,200 to 16,900 years. They are represented by mean daily insolation predictions at 65 degrees north latitude during June in Figure 4.

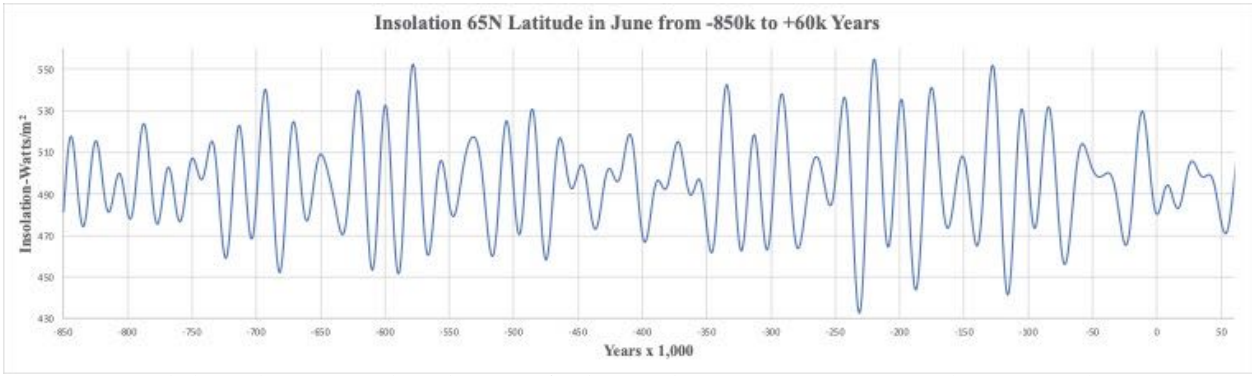

Figure 4. Mean-daily-insolation at 65N latitude in June for the period -850,000 to +60,000 years (IMCCE, 2018).

However, the number of prominent temperature excursions indicated in paleoclimate data is at best 13, which is represented by EPICA Dome C ice core data from Antarctica in Figure 5. This graph is a temperature reconstruction from ice core data using deuterium as a proxy; however, it is model dependent. There are physical effects that can affect the dating of temperature changes inferred from ice cores, which are discussed further in Section 3 where model predictions are compared with paleoclimate time series data.

Reconciling the 74 transitions of Figure 4 in terms of timing and amplitude with the prominent temperature excursions in Figure 5 is a formidable theoretical challenge. These features are affected by eccentricity, precession, and obliquity cyclical behaviors, which have been computed from -250 million to +250 million years (IMCCE, 2018; Laskar et al., 2004). According to the Milankovitch hypothesis, their determination provides a consistent temporal calibration that should correlate insolation changes with features in the paleoclimate data.

Figure 5 indicates that steep rises and subsequent major temperature declines are comparatively infrequent; however, the timescale of these changes is roughly 10,000 years, which approximately

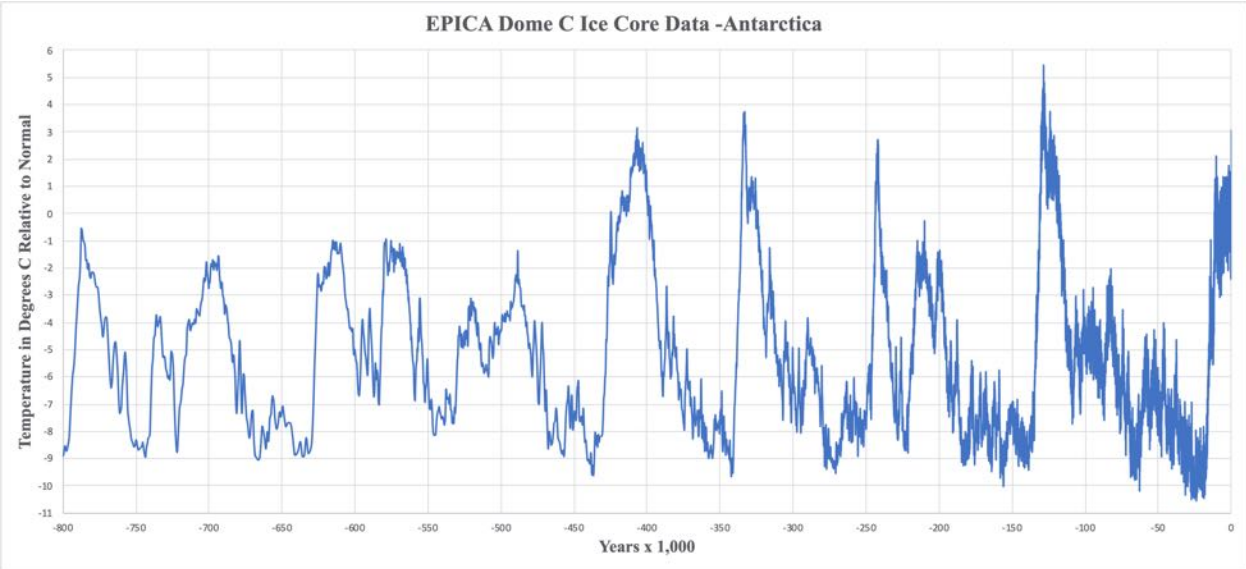

Figure 5. EDC ice core data based on a temperature reconstruction model using deuterium as a proxy presented in degrees centigrade relative to normal from -800,000 years to the present (NCEI, 2007).

coincides with the average precession half-cycle. What, if any, relationship is there between insolation changes and prominent features in the paleoclimate data? Are there specific insolation changes that are special, or are there trends in the insolation over time that correlate with significant changes in the paleoclimate data? To gain some insight into correlations, one might consider the largest changes in insolation from successive minima to maxima, and vice versa to see if these influenced the paleoclimate data more than other insolation changes. Such an approach would also capture insolation trends (as opposed to just individual changes) that could explain certain reoccurring features in the paleoclimate data over time.

Since the obliquity primarily affects the angular distribution of the solar irradiance over the earth's surface with a comparatively small effect on its amplitude over long cycles and the precession index is the primary driver of the insolation amplitude over shorter cycles, the product of the two contributions, the partition model, should well approximate the insolation at maxima and minima. This approximation separates these two effects over time and allows for their time series comparison with the paleoclimate data that implicitly includes the quasiperiodic nature of the three celestial parameters.

2. Methodology

The partition model presented below in Section 3 is not a climate model. There is no inclusion of any aspect of the earth's climate in the model. It is a parameter-free kinematic model based on the three celestial motions of the earth and the sun's rays. The model provides a set of points in time for the obliquity and precession index contributions that represent the percentage change between successive mean-daily-insolation extrema at 65N in June. The model predictions for the insolation are compared with the corresponding theoretical calculations of J. Laskar et al. (IMCCE, 2018; Laskar et al., 2004) showing excellent agreement. An interpolation is made between the set of points for the obliquity and precession index contributions that enables a wave description of these separate contributions to the insolation. In Section 4, the interpolated predictions are compared with the EDC ice core dataset and interpreted using waves and their interference. In Section 5, an estimate for the Holocene warm period termination is presented. Section 6 summarizes the principal results.

3. The Partition Model

This paper assumes the percentage change between successive mean-daily-insolation maxima and minima at 65 degrees northern (65N) latitude during the summer solstice (June) over the last 800,000 years, substantially influenced the prominent features in paleoclimate data such as the EDC dataset depicted in Figure 5.

The main point of this paper is to provide insight into the insolation's time-dependent wave behavior through its separation into precession index and obliquity contributions. Both quasiperiodic behaviors are shown to correlate with the prominent features in paleoclimate data over the last 800,000 years in Section 3.

The separation is accomplished, in part, through an application of the computational tool developed by J. Laskar et al. (IMCCE, 2018; Laskar et al., 2004). The eccentricity, precession, obliquity, and insolation parameters are specified at a time with a temporal resolution of 100 years using Laskar's tool. There are no free parameters in the model.

The insolation, Q, is assumed to be of the form,

$$Q = A \cdot B, \tag{1}$$

where A and B are respectively the precession index and obliquity contributions to the insolation. In Appendix A, B is shown to depend on latitude and the sun's declination angle. Because daylight hours depend on latitude and the sun's declination angle, the mean-daily-insolation, $\overline{Q}$, is dependent on the mean-daily-obliquity contribution, $\overline{B}$. By averaging equation (1) over daylight hours, the mean-daily-insolation is given by

$$\overline{Q} = A \cdot \overline{B} \tag{2}$$

It is straightforward to show from equation (2) that a fractional change in $\overline{Q}$ produced through changes in A and $\overline{B}$ is approximately given by the sum of the fractional contributions,

$$\frac{\Delta\overline{Q}}{\overline{Q}_i} \cong \frac{\Delta A}{A_i} + \frac{\Delta\overline{B}}{\overline{B}_i}, \tag{3}$$

where $\frac{\Delta A}{A_i}$ and $\frac{\Delta\overline{B}}{\overline{B}_i}$ are respectively the fractional precession index and obliquity contributions to the fractional change in the mean-daily-insolation, $\frac{\Delta\overline{Q}}{\overline{Q}_i}$, with $\Delta\overline{Q} = \overline{Q}_f - \overline{Q}_i$, $\Delta A = A_f - A_i$, and $\Delta\overline{B} = \overline{B}_f - \overline{B}_i$ are the respective changes in the mean-daily-insolation, and the precession index and obliquity contributions to the mean-daily-insolation with the subscripts, i and f, designating the initial and final states. The correction cross-term, $\frac{\Delta A}{A_i} \cdot \frac{\Delta\overline{B}}{\overline{B}_i}$, to equation (3) will be shown to be negligible.

The approximation represented by equation (3) implies that the precession index and obliquity contributions to the mean daily insolation simply add. As will be demonstrated in Section 3.3, this translates into the superposition of a precession index wave and an obliquity wave. This separation also enables each of these waves to be compared with EDC data as a time series.

3.1 Precession Index Contribution

The earth's eccentricity has varied by more than an order of magnitude from about 0.004 to 0.05 during the last 800,000 years. The key to understanding the eccentricity's effect on the insolation at northern latitudes during the summer solstice is its change from the time the earth's axis points toward the sun at perihelion to the time it points toward the sun at aphelion. While the timescale of the precession index contribution to the insolation is affected by the eccentricity, its short-term half-cycle is primarily due to the precession.

The comparatively small eccentricity changes over these precession half-cycles enable the approximate determination of the precession index contribution to the fractional change between mean-daily-insolation extrema. As discussed further below, the precession index contribution to the percentage change between successive insolation extrema at 65N during June takes the form of a quasiperiodic wave; however, its half-cycle durations differ from those of the precession.

Assuming the insolation depends on the inverse distance squared from the sun multiplied by an overall constant, the fractional change of the precession index contribution during a perihelion to aphelion half-cycle transition is given by

$$\frac{\Delta A_{p\to a}}{A_p} = \frac{(1-e_p)^2}{(1+e_a)^2} - 1, \tag{4}$$

where the perihelion subscript, p, and aphelion subscript, a, are the initial and final states, respectively. Equation (4) is well approximated by

$$\frac{\Delta A_{p\to a}}{A_a} \approx -2\left(e_a + e_p\right) + e_p^2 + 4e_a e_p + 3e_a^2\,, \tag{5}$$

where the linear term dominates. Similarly, in transitioning from aphelion to perihelion, the corresponding fractional precession index contribution is given by

$$\frac{\Delta A_{a\to p}}{A_a} = \frac{(1+e_a)^2}{(1-e_p)^2} - 1, \tag{6}$$

which is also well approximated by

$$\frac{\Delta A_{a\to p}}{A_a} \approx 2\left(e_a + e_p\right) + e_a^2 + 4e_a e_p + 3e_p^2, \tag{7}$$

where again the first term dominates, and the subscripts have corresponding interpretations. The eccentricity, e, depends on time and is specified by Laskar's tool at the time of each mean-daily-insolation maximum and minimum during June at 65N latitude.

In deriving equations (4) and (6), the earth-sun distances at perihelion, $R_p = a\cdot\left(1-e_p\right)$, and aphelion, $R_a = a\cdot(1+e_a)$, are used, where, a, is the semi-major axis of the earth's orbit. The semi-major axis is assumed constant during an insolation transition between successive extrema, which implies eccentricity changes result from changes in the semi-minor axis. Also, because the

eccentricity is a slowly varying function of time, differences in the time specification of insolation extrema and when the earth's axis successively points toward the sun at perihelion and aphelion and vice versa have a comparatively small impact on the insolation. An error analysis that supports this conclusion is presented in the next subsection.

3.2 Obliquity Contribution

The comparatively small and gradual change in the earth's tilt angle also enables the approximate determination of the obliquity contribution to the fractional change between successive mean-daily-insolation extrema. By specializing to the summer solstice (the sun's declination angle equals the obliquity angle), in Appendix A, the fractional obliquity contribution to successive mean daily insolation during June is shown to be of the form,

$$\frac{\Delta\overline{B}}{\overline{B}_i} = \frac{h_f \cdot \sin\emptyset \cdot \sin\theta_f + \cos\emptyset \cdot \cos\theta_f \cdot \sin h_f}{h_i \cdot \sin\emptyset \cdot \sin\theta_i + \cos\emptyset \cdot \cos\theta_i \cdot \sin h_i} - 1, \tag{8}$$

where $\emptyset$ is the latitude $= 1.134$ radians or $65N$, and θ_i and θ_f are the initial and final obliquity angles specified in radians with h_i and h_f the initial and final hour angles determined by,

$$h_j = \cos^{-1}\left(-\tan\emptyset \cdot \tan\theta_j\right), \tag{9}$$

which is also in radians. The obliquity range, $0.386 \leq \theta \leq 0.428$ radians, implies a maximum percentage obliquity contribution to successive mean-daily-insolation extrema during June at 65N latitude is about 8.6% from equations (8) and (9); however, this maximum is never realized (see further discussion below). The obliquity angle, θ, is specified by Laskar's tool at the time of each mean-daily-insolation maximum and minimum at 65N latitude during June. For successive insolation extrema transitions, equations (8) and (9) are surprisingly well approximated by

$$\frac{\Delta\overline{B}}{\overline{B}_i} \approx 2 \cdot \left(\theta_f - \theta_i\right). \tag{10}$$

The linear terms in equations (5), (7), and (10) can be used to provide reasonable "back of the envelope" estimates for the fractional change between successive mean-daily-insolation extrema at 65N latitude during June.

3.3 The Wave Description

The more accurate partition model predictions are utilized by substituting equations (4), (6), (8), and (9) into equation (3) to compare the model predictions with the corresponding Laskar predictions. This comparison is shown in Figure 6.

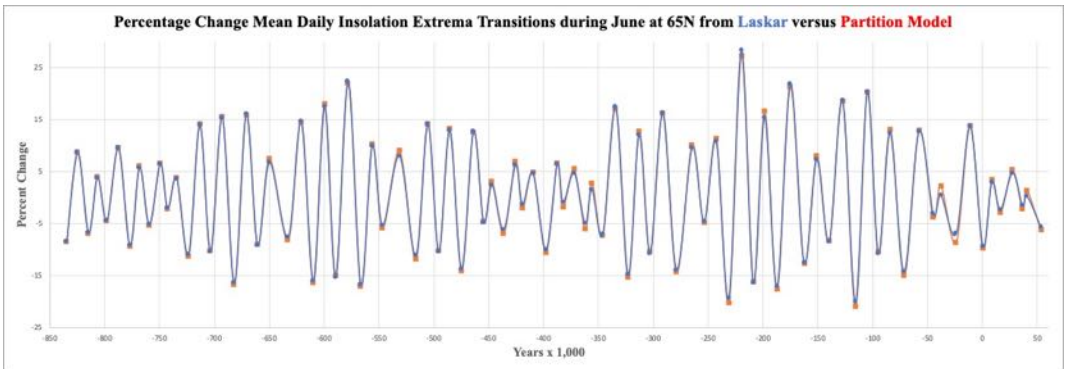

Figure 6. Comparison of the partition model approximation to the percentage change between successive mean-daily-insolation extrema at 65N latitude in June with the predictions of J. Laskar et al. in Figure 3.

The blue dots follow from Laskar's tool, and the red dots are partition model estimates for the percentage change between successive mean-daily-insolation extrema at 65N latitude during June. A point wise error analysis of Figure 6 is represented in Figure 7,

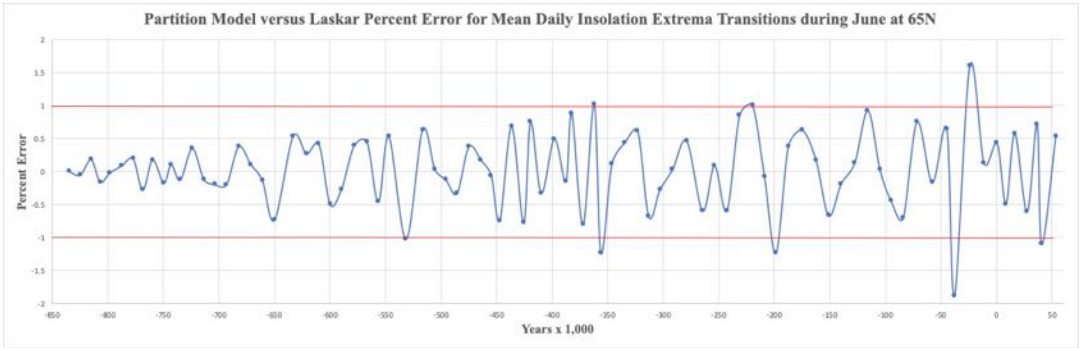

Figure 7. An analysis of Figure 7 indicates a + or -1% error bound on most points (horizontal red lines) with several points between + or -1 and + or -2%.

For most points, the error is bounded by + or -1%. The comparatively few exceptions are of no consequence to the analysis presented below.

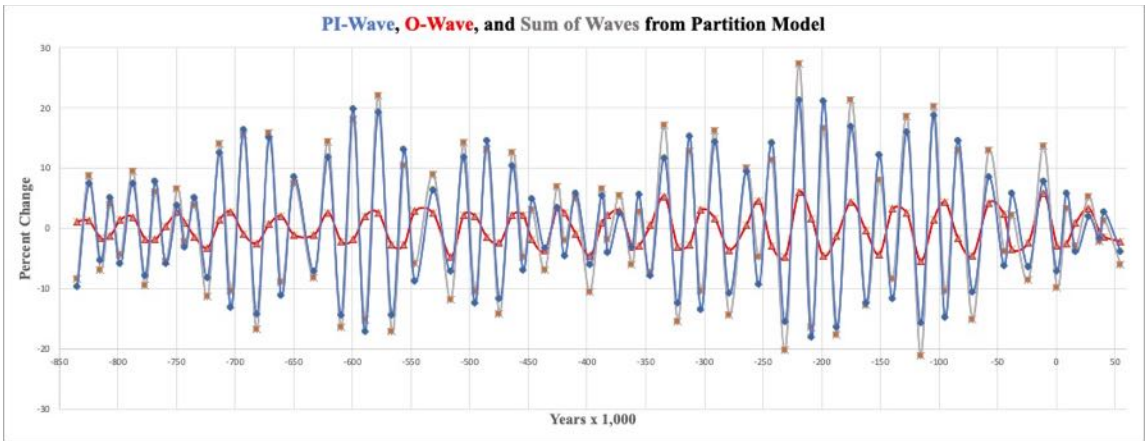

Figure 8. Partition model estimates for the precession index wave (blue curve), obliquity wave (red curve), and their sum (grey curve with red dots) associated with the percentage change between successive mean- -daily-insolation maxima and minima at 65N latitude during June from -844,200 to +53,500 years (IMCCE, 2018).

The complex "beat structure" in Figure 6 results from the superposition of the precession index and obliquity wave contributions to the percentage change between successive mean-daily- insolation extrema, which follow from equations (3), (4), (6), (8), and (9) and are represented in Figure 8.

The values greater or less than zero represent increasing or decreasing changes from each contribution to successive mean-daily-insolation extrema transitions. They, therefore, provide systematic trends associated with mean daily insolation changes over time, which are not evident in Figures 4 and 6. These increasing and decreasing trends will be shown to correlate with the prominent features in paleoclimate data.

Note that the precession index and obliquity contributions to successive mean-daily-insolation extrema from equations (4), (6), (8), and (9) contribute to the neglected cross-term corrections to equation (3). At best, these corrections are an order of magnitude less than the leading terms, which validates equation (3).

The three curves in Figure 8 are based on best fits to a sparse set of points. Nevertheless, the curves provide quantitative estimates, and qualitative behaviors as well as a conceptual language involving waves that will be exploited below to physically describe the prominent features of the EDC ice core data of Figure 5.

The obliquity contribution (red curve) in Figure 8 will be referred to as the O-Wave. It appears as a quasiperiodic wave of varying half-cycle duration having a narrowly bound amplitude. Its contributions range from about 6% (-219,600 years) to -5% (-115,700 years).

The precession index contribution (blue curve) will be referred to as the PI-Wave of recurring wave packets comprised of a precession carrier wave modulated by an eccentricity wave. It is contribution ranges from about 21% (-219,600 years) to -18% (-208,700 years). Note that the eccentricity primarily amplifies and reduces the insolation in a quasiperiodic manner through recurring PI wave packets.

The grey curve is the sum of the O-Wave and PI-Wave contributions. In terms of magnitude, the PI-Wave contribution to the insolation dominates the O-Wave. As will be demonstrated in the next section, the insolation trends represented by the PI-Wave approximately correlate with the prominent features of the EDC data. These aspects of the PI-Wave contradict the original Milankovitch Theory hypothesis (Milankovitch, 1998), which emphasizes the role of the obliquity in the occurrence of ice ages.

4. Time Series Comparison of the Model Predictions and EDC data

Because of the earth's highly complex climate system and unknown conditions in the past, its response to external effects such as celestial mechanical forcing is very challenging to predict. Adding to this complexity are internal effects within the earth system that can also affect its climate, such as volcanic eruptions, albedo changes, etc. Hence, the detailed behavior of the earth's climate between and during interglacial periods is far beyond the scope of this paper. Nevertheless, the predictions from the partition model will be used to interpret the EDC data. This semi-quantitative approach indicates that there are correlations between celestial mechanical forcing and prominent features in the data.

The comparison of EDC data modified by Marine Isotope Stage (MIS) designations (Berger et al., 2015) with the PI-Wave of Figure 8 is represented in Figure 9.

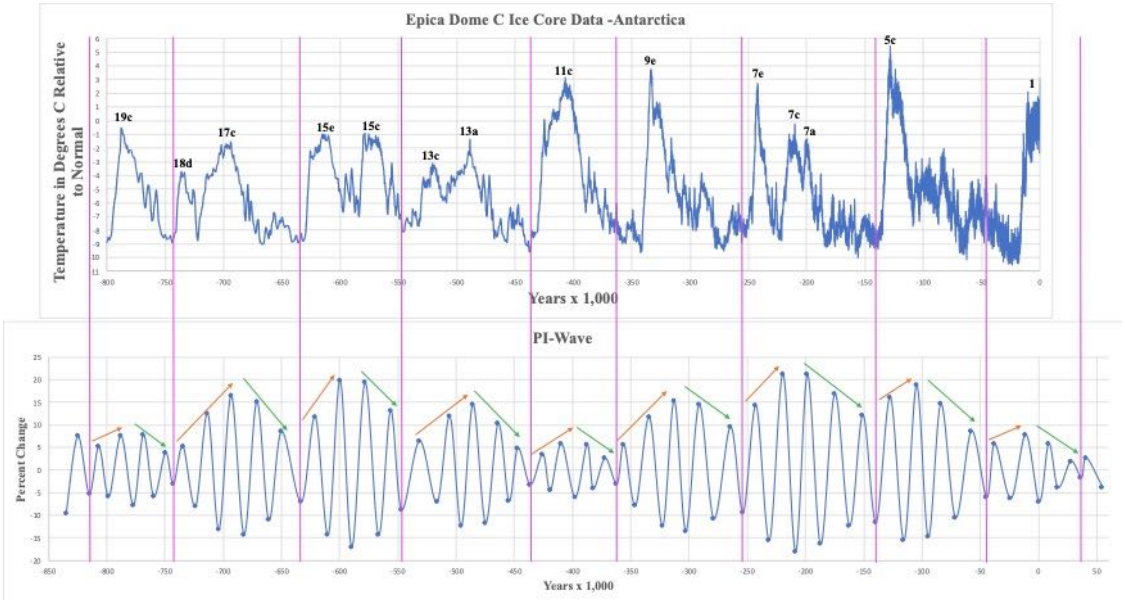

Figure 9. PI recurring wave packets (judiciously defined by purple vertical lines) approximately correlate with interglacial and glacial periods over the last 800,000 years. Precession carrier wave maxima trends qualitatively correlate with increasing temperature trends (red arrows) and decreasing maxima trends (green arrows) with decreasing temperature.

Visually, the quasiperiodic PI wave packets, which are specified by the vertical purple lines, roughly correlate with recurring interglacial and glacial periods. To determine occurrences of interglacial and glacial periods, simply follow the recurring PI wave packets. However, the relationship between the timing of prominent temperature excursions and the partition model predictions also depends on the O-Wave contributions (see further discussion below). Nevertheless, increasing temperatures in the EDC data coincide with increasing precession carrier wave maxima (red arrows), while declining temperature trends follow the decreasing trend in precession carrier wave maxima (green arrows). These amplitude trends are primarily due to eccentricity changes. The eccentricity during precession carrier wave cycles amplifies and reduces the insolation over substantial periods, which roughly correlate with the inception and termination of interglacial periods.

Note that some temperature trends are interrupted by precession carrier wave amplitude reductions that appear to "split" the temperature peaks into MIS pairs, namely, 18d-17c, 15e-15c, 13c-13a, 7e-7c, and 7c-7a (see further discussion below). Also, note the similarity in Figure 9 between the wave packet to the far left (associated with MIS 19c) and the last one to the far right (associated with MIS 1), which is the Holocene, but more about this relationship in the next section.

The O-Wave contribution to the percentage change of successive mean-daily-insolation extrema at 65N during June also qualitatively correlates with EDC temperature excursions as indicated in Figure 10. The comparison in Figure 10 indicates that both data sets have similar quasiperiodic behaviors with the O-Wave systematically lagging the EDC data (see discussion below). It also indicates that there were 20 O-Wave maxima and 13 prominent temperature excursions with numerous temperature "bumps" in between over the last 800,000 years. Also note that from -430,000 years to the present, the obliquity wave maxima tend to be higher, and the minima lower than the period -800,000 to -430,000 years. This behavior may, in part, account for the systematically higher and lower

temperatures during the period -430,000 years to present compared to the earlier period often referred to as the mid-Brunhes Climate Transition.

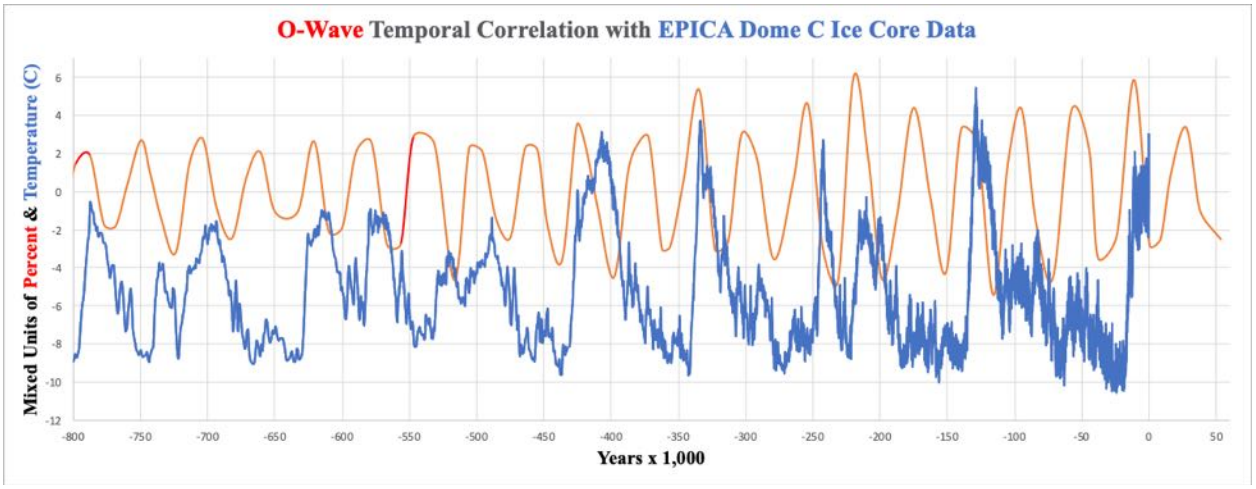

Figure 10. O-Wave predictions from the partition model and EDC data indicate a qualitative temporal correlation between O-Wave maxima and EDC temperature peaks. The O-Wave curve is constructed from 85 data points while the EDC data involves 5,788 points.

The temporal correlation between the O-Wave oscillations and EDC temperature excursions can be improved by shifting O-Wave data by +10,000 years as indicated in Figure 11.

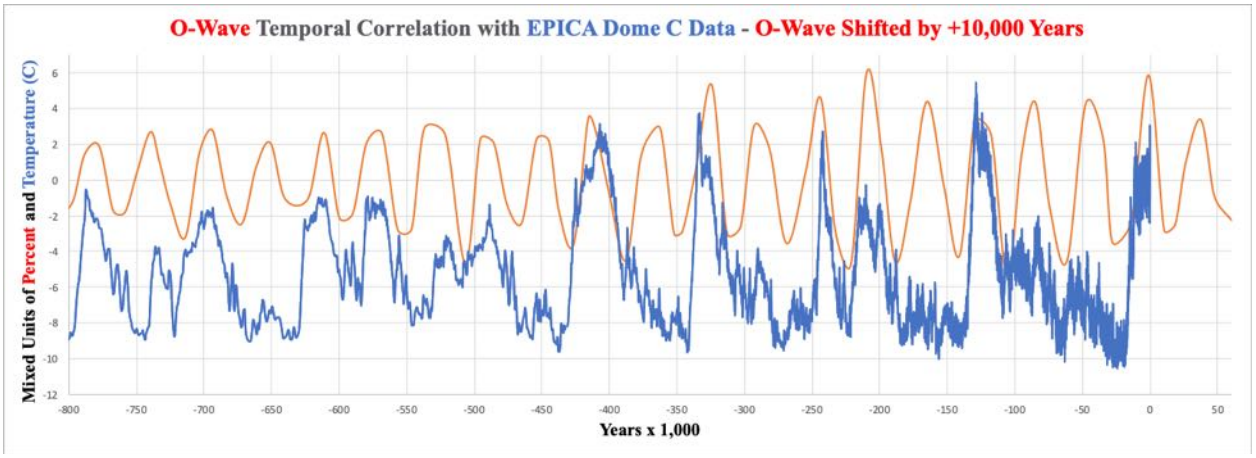

Figure 11. O-Wave predictions from partition model and EDC data with the O-Wave temporally shifted by +10,000 years indicating an improved qualitative correlation between O-Wave maxima and EDC temperature peaks.

Note, the 10,000-year shift is comparable to the average precession carrier wave half-cycle duration. The timing differences between the O-Wave contribution and the temperature excursions are ameliorated through interference between the PI- and O-Wave.

Utilizing the above wave taxonomy, interglacial periods can be classified into two types. Those of Type I occur over one precession carrier wave cycle. During such a cycle, there is an approximate constructive interference between the precession carrier and O waves. Those of Type II occur over two precession carrier cycles; however, there is constructive and destructive interference between the precession carrier and O waves during such cycles.

Using MIS designations, those of Type I are 19c, 15e, 15c,13c, 9e, 7e, 5e, and 1, which are represented in Figure 12.

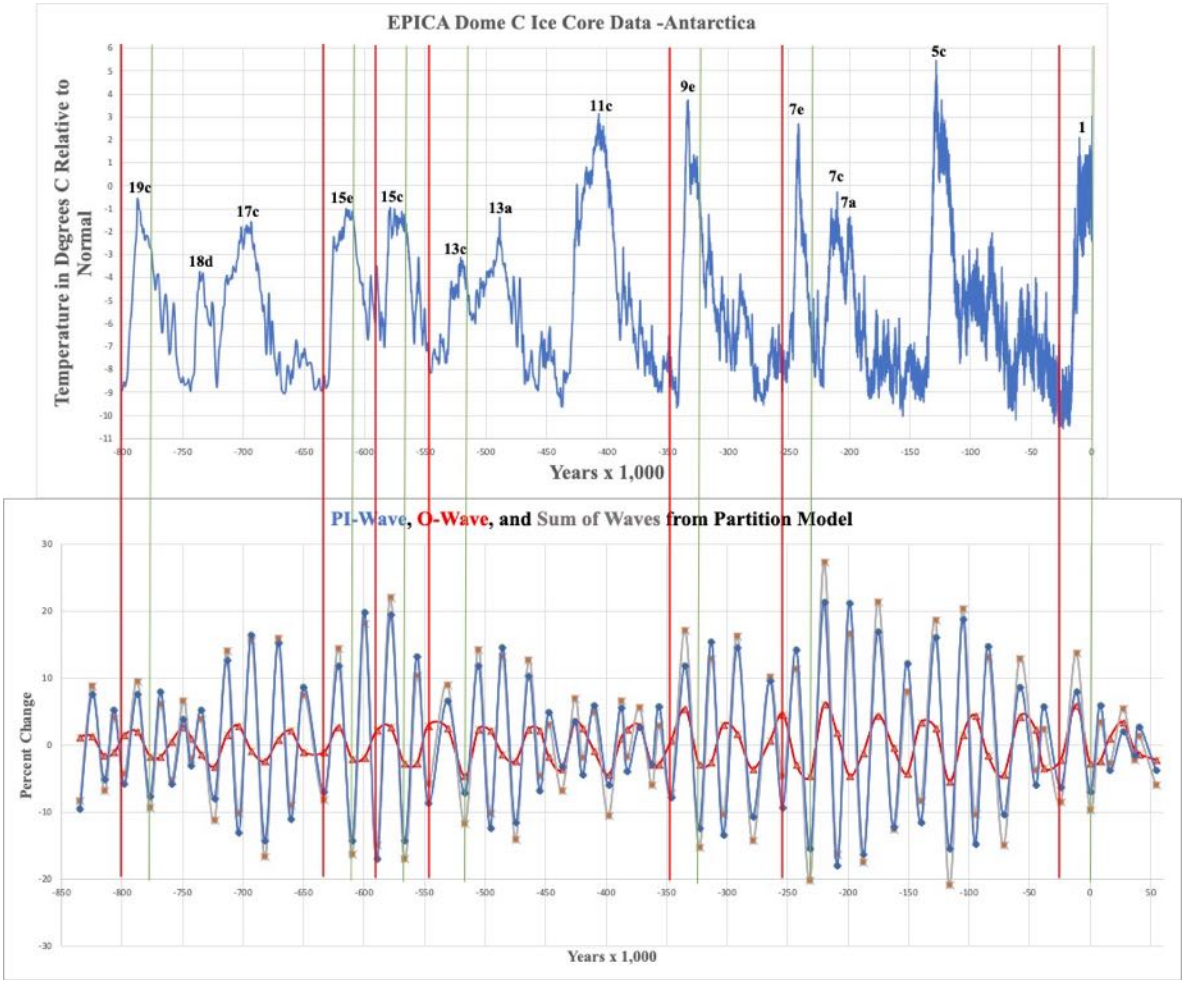

Figure 12. Type I interglacial initiations (red vertical lines) are followed by interglacial terminations (green vertical lines). Initiations coincide with concurrent PI-Wave, and O-Wave increases to the right of the red vertical lines, and terminations coincide with corresponding concurrent declines ending in green vertical lines.

Each pair of vertical red and green lines extending across both graphs relates the duration of each precession carrier cycle and its corresponding MIS interglacial. For Type I, all PI-Wave contributions constructively interfere with O-Wave contributions except for MIS 7e (see further discussion below). Starting from the right of each vertical red line, both contributions concurrently increase to approximately synchronized maxima associated with the red dots of the grey curve and then decline concurrently to the vertical green lines terminating on the red dots of gray curve minima. The vertical green lines define all interglacial terminations, which are comparatively sharp. Note the role of the O-Wave is to enhance (constructive interference) the precession carrier wave maxima and minima as indicated by the red dots associated with grey curve maxima (excluding for MIS 7e) and minima (including MIS 7e). The termination of MIS 1, the Holocene, will be discussed in the next section.

For MIS 7e, the PI- and O-Wave contributions are initially out of phase by about ¼ of an O-Wave cycle; however, they partially constructively interfere as the PI-Wave contribution increases to the right of the indicated vertical red line. The duration of this interglacial is likely cut short because the O-Wave contribution subsequently destructively interferes with the PI-Wave contribution. However,

MIS 7e terminates like all others of Type I as indicated by the deep minimum at the green line (the grey curve red dot minimum).

Note also, the delay in the initiation of interglacial MIS 13c, which has the longest precession carrier wave cyclical duration of about 30,000 years. Its precession carrier wave maximum represents a decline from the earlier maximum in Figure 12. Note the O-wave contribution is out of synchronization, which broadens the insolation maximum. Also, the amplification rate of the insolation during this period is comparatively low due to its long duration. This delay is described further below, along with another initiation delay associated with a Type II interglacial.

The interglacial periods of Type II are MIS 18d, 17c, 13a, 11c, and 7c-7a. The latter hyphenated designation is further explained below. Each of these periods involves a pair of precession carrier wave maxima trending higher, as depicted in Figure 13.

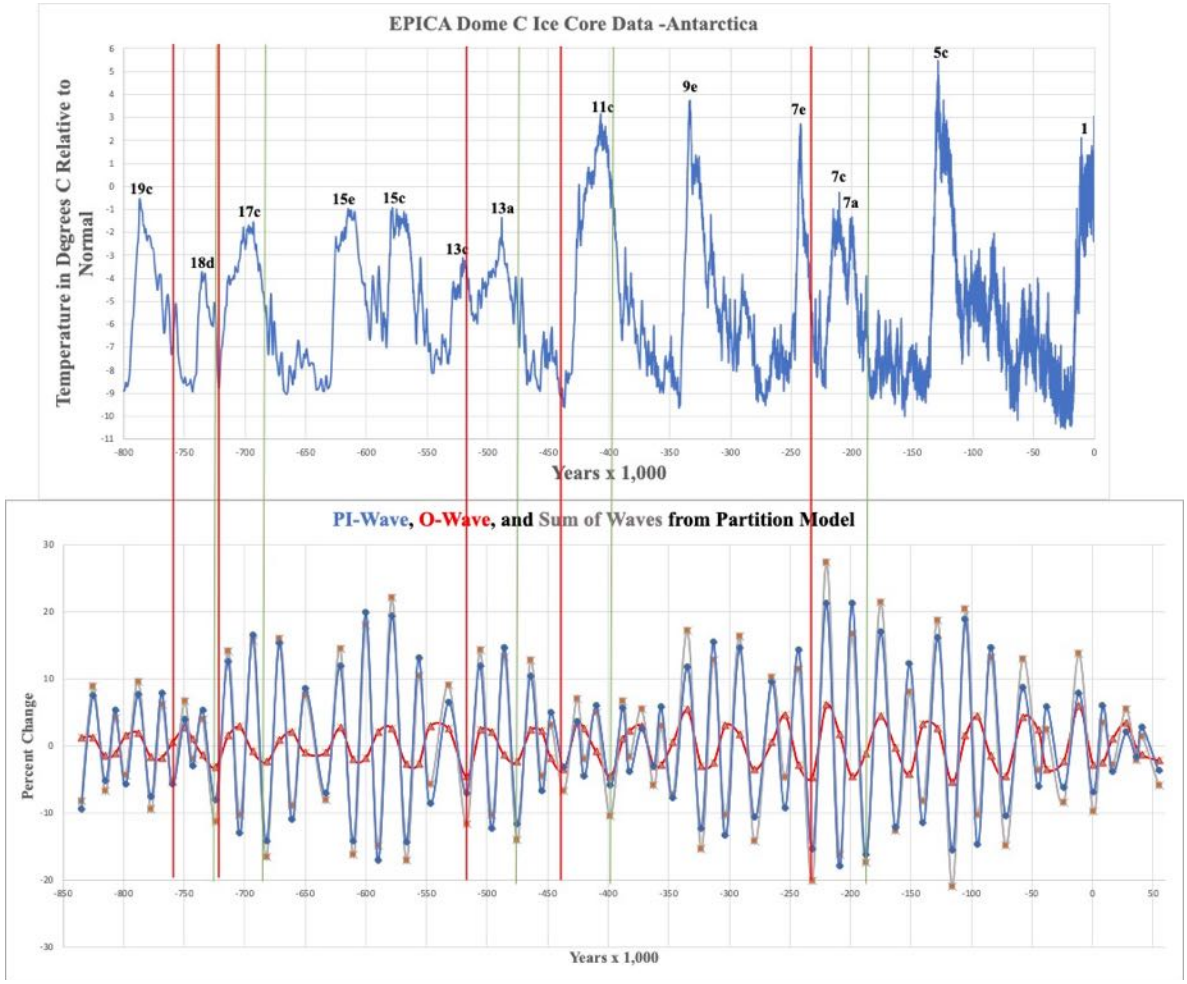

Figure 13. Type II interglacial initiations (red vertical lines) are followed by interglacial terminations (green vertical lines). Initiations coincide with concurrent PI-Wave and O-Wave increases to the right of the red vertical lines, while terminations coincide with in phase PI-Wave and O-Wave minima that coincide with corresponding green vertical lines. Note that the pair of green and red lines associated with the MIS 18d-17c split the interglacial.

Again, the pair of vertical red and green lines identify the temporal extent of two precession carrier wave maxima and minima and their corresponding interglacial period. The O-Wave contributions occur over a longer half-cycle than the Type I set. In all cases, an O-Wave maximum is approximately

in phase with the first precession carrier wave maximum (constructive interference). The O-Wave is then out of phase with the next precession carrier wave minimum and maximum (destructive interference). Eventually, the O-Wave contribution ends approximately in phase with the final precession carrier wave minimum except for MIS 7c-7a, which is about ¼ of an obliquity wave cycle out of phase (about 11,000 years). However, in the latter case, the O-Wave contribution is negative at the second precession carrier wave minimum, so it constructively contributes to the MIS 7a termination as indicated by the deep minimum at its green vertical line (red dot minimum of the grey curve).

MIS 7c-7a appears to be an interglacial that is split in two. It is associated with successive precession carrier wave maxima and minima that have the largest magnitudes over the last 800,000 years. There is a concurrent decline in the precession carrier wave and O-Wave contributions between the precession carrier wave peaks. The timing of this concurrent decline likely accounts for the split in the MIS 7c-7a interglacial. However, the MIS 7a temperature peak is of a very short duration, likely due to the destructive interference between the second precession carrier wave peak and the O-Wave. Note that MIS pairs 18d-17c, 15e-15c, 13c-13a, and 7e-7c also appear to be split by PI- and O-Wave cyclical behaviors.

All Type I and II interglacial durations are approximately determined by their precession carrier wave durations. However, there are delays in the initiation of MIS 18d (5,000–7,000 years) and MIS 13c (11,000–13,000 years). For MIS 18d, the precession carrier wave maximum to the right of the red line is a part of an insolation decline despite its enhancement from the O-Wave contribution (red dot on grey curve). The subsequent second precession carrier wave maximum (MIS 18d is of Type II) is even less by about 2%. This feature may account for the comparatively small MIS 18d temperature excursion. The relatively low rate of increasing insolation may also account for the comparatively small MIS 13c temperature excursion.

Both MIS 18d and 13c also represent deep ice cores (time is a function of core depth), where physical effects can affect the estimated time of these interglacial inceptions and terminations using ice core models. It has been noted (Parrenin et al., 2007) that the most significant timing discrepancies between paleoclimate datasets EDC and LR04 benthic $\delta^{18}O$ occur for MIS 18d and 13c. This comparison suggests that the partition model predictions for the timing of interglacial initiations and terminations could be correct and that another examination of the EDC data may resolve the timing discrepancies between the partition predictions presented here and the data.

Overall, the rates of insolation amplification and reduction as indicated by the recurring PI wave packets (enhanced by the obliquity contribution) appear to correlate with rising and declining EDC temperature excursions. And all interglacial terminations coincide with the same celestial mechanical forcing conditions.

5. Estimating the Holocene Warm Period Termination

To discuss the duration of interglacial terminations, a quantitative criterion is required that can be used across 800,000 years to define the interglacial termination period. For an interglacial, that criterion is the period from the PI-Wave maximum (second maximum for Type II) to the successive synchronized minimum.

The analysis presented above indicates that MIS 1 is a Type I interglacial. As such, it is expected to terminate because of PI- and O-Wave constructive interference. The MIS 1 one cycle classification

indicates that MIS 11c is an unlikely analog because it is Type II, which has been proposed in the literature (Berger et al., 2003; Rohling et al., 2010).
MIS 19c has also been identified as a possible Holocene analog based solely on the behavior of celestial parameters and comparable mean-daily-insolation changes (Vavrus et al., 2018). The analysis presented below addresses the similarities and differences between MIS 19c and MIS 1 based on PI- and O-Wave contributions to the percentage change between successive mean-daily-insolation extrema at 65N latitude during June.

As pointed out earlier in Figure 9, the O-Wave half-cycle durations of MIS 19c and MIS 1 are similar. They both are associated with an O-Wave cycle duration of about 37,000 years, with approximate half-cycles of 27,000 years on the upside and 10,000 years on the downside. They also have comparable declines in mean-daily-insolation from their maxima to minima. For MIS 19c, the decline is about 48 $W/m^{2,}$ while for MIS 1, it is about 50 W/m^2.

Their main difference is the estimated duration of their precession carrier wave cycle and half-cycle durations. For MIS 19c, the precession carrier wave cycle duration is about 21,000 years, while for MIS 1, it is about 24,000 years. This difference indicates that MIS 1 will likely be a longer interglacial than MIS 19c. In terms of interglacial terminations, the MIS 19c downside precession carrier wave half-cycle duration is about 10,500 years, while for MIS 1, it is about 11,600 years.

In Figures 12 and 13, Type I and II terminations end on grey curve red dot minima that involve O-Wave enhancements (constructive interference) to precession carrier wave minima. The following table summarizes the termination estimates for each MIS based on their downside precession carrier wave half-cycle duration.

Table I: MIS termination duration estimates based on the last precession carrier wave peak to the vertical green line in Figures 12 and 13.

Type I	MIS #	Termination (years)
	19c	10,500
	15e	11,100
	15a	11,700
	13c	14,800
	9c	11,400
	7e	11,500
	5e	11,800
	1	11,600
Type II	18d	10,800
	17c	11,100
	13a	10,800
	11c	11,800
	7c-7a	11,200

These termination estimates are all comparable (within hundreds of years of each other) in duration except for MIS 13c, which has the longest cyclical duration and the largest downside precession carrier wave half-cycle duration of 14,800 years.

Assuming the vertical green line for MIS 1 in Figure 12 is accurate, its termination will occur at 500 years from the present based on just celestial mechanical forcing. This estimate coincides with the local minimum in insolation using Laskar's tool as indicated in Figure 14.

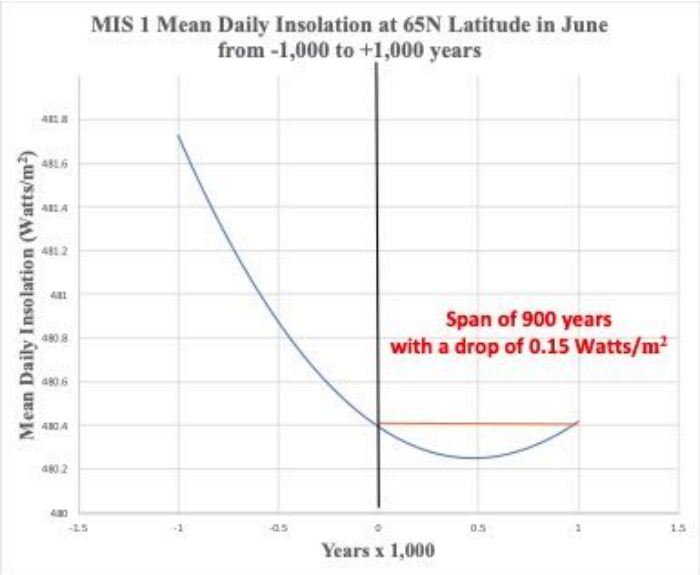

Figure 14. MIS 1 mean-daily- insolation at 65N latitude during Junefrom -1,000 to +1,000 years. The shallow minimum at +500 years measured from the vertical black line estimates the Holocenetermination, which coincides with the vertical green line in Figure 12.

It is hard to imagine, given other uncertainties, that an additional 0.15 W/m^2 decline of insolation from the present to 500 years in the future can make much of a difference regarding the termination of the current Holocene warm period. Given the very shallow minimum and the likelihood that the effects causing a temperature descent are cumulative, a more reasonable low-resolution estimate for the resolution estimate for the termination would be sometime within the next 500 years.

MIS 19c shares the same MIS 1 feature as indicated in Figure 15, which also has a relatively shallow minimum over 1,100 years. Note that all other interglacial terminations share this common feature.

Given the consistent recurrence of the interglacial terminations based on celestial mechanical forcing over the last 800,000 years, it is likely that there is a common physical climate mechanism that accounts for interglacial terminations. Milankovitch Theory focuses on northern latitudes at or greater than 65N because of the potential for ice sheet growth due to the decline in mean-daily-insolation at these latitudes during June over thousands of years. The substantial reduction in the mean-daily-insolation over the last 11,100 years for the Holocene has likely had a cooling effect on the air over a range of latitudes. This latitudinal range is due to a tradeoff between increasing insolation as the latitude decreases (the obliquity has decreased over the last 11,100 years) along with a concurrent decline in daylight hours. As examples, Figures 16 and 17 demonstrate the extensive nature of this latitudinal effect for MIS 19c and 1,

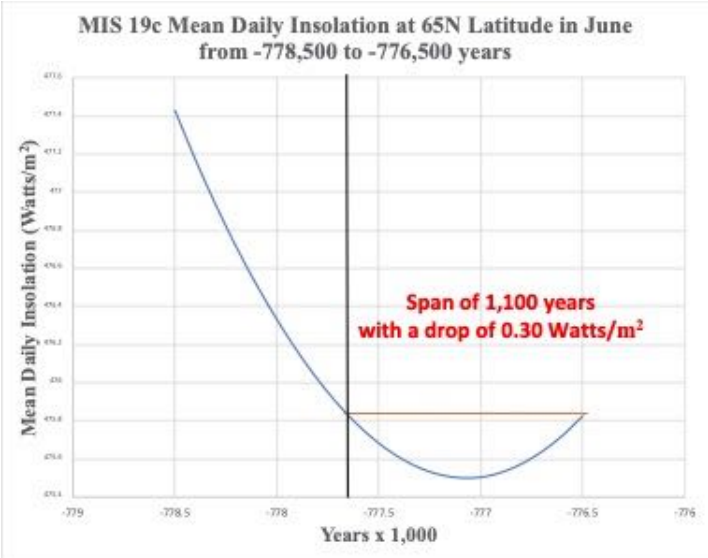

Figure 15. MIS 19c mean-daily-insolation at 65N latitude during June from -778,500 to -776,500 years. The shallow minimum at 600 years measured from the vertical black line is a termination estimate that coincides with the vertical green line in Figure 12

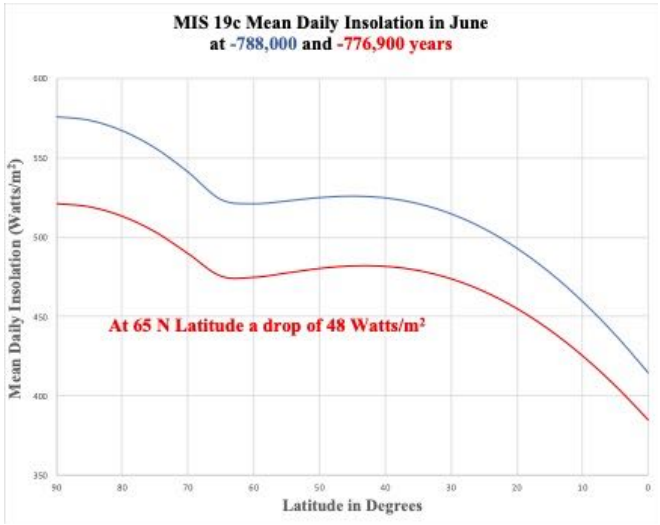

Figure 16. Latitudinal effect on mean-daily-insolation over a period of 11,100 years for MIS 19c (IMCCE, 2018).

This gradual reduction in mean-daily-insolation during June over the last 11,100 years enables air at northern latitudes to more readily cool during the winter solstice (the hour angle significantly decreases), which has the potential to increase the dense cold air volume at northern latitudes. Similar insolation reductions have occurred many times over the last 800,000 years; however, the specific physical mechanism within the earth's climate system that couples to such insolation reductions to cause a temperature descent into a glacial remains uncertain. It is therefore impossible to predict the consequences of this insolation condition on the earth's climate in detail because of our poor understanding of the earth's climate. The best that can be expected is relying on the recurring pattern described in this paper.

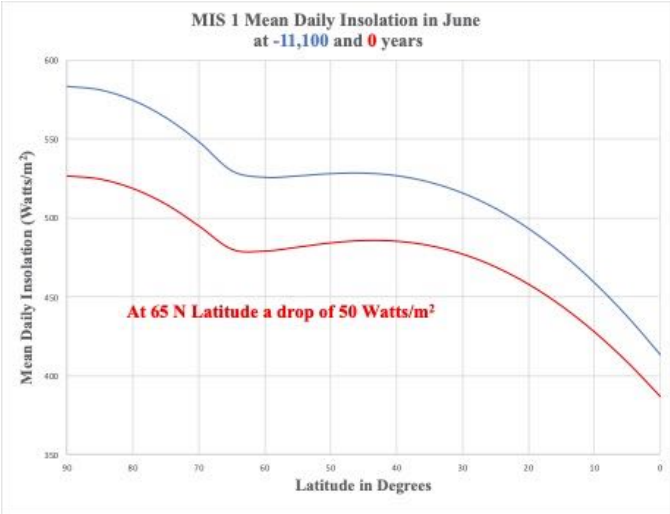

Figure 17. Latitudinal effect on mean-daily-insolation over a period of 11,100 years for MIS 1 (IMCCE, 2018).

However, in recent times, the cold air volume above 60N latitude has produced extreme weather events associated with an instability of the polar vortex - stable cold, dense air counter-rotating at northern latitudes - that is kept in check by the jet stream. The specific conditions that produce these events are not well understood due to the lack of a reliable theory of the earth's climate. At best, there are models (Lawrence et al., 2020) that attribute different physical mechanisms to these events. However, the recurrence of such events over an extended period can result in ice and snow accumulation that can change the earth's albedo, producing cooler climates because of gradual changes in the earth's heat engine. The monitoring of trends in the earth's albedo may provide a way of anticipating an eventual temperature descent into the next ice age.

It is essential to keep in mind that the above estimated MIS 1 termination is tentative. Nevertheless, based solely on the earth's celestial motions and the sun's rays, the Holocene termination is likely to happen as all other interglacial terminations over the last 800,000 years.

6. Summary

The partition model presented in this paper is a kinetic model based on the earth's celestial motions and the sun's rays. Its predictions reveal a recurring pattern over 800,000 years consistent in its interpretation of paleoclimate data and, in particular, interglacial terminations. The results regarding the future occurrence of an ice age are a simple extrapolation of the recurring pattern. If anything, it is a very conservative, albeit limited, approach to inferring when the next ice age will occur based solely on celestial mechanics and the sun's rays.

The model also provides additional insight into the roles of the precession index and obliquity contributions to the insolation described as a wave. In particular, the recurrence of interglacial and glacial periods over the last 800,000 years approximately correlates with the quasiperiodic behavior of PI wave packets. This correlation is reinforced by the quasiperiodic behavior of the O-Wave contribution to the insolation. In addition, all interglacial terminations involve constructive interference between the PI and O waves. Finally, interglacial durations approximately coincide with the number and duration of precession carrier wave cycles.

Based solely on celestial mechanical considerations and the sun's rays, the estimated Holocene termination will likely occur at 500 years from the present. The estimated duration of the glacial period that will follow this termination is about 36,000 years based upon the temporal duration of the precession index wave packet of Figure 12. After this period, there will likely be another increase in temperature, but the magnitude cannot be determined based solely on the partition model. To accomplish that would require a detailed climate model that consistently reproduces the features of the paleoclimate data over the last 800,000 years, which is far beyond the scope of this paper.

In terms of discrepancies, the comparison between the partition model predictions and EDC data indicates two interglacial inception timing issues. There are inception delays associated with MIS 18d and 13c (see Parrenin et al., 2007 for similar discrepancies between LR04 Benthic and EDC datasets); however, these may be due to physical effects related to the timing inferred from deep ice cores. Nevertheless, the considerable consistency of the PI and O waves predicted by the partition model over 800,000 years with data should motivate further examination of the timing inferred from EDC deep ice cores.

Finally, the consistency of the partition model predictions makes the search for a common physical mechanism within the earth's climate system that causes temperature descents into glacial periods more compelling. It is likely that a cumulative climate effect occurs over an extended period (the next 500 years) that eventually tips the earth into a persistent temperature descent concurrent with the decline in precession carrier wave maxima. This trend very likely impairs recovery until there is a return to increasing precession carrier wave maxima as Figure 12 indicates. Identifying the specific physical mechanism that causes this descent is far beyond the scope of this paper. Nevertheless, the potential expansion of the cold air volume at northern latitudes due to significant declines in insolation over the last 11,100 years should be investigated as a possible cause. Given recurring PI wave packets and their correlation with interglacial and glacial periods over the last 800,000 years, the possible catastrophic consequences to the future of civilization from another ice age should provide ample motivation to intensify scientific research in this vitally important area.

Funding

None

Guest-Editor: Martin T. Hovland; Reviewer: anonymous

Acknowledgments

I would like to acknowledge numerous exchanges with Professor William H. Smith of Washington University, St. Louis, concerning Milankovitch Theory. I would especially like to thank Dr. Patrick Frank and Patrice Poyet for reading the manuscript and making numerous helpful suggestions that measurably improved the clarity and presentation of the results. I am also indebted to Bruce Bauer, Data Manager, World Data Service for Paleoclimatology and NOAA National Centers for Environmental Information (NCEI) Climatic Science and Services Division – Paleoclimatology Boulder, CO for providing the relevant paleoclimate datasets. Finally, I would like to express my gratitude to Dr. Jacques Laskar for directing me to the wonderful computational tool he and his colleagues created, which enabled all the computations in this paper.

Appendix A

This section aims to derive equations (8) and (9) using light rays and vector analysis. The sun's light rays hit the earth with uniform intensity at angles relative to tangential planes over the earth's surface. However, there is a point on the earth where the rays are perpendicular to a tangential plane, the subsolar point. As the earth rotates, this point moves westward and north and south due to the earth's obliquity and orbit in a wavelike pattern completing an entire cycle over a year.

For an observer at a point on the earth looking vertically, there is a component of a solar ray parallel to the vertical and another tangential. The vertical component is of interest in determining the obliquity contribution to the insolation, while the tangential component is assumed lost. The key quantity to determine is the time-dependent zenith angle between an observer vector pointing vertically and the declination vector pointing from the earth's center to the subsolar point. The partition model assumes that the cosine of this angle times an overall constant determines the obliquity contribution to the insolation. Because the observer and subsolar point move relative to the sun, the mean daily insolation is the average of the cosine of the zenith angle over daylight hours.

The relevant angles and vectors defined with respect to the earth's body fixed rotating axes are represented in the following diagram,

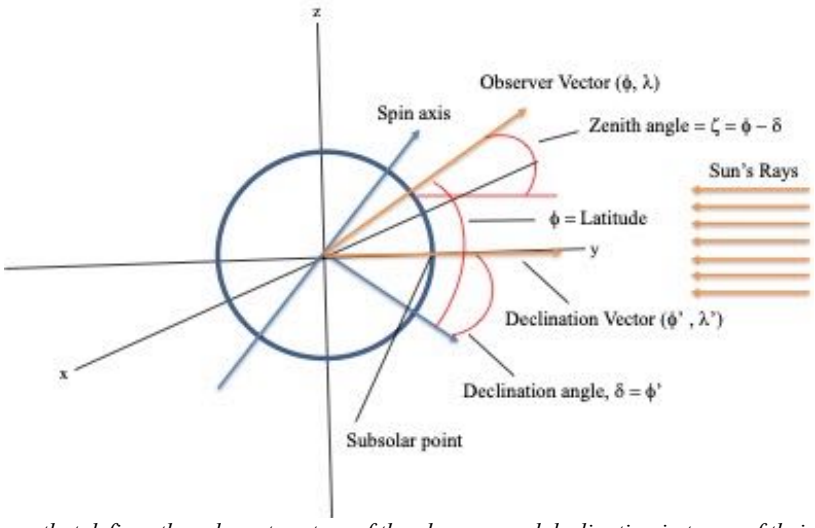

Figure 1A. A diagram that defines the relevant vectors of the observer and declination in terms of their latitudes and longitudes, (f , l) and (f'= d, l'), respectively defined with respect to rotating body fixed axes. The observer latitude and the declination angle, d, determine the zenith angle, z.

The observer unit vector in the rotating body-fixed frame is given by

$$\vec{V}_o = \cos(\emptyset) \cdot \cos(\lambda)\,\vec{\imath} + \sin(\phi) \cdot \cos(\lambda)\,\vec{\jmath} + \sin(\lambda)\,\vec{k}, \qquad (1A)$$

and the declination unit vector is given by

$$\vec{V}_\delta = \cos(\emptyset') \cdot \cos(\lambda')\,\vec{\imath} + \sin(\phi') \cdot \cos(\lambda')\,\vec{\jmath} + \sin(\lambda')\,\vec{k}, \qquad (2A)$$

where $\emptyset' = \delta$, the declination angle. The cosine of the zenith angle is simply the scalar product of equations (1A) and (2A) given by

$$\vec{V}_o \cdot \vec{V}_\delta = \cos(\zeta) = \sin(\phi) \cdot \sin(\delta) + \cos(\phi) \cdot \cos(\delta) \cdot \cos(h), \quad (3A)$$

where $h = \lambda' - \lambda$ is the hour angle, which for sunrise and sunset is determined by $cos(\zeta) = 0$ or

$$h_0 = cos^{-1}(-\tan(\emptyset) \cdot \tan(\delta)), \quad (4A)$$

which equals equation (9) for the summer solstice when $\delta = \theta$, the earth's obliquity angle.

For the partition model, we assume the obliquity contribution to the insolation during the summer solstice is of the form

$$B = G \cdot \big(sin(\phi) \cdot sin(\theta) + cos(\phi) \cdot cos(\theta) \cdot cos(h) \big) \quad (5A)$$

where G is an overall constant. The mean daily obliquity contribution to the mean daily insolation, $\bar{Q}$ of equation (2) is obtained by averaging equation (5A) over daylight hours given by

$$\bar{B} = \frac{G}{2 \cdot \pi} \cdot \int_{-h_0}^{h_0} (sin(\phi) \cdot sin(\theta) + \cos(\phi) \cdot cos(\theta) \cdot cos(h)) \; dh \quad (6A)$$

$$= \frac{G}{\pi} \cdot \big(h_0 \cdot \; sin(\phi) \cdot sin(\theta) + \cos(\phi) \cdot cos(\theta) \cdot sin(h_0) \big), \quad (7A)$$

from which equation (8) follows straightforwardly with h_0 determined by equation (4A) with $\delta = \theta$.

References

Berger, A., Loutre, M.F. and Crucifix M., The Earth's Climate in the Next Hundred Thousand Years (100 kyr), Surv. Geophys., Vol. 24, pp. 117–138, https://link.springer.com/article/10.1023/A:1023233702670, 2003.

Berger, A., Crucifix, M., Hodell, D.A, Mangili, C., McManus, J.F., Otto-Bliesner, B., Pol, K., Raynaud, D., Skinner, L.C., Tzedakis, P.C., Wolff, E.W., Yin, Q.Z., Abe-Ouchi, A., Barbante, C., Brovkin, V., Cacho, I., Capron, E., Ferretti, P., Ganopolski, A., Grimalt, J.O., Hönisch, B., Kawamura, K, Landais, A., Margari, V., Martrat, B., Masson-Delmotte, V., Mokeddem, Z., Parrenin, F., Prokopenko, A.A., Rashid, H., Schulz, M., and Vazquez Riveiros, N., Interglacials of the Last 800,000 Years, Rev. Geophys, Review Article, pp. 1-58, https://agupubs.onlinelibrary.wiley.com/doi/full/10.1002/2015RG000482, 2015.

Berger, W.H., Milankovitch Theory - Hits and Misses, Scripps Institution of Oceanography, Technical Report, pp. 1-35, https://escholarship.org/uc/item/95m6h5b9, 2012.

Gradstein, F., Ogg, J., and Smith, A., A Geologic Time Scale 2004, Cambridge University Press, Book, pp. 1-589, https://www.cambridge.org/core/books/geologic-time-scale-2004/ACED6139A9320FC9CA982E316FFF3E38, 2005.

Hays, J.D., Imbrie, John, and Shackleton, N.J., Variations in the Earth's Orbit: Pacemaker of the Ice Ages, Science, Vol. 194 (4270): pp. 1121–1132, https://www.science.org/doi/10.1126/science.194.4270.1121, 1976.

Huybers, P., Combined Obliquity and Precession Pacing of Late Pleistocene \Deglaciations, Nature, Vol. 480, pp. 229–232, https://www.nature.com/articles/nature10626, 2011.

Imbrie, J., Astronomical Theory of the Pleistocene Ice Ages, Icarus, Vol. 50 (2-3), pp. 408-422, https://www.sciencedirect.com/science/article/abs/pii/0019103582901324, 1982.

Imbrie, J., and Imbrie, K. P., Ice Ages: Solving the Mystery, Harvard University Press, Book, pp.1-224, https://www.hup.harvard.edu/catalog.php?isbn=9780674440753, 1986.

IMCCE, Virtual Observatory Solar System Portal, CNRS Observatory, Paris, http://vo.imcce.fr/insola/earth/online/earth/online/index.php, 2018. Numerical calculations in this paper make considerable use of data generated from this computational tool.

Jouzel, J., A Brief History of Ice Core Science over the Last 50 Years, Clim. Past, Vol. 9, pp. 2525-2547, https://cp.copernicus.org/articles/9/2525/2013/, 2013.

Laskar, J., Robutel, P., Joutel, F., Gastineau, M., Correia, A.C.M., and Levrard, B., A Long-Term Numerical Solution for the Insolation Quantities of the Earth, Astron. Astrophys., Vol. 428, pp. 261-285, https://www.aanda.org/articles/aa/full/2004/46/aa1335/aa1335.html, 2004.

Lawrence, Z.D., Perlwitz, J., Butler, A.H., Manney, G.L., Newman, P.A., Lee, S.H., and Nash, E.R., The Remarkably Strong Artic Stratospheric Polar Vortex of Winter 2020: Links to Record Breaking Arctic Oscillation and Ozone Loss, J. Geophys. Res.-Atmos., Vol. 125, pp. 1-21, https://doi.org/10.1029/2020JD034190, 2020.

Lisiecki, LE. and Raymo, M.E., A Pliocene-Pleistocene Stack of 57 Distributed Benthic $\delta^{18}O$ Records, AGU Paleoceanography and Paleoclimatology, Vol. 20 (PA1003), pp.1-17, https://agupubs.onlinelibrary.wiley.com/doi/epdf/10.1029/2004PA001071, 2005.

Lisiecki, L., Links between Eccentricity Forcing and the 100,000-Year Glacial Cycle, Nature Geoscience, Vol. 3, pp. 349–352, https://www.nature.com/articles/ngeo828, 2010.

Meyers S.R., Sageman B.B., and Pagani M., Resolving Milankovitch: Consideration of Signal and Noise, Am. J. Sci., Vol. 308 (6), pp. 770-786, https://www.ajsonline.org/content/308/6/770, 2008.

Milankovitch, M., Canon of Insolation and the Ice-Age Problem, Royal Serb. Acad., Spec. Publ., pp. 1-634, https://www.amazon.com/Insolation-Ice-Age-Problem-Milankovic-Milankovitch/dp/8617066199, 1998.

NCEI, EPICA Dome C – 800KYr Deuterium Data and Temperature Estimates, https://www.ncei.noaa.gov/access/paleo-search/study/6080, 2007.

Parrenin, F., Barnola, J.-M. , Beer, J., Blunier, T., Castellano, E., Chappellaz, J., Dreyfus, G., Fischer, H., Fujita, S., Jouzel, J., Kawamura, K, Lemieux-Dudon, B., Loulergue, L., Masson-Delmotte, V., Narcisi, B., Petit, J.-R., Raisbeck, G., Raynaud, D., Ruth, U., Schwander, J., Severi, M., Spahni, R., Steffensen, J.P., Svensson, A., Udisti, R., Waelbroeck, C., and Wolff, E.W., The EDC3 Chronology for the EPICA Dome C Ice Core, Clim. Past., Vol. 3, pp. 485-497, Figure 3, pp. 491, https://cp.copernicus.org/articles/3/485/2007/, 2007.

Roe, G., In defense of Milankovitch, Geophysical Research Letters, Vol. 33 (L24703), https://agupubs.onlinelibrary.wiley.com/doi/abs/10.1029/2006GL027817, pp. 1-5, 2006.

Rohling, E.J., Braun, K., Grant, K., Kucera, M., Roberts, A.P., Siddall, M, Trommer, G., Comparison between Holocene and Marine Isotope Stage -11 Sea Level Histories, Earth Planet. Sc. Letters, Vol. 291 (1-4), pp. 97–105, https://www.sciencedirect.com/science/article/abs/pii/S0012821X1000018X?via%3Dihub, 2010.

Vavrus, S.J., He, F., Kutzbach, J.E., Ruddiman, W.F., and Tzedakis, P.C., Nature: Scientific Reports, Vol. 8 (10213), pp. 1-12, https://www.nature.com/articles/s41598-018-28419-5, 2018.

Wunsch, C., Quantitative Estimate of the Milankovitch-Forced Contribution to Observed Quaternary Climate Change, Quaternary Sci, Rev., Vol. 23 (9-10), pp. 1001-1012, https://www.sciencedirect.com/science/article/abs/pii/S0277379104000575, 2004.

Zachos, J., Pagani, M., Sloan, L., Thomas, E., and Billups, K., Trends, Rhythms, and Aberrations in Global Climate 65Ma to Present, Science, Vol. 292(5517), pp. 686-693, https://www.science.org/doi/abs/10.1126/science.1059412, 2001.

Clear Thinking About Atmospheric CO_2

Correspondence to
David.andrews@umontana.edu
Vol. 3.1 (2023)
pp. 33-45

David E. Andrews

Department of Physics and Astronomy (retired)
University of Montana
Missoula, MT, USA

Abstract

Several articles have been published in this journal purporting to show that the well-documented rise in atmospheric CO_2 is a natural phenomenon rather than human caused. This note reviews the overwhelming case that human activities are the cause. It identifies specific misunderstandings about the carbon cycle and errors in the interpretation of radiocarbon data contained in these papers. Most importantly, misconceptions about the conclusions that can and cannot be drawn from the present composition of the atmosphere are highlighted.

Keywords: carbon cycle; net global uptake; radiocarbon; bomb pulse; isoflux

Submitted 03-12-2022, Accepted 06-02-2023. https://doi.org/10.53234/scc202301/20

1. Introduction

A cornerstone of the argument that humans are responsible for climate change is the consensus among climate scientists that human activities such as the burning of fossil fuels have caused the rise of atmospheric CO_2 concentration during the Industrial Era, all of it. This is perhaps the most well-established piece of the case for anthropogenic global warming. Yet a few dissenters continue to argue that natural sources are the primary cause of the increase. Papers in Science of Climate Change such as (Harde and Salby 2021), (Berry 2021), and (Schroder 2022), and in Health Physics (Skrable et al. 2022a; 2022b) conclude that human emissions have made a relatively small contribution. While these papers have no impact on mainstream climate science, they may confuse lay readers who read their conclusions but do not have the tools to critically analyze them. Most active climate scientists ignore such papers if they are even aware of them. But this author believes that it is a mistake to allow misconceptions and errors go unchallenged. The errors need to be clearly spelled out in front of those same lay audiences, to ensure that the development of public policy is based on sound science. The arguments made here are limited to the question of responsibility for atmospheric CO_2 increases and are not original with the author.

A simple and compelling argument that human emissions, not natural sources, have caused the increase will be presented in Section 2. But that will still leave the question of how these authors came to their mistaken conclusions. It will be unnecessary to scrutinize details of their individual calculations because they share a common misconception discussed in Section 3. The quantity that all the papers attempt to calculate, or infer from data, is the fraction of carbon in the present atmosphere that was once contained in a fossil fuel. They call this the "human contribution", or the "fossil component", or "the fraction due to fossil fuel burning". Although at first glance this quantity seems to be a valid measure of human impact, in fact it is not. As we will see, the dynamic atmosphere is more subtle. Finally, in an Appendix, we discuss the misanalysis of radiocarbon data. Errors in earlier papers (Berry 2019) and (Harde 2017; 2019) have been noted before (Andrews 2020). The modified model of (Harde and Salby 2021), an attempt to correct

Harde's earlier mistake, is not credible.

2. Human Emissions Cause the Increase

I cite the results of (Ballantyne et al. 2012) who combine all land and sea reservoirs both for simplicity and to avoid uncertainties in the magnitude of changes in individual non-atmospheric reservoirs. Very good measurements are in hand of total atmospheric carbon accumulation between 1960 and 2010. Ballantyne uses CO_2 concentration data from a network of approximately 40 marine boundary sites (the NOAA/ESRL flask network) and converts to pentagrams of carbon in the total atmosphere with the factor 2.124 PgC/ppm. The uncertainty quoted takes into account sampling errors. Good estimates of human emissions are also in hand. Ballantyne uses emission data from the Carbon Dioxide Information Analysis Center, BP, and the Emissions Database for Global Atmospheric Research. Carbon conservation then yields a good estimate of "Net Global Uptake" during that period. Ballantyne's Figure 2 numbers are shown schematically in Figure 1 below.

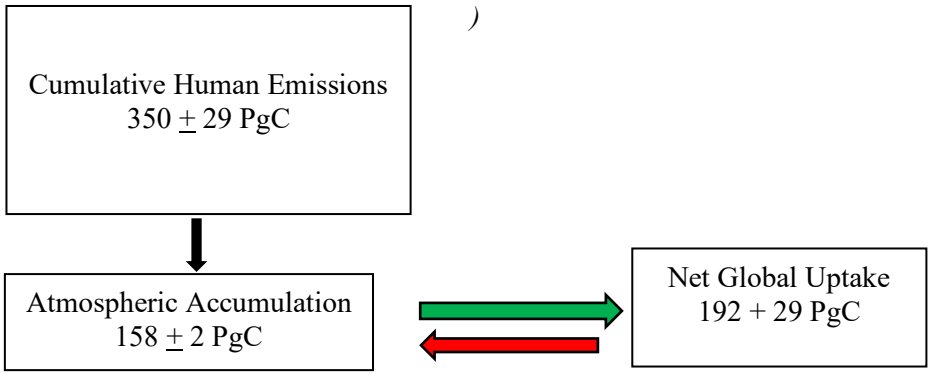

Fig 1: Total carbon changes 1960-2010 from Ballantyne (2012)
(1 PgC = 1 billion metric tons of carbon)

The positive Net Global Uptake for this period is the *net* quantity of carbon that has moved from the atmosphere into land/sea reservoirs. It is the difference between much larger gross exchanges in both directions. Differences between large, similar numbers usually contain large errors, but in this case carbon conservation allows Net Global Uptake to be determined more accurately than either gross exchange. The qualitative observation that humans have put more carbon into the atmosphere than has remained applies not only to the fifty-year span shown, but throughout the Industrial Era, and is seen in the Mauna Loa data sets used by most authors.

Because the carbon from human emissions during this period exceeds the rise in atmospheric *total carbon*, we know immediately that land and sea reservoirs together have been net sinks, not sources, of *total carbon* during this period. We can be sure of this without knowledge of the detailed inventory changes of individual non-atmospheric reservoirs. This is not a model dependent result. It is a simple statement based on carbon conservation, data on emissions and atmospheric levels, and arithmetic. Note that this conclusion contains no assumption whatsoever about the constancy of natural carbon in this period. In fact, the primary conclusion of Ballantyne is that non-atmospheric natural reservoirs have, during the 50-year period studied, not only increased their carbon inventory, they have also increased the rate at which they are doing so in response to the higher atmospheric levels. Nor does the conclusion rely on treating "human" and "natural" carbon differently as (Harde and Salby 2021) and (Berry 2021) both allege. Net Global Uptake is simply what is left over after atmospheric accumulation has been subtracted from total emissions. If more carbon was injected into the atmosphere by human activities than stayed there, it had to have gone somewhere else. It is also a statement that has been made many times before (Cawley 2011); (Richardson 2013); (Denning et al. 2022).

The red arrow in Figure 1 represents processes which transfer carbon from land/sea inventories to the atmosphere: outgassing of oceans, outgassing of freshwater ponds, decay of vegetation, human breathing, even volcanos. (Ballantyne attributes a temporary stabilization of Net Global Uptake in the 1990's to the eruption of Mt Pinatubo in 1991, among other things.) (Schroder 2022), like (Harde and Salby 2021), speculates that outgassing from oceans due to temperature increases is a major factor in atmospheric CO_2 rise. *The data in Figure 1 falsify this hypothesis*. Processes like outgassing are part of the carbon *cycle* and are accompanied by processes by which carbon is transported from the atmosphere to the oceans, represented by the green arrow. Discussing credits without discussing debits is bad accounting. The green arrow includes the dissolution of CO_2 in the oceans and freshwater ponds, and photosynthesis. If the rates of natural outgassing-like processes (red arrow) were exceeding the rates of natural processes by which carbon is removed from the atmosphere to land/sea reservoirs (green arrow), then they would cause Atmospheric Accumulation to exceed Cumulative Human Emissions, making Net Global Uptake negative. The data for the period 1960-2010 cited by Ballantyne clearly say otherwise. If outgassing-like processes were important sources of new carbon that had not been in the atmosphere in recent centuries, then they would have a radiocarbon signature showing that. They do not.

Ballantyne chose to study a limited 50-year period with the best data in order to understand how the natural sinks were changing with time. During this period, Net Global Uptake was always positive. This has not always been the case. For example, 56 million years ago natural processes caused atmospheric CO_2 to increase by about 10,000 GT over a period of several thousand years. (Voosen 2022). Since human emissions were zero 56 million years ago, Net Global Uptake was then clearly negative. Natural non-atmospheric carbon reservoirs were then net sources, unlike in the present era. The present anthropogenic sources are an order of magnitude larger.

We note that (Beck 2022) presents a record of atmospheric CO_2 levels in the first half of the 20th century that differs markedly from the US Energy Information Administration data set used by most authors (EIA 2022.) Beck assembled this record from observations at multiple locations, by multiple researchers using multiple techniques. This author has no insight into reasons for the discrepancy between the two records. The Beck record shows a substantial rise in atmospheric CO_2 between about 1920 and 1940, a rise which exceeds anthropogenic emissions in that period. Therefore, Net Global Uptake was negative in those years according to the Beck record, though it was positive according to the EIA record. In the Beck record, CO_2 levels then fall rapidly from 1940 to 1950. No reason is given for the change in the sign of Net Global Uptake, i.e, for the sudden switch around 1940 of natural reservoirs from sources to sinks. Both data sets agree that averaging over the entire period from 1900 to 1960, anthropogenic emissions exceeded atmospheric CO_2 rise and natural reservoirs were net sinks. It is worth remarking that over 70% of the CO_2 rise in the Industrial Era has occurred since 1960, a period in which Beck does not challenge EIA data, and a period in which natural reservoirs have clearly been sinks. This is the period which is depicted in Figure 1.

In their quest to determine the fraction of anthropogenic carbon in the present atmosphere Harde and Salby, Berry, and Schroder focus on anthropogenic and natural carbon separately. This complicates their analysis and they miss the simple conclusions made here. What they do find is that natural carbon is accumulating in the atmosphere faster than human carbon, *and indeed it is!* Nothing in the analysis presented here conflicts with this fact. We will see in Section 3 why this happens. Anthropogenic carbon can be the cause of the entire Industrial Age increase without being a large part of the present atmospheric composition. Of course, it is the *total* atmospheric carbon that impacts climate, and the above analysis leaves no doubt where the increase in the total is coming from. Tracking anthropogenic carbon separately from natural carbon is a distraction, which is why few papers in the serious peer-reviewed literature do so.

As a final comment for this section, note that a positive Net Global Uptake is not only measured, but also completely expected. The higher partial pressure of CO_2 in the atmosphere in 2010 compared to 1960 leads, by Henry's Law, to higher carbonate concentrations in the oceans. Ocean acidification has been observed and confirms what Net Global Uptake tells us: the primary

reservoir, the oceans, have on balance globally been taking in net carbon, even while outgassing net carbon at some locations. Natural processes mitigate anthropogenic caused CO_2 rise; they do not enhance it.

3. Why "Natural Carbon" accumulates in the atmosphere over "Human Carbon"

3.1 The concept of isofluxes

The two-way carbon exchanges between the atmosphere and other reservoirs shown in red and green in Figure 1 are each much larger than their difference which Net Global Uptake measures. In other words, the flows in either direction are almost balanced, though a small net excess flows out of the atmosphere. What some do not necessarily appreciate is the consequence of these balanced two-way exchanges. Balanced exchanges are equivalent to simple mixing. Carbon in the atmosphere mixes with carbon in the oceans in the course of dissolving in one place and outgassing in another.

Because of the mixing, composition differences between the carbon inventories of different reservoirs tend to decrease. This is no different than say, pouring 30% of an alcohol and water mixture back and forth between two containers. If Container A started with a higher alcohol concentration than Container B, after several transfers the two concentrations will have become more equal. Even with no net exchange of liquid, a net exchange of alcohol between containers will have occurred. In the same way, even with little or no net exchange of carbon between the atmosphere and oceans, a substantial net exchange of, for example ^{14}C can occur. The phenomenon of isotope flow between reservoirs by this process has a name among specialists: isotope disequilibrium fluxes or "isofluxes" (Levin et al. 2010). The direction of the isoflux flow always tends to reduce the composition difference between the two reservoirs. It is simply about mixing.

3.2 Understanding the bomb pulse with isofluxes

We can illustrate the workings of isofluxes by looking at some atmospheric ^{14}C data. Figure 2 shows two measures of atmospheric radiocarbon from 1920 to 2015. The line in green is of "$\Delta^{14}C$" (left axis), the standard variable by which the ^{14}C community presents data, from 1915 to 2015. Only northern hemisphere data from (Graven et al. 2017) is shown, to align with the data used by (Harde and Salby 2021). The most prominent feature of this graph is the "bomb pulse", the dramatic increase in atmospheric ^{14}C from atmospheric nuclear testing in the 1950's and early 1960's, before the 1963 Test Ban Treaty. Clearly this perturbation presents an opportunity to learn about exchange processes.

$\Delta^{14}C$ measures the fractional deviation of the *specific activity* of a sample from a standard, in parts per thousand (‰):

$$\Delta^{14}C = 1000\left[\frac{A_{measured}}{A_{standard}} - 1\right] \quad (1)$$

That is, it describes what *fraction of the carbon* in a sample is ^{14}C. It does not, in general, measure the concentration of ^{14}C i.e., the *fraction of the sample* that is ^{14}C. It can be used as a proxy for concentration only when the total carbon in a sample is fixed, as it is in a liter of oxalic acid. The $^{14}C/^{12}C$ ratio (or $^{14}C/C_{total}$) is not only what is most directly measured, but also what is useful for ^{14}C dating. The standard used depends on the measurement technique. Common $A_{standards}$ are 226 Bq/kgC or 1.176×10^{-12} mole^{14}C/moleC. [See (Stuiver and Polach 1977), (Stenstrom et al. 2011), (Andrews 2020).]

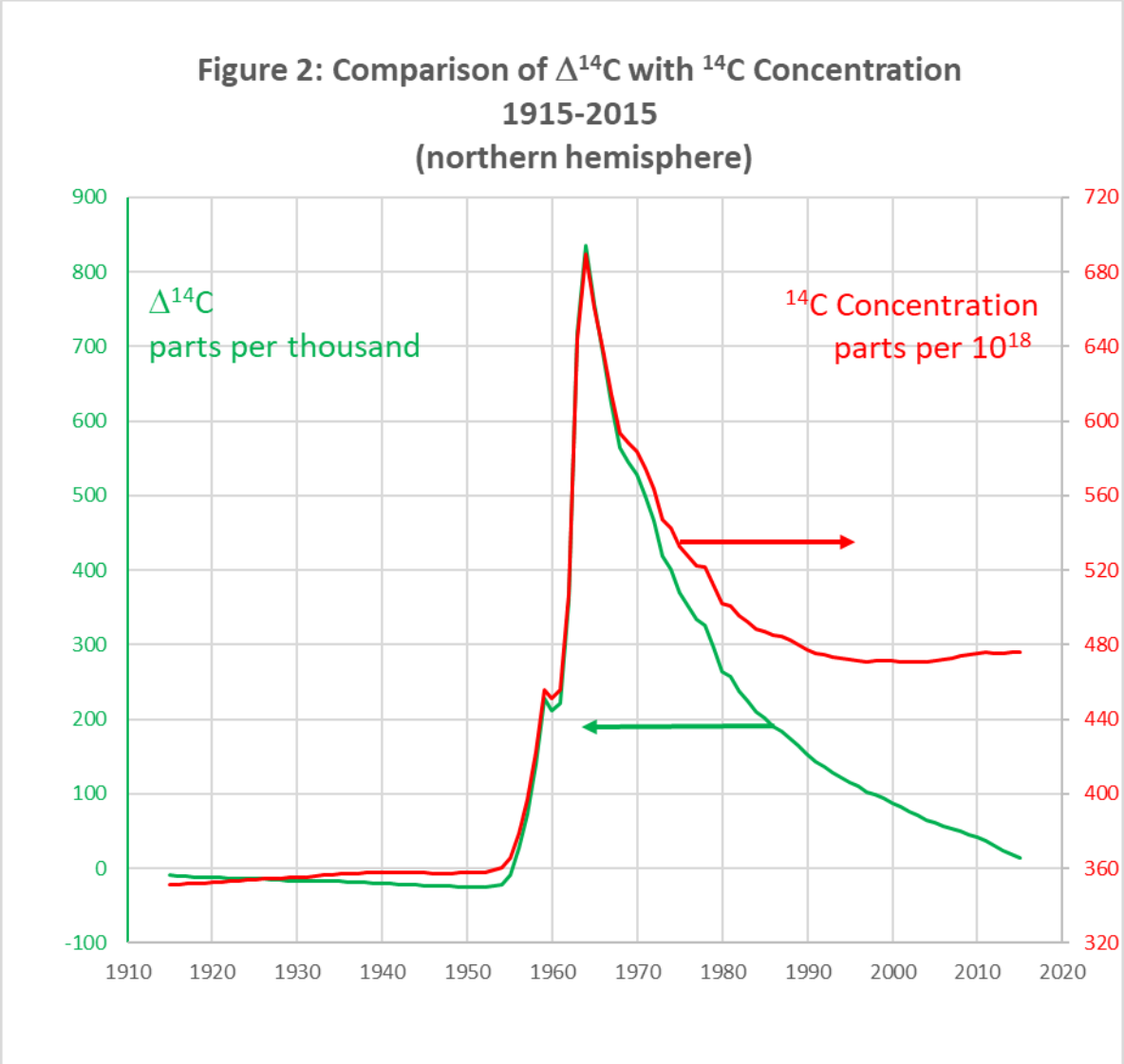

Fig 2. Northern Hemisphere Atmospheric Radiocarbon 1915-201. $\Delta^{14}C$ measures the fraction of carbon in a sample that is ^{14}C compared to a standard. ^{14}C Concentration is the molar fraction of the atmosphere which is ^{14}C.

Figure 2 also shows in red the atmospheric ^{14}C *concentration* (right axis) during the same period, calculated from the same $\Delta^{14}C$ and data on total atmospheric carbon concentration from the US Energy Information Administration (EIA 2022). After the "bomb pulse", the ^{14}C concentration did not return to its 1950 value. It remained about 30% higher.

While nuclear testing was increasing the specific activity of the atmosphere, the "Suess effect" was decreasing it. ^{14}C is naturally produced in the upper atmosphere from cosmic rays at a more or less steady rate, and carbon cycle processes distribute it to the oceans and biosphere. (See the Appendix for a discussion of small variations in the natural production rate of ^{14}C.) Because the half-life of ^{14}C is about 5730 years, fossil fuel carbon which has been isolated from the atmosphere for much longer times is essentially devoid of ^{14}C; it is "cold". When released into the atmosphere by fossil fuel burning, this cold carbon reduces the specific activity (measured by Bq/kgC or by the $^{14}C/C_{tot}$ ratio) by simple dilution. This effect was noticed in (Suess 1955). Wood produced in 1950 had lower specific activity than wood produced in 1900 because of the presence of cold anthropogenic carbon in the atmosphere, diluting the cosmic-ray-produced component and potentially complicating ^{14}C dating.

Using the concept of isofluxes caused by two-way exchanges (mixing), we can understand fine details of both $\Delta^{14}C$ and concentration shown in Figure 2:

- From 1915 until the early 1950's, the addition of anthropogenic cold carbon into the atmosphere by fossil fuel burning lowered $\Delta^{14}C$ via the Suess effect, as shown by the slightly decreasing green curve. With $^{14}C/C_{tot}$ now lower in the atmosphere than in the oceans, an isoflux of ^{14}C moved from the oceans to the atmosphere, causing a small but clear rise in the red curve during the same period. This is perhaps a first hint that exchange processes cause subtle effects: *adding cold carbon to the atmosphere ended up increasing its ^{14}C concentration!*
- The atmosphere was left with a much higher $^{14}C/C_{tot}$ than the oceans after the bomb testing ceased. Mixing between the atmosphere and other reservoirs by two-way exchanges brought both measures of atmospheric radiocarbon down between 1965 and 1990. The characteristic time for the mixing can be seen to be about one decade.
- While two-way exchanges were diminishing the "bomb pulse", anthropogenic cold carbon was being added to the atmosphere. Eventually, around 2000, $^{14}C/C_{tot}$ in the atmosphere was again less than it was in the oceans for the first time since the early 1950's. The isotope gradient had reversed sign. This again caused a net flow, an isoflux, of ^{14}C from the oceans to the atmosphere. The red curve began increasing again, just as it had between 1915 and 1950.

The narrative here is qualitative, but quantitative analyses have been performed by (Caldiera et al.1998), and more recently by (Graven et al. 2020). The Caldeira analysis preceded and anticipated the rise in ^{14}C concentration beginning about 2000. Successful predictions are the hallmark of good science.

3.3 Applying the isoflux concept to "human" and "natural" carbon

If we think of human (anthropogenic) and natural (all other) carbon as two types of carbon whose fraction can be different in different environmental reservoirs, not unlike the situation with isotopes, then the concept of mixing via two-way balanced exchanges can be applied. The net result of exchanges will again be a tendency to reduce differences between the human fraction in the atmosphere and the human fraction in the other reservoirs. Fossil fuel burning creates an excess of anthropogenic carbon in the atmosphere's composition, compared to land and sea. The "isoflux-like" flows will therefore move natural carbon into the atmosphere and human carbon out of it.

We can make a rough quantitative estimate of what these flows do to the atmospheric composition. From the bomb pulse data, we know the mixing time is about one decade. Were human emissions to abruptly stop, isoflux-like flows would cause the atmospheric human fraction to approach the land/sea human fraction, a quite small number, in a couple of decades. Therefore, it is the last decade's worth of human emissions, which have yet to be diluted from exchange processes, which dominate the present value of the atmosphere's "human component."

3.4 Measuring and interpreting the human component of atmospheric CO_2

This rough estimate of the present human component can be corroborated by data on the present specific activity of the atmosphere. (Skrable et al. 2022a)'s initial analysis of this was compromised by wrong input data for the specific activity and a lack of appreciation of the lingering effects of bomb carbon. In a follow-up paper, (Skrable et al. 2022b) used for the specific activity record a "no bomb scenario" model developed by (Graven et al. 2020). Although this means that the input data used is itself model dependent, that is of no concern here. The Skrable papers developed a simple formula to measure the human carbon fraction of the atmosphere in any year, based on the observed magnitude of the Suess effect. They take the 2018 "no bomb scenario" atmosphere to contain a mixture of cold carbon ($\Delta^{14}C = -1000$) and carbon with $\Delta^{14}C = 0$. (Had

no nuclear testing occurred, the 2018 value of $\Delta^{14}C$ would be -.130 in Graven et al.'s "no bomb scenario".) This leads to Skrable et al.'s inferred measurement via isotope analysis of what they call the "fossil fraction". This quantity is what Berry, Harde and Salby, and Schroder attempt to calculate. This is the quantity that (Segalstad 1992) inferred from ^{13}C data. These authors all equate this fraction to the fraction of human responsibility for CO_2 increase.

The number (Skrable et al. 2022b) get for the fossil component in 2018 is 321 GT CO_2, (87 GT C). This is 32% of the atmospheric carbon increase since 1750, motivating them to declare it to be "much too low to be the cause of global warming". *But they ignored mixing from two-way, nearly balanced exchanges in jumping to this conclusion* (Schwartz et al. 2022), (Andrews 2022) It is noteworthy that the 321 GT CO_2 number they get is quite comparable to the 346 GT CO_2 of human emissions in the years 2009-2018, the last decade of their data set. All that they have really measured is the anthropogenic carbon emitted in roughly the past decade. That is about all the information that can be extracted from the present atmospheric composition. Mixing has obscured the earlier history. But that is no problem. We learned in Section 2 why atmospheric CO_2 is increasing.

The Skrable analysis illustrates that the measured Suess effect is substantially smaller than it would have been without isofluxes. This was noted by Suess himself: "The decrease [in specific activity] can be attributed to the introduction of a certain amount of C^{14}-free CO_2 into the atmosphere by artificial coal and oil combustion *and to the rate of isotopic exchange between atmospheric CO_2 and bicarbonate dissolved in the oceans*" [italics added]. In the same paper Suess began the rich history of using radiocarbon to learn about atmospheric processes when noting "the rate by which this CO_2 exchanges must be greater than previously assumed" (Suess 1955).

3.5 A helpful analogy

We have seen that the statement "Human carbon in the present atmosphere is only 30% of the Industrial Age increase" is not the same as "Human emissions caused only 30% of the increase." As the disconnect between current inventories and fundamental causes is subtle, an analogy may be helpful for understanding it. (Cawley 2011) proposed a good one, worth repeating verbatim here:

"Consider a married couple, who keep their joint savings in a large jar. The husband, who works in Belgium, deposits six euros a week, always in the form of six one-euro coins minted in Belgium, but makes no withdrawals. His partner, who works in France, deposits 190 euros a week, always in the form of 190 one-euro coins, all minted in France. Unlike her husband, however, she also takes out 193 euro per week, drawn at random from the coins in the jar. At the outset of their marriage, the couple's savings consisted of the 597 French-minted one-euro coins comprising her savings. Clearly, if this situation continued for some time, the couple's savings would steadily rise by 3 euros per week (the net difference between total deposits and withdrawals). It is equally obvious that the increase in their savings was due solely to the relatively small contributions made by the husband, as the wife consistently spent a little more each week than she saved."

Cawley goes to the trouble of showing with a Monte Carlo simulation that, after some time, Belgian coins make up only 3% of the inventory, even though they accounted completely for the savings increase. In a like manner human carbon, while a relatively small percentage of carbon in the present atmosphere, is completely responsible for the increase. A net sink of total carbon can raise natural carbon levels elsewhere, but it cannot raise total carbon levels elsewhere.

4. Summary

Since this article was first drafted, (Harde and Salby 2022) has been published. Unfortunately the newer paper contains the same fatal flaws as the earlier papers already discussed. We can use it to summarize those flaws:

- (Harde and Salby 2022) focuses on tropical temperature dependent outgassing, a regional

analysis. No doubt it contains some insights. But like the other papers critiqued it ignores the well-established fact that Net *Global* Uptake is solidly positive in the current era as the authors should know. All credible models need to be constrained by this simple observation.

- (Harde and Salby 2022) correctly notes that natural emissions and absorptions approximately balance. The mixing that results surely modifies isotope distributions as discussed in Section 3. Isoflux effects explain and dominate the evolution of ^{14}C distributions, both specific activity and concentration, over the last 100 years as described in Section 3.2. Isoflux effects can change carbon isotope distributions without changing total carbon distributions. These authors ignore them and mistakenly believe that total carbon changes mimic isotope changes. See the appendix for further criticism of the radiocarbon model of these authors.

Scientific progress depends upon original ideas challenging the consensus. Scientific progress also relies on the use of empirical data to weed out ideas that may be original but are also just plain wrong. That progress is helped when the originators of the wrong ideas acknowledge their errors and find constructive ways to contribute. That does not always happen, and it is not happening in the present case. The unconventional ideas critiqued here have been around for well over a decade. It should not have been necessary for this article to refer to a 2011 paper to, once again, refute them.

As an example of authors' clinging to old and discredited ideas, we will describe (Harde and Salby 2021)'s attempt to salvage Harde's model by designing (inventing?) a background to transform the true concentration curve (red in Figure 2) to the curve they originally thought was the concentration (green in Figure 2). As the analysis here is not part of the main argument of this paper, it is relegated to an appendix. For a credible model of the evolution of the bomb pulse, see Section 3.2 or the quantitative and peer-reviewed analyses cited.

Appendix: Clinging to wrong ideas: the radiocarbon model of Harde and Salby

The two curves in Figure 2 describing atmospheric radiocarbon history were confused by (Berry 2019) and by (Harde 2017;2019), as pointed out by (Andrews 2020). They wrongly believed that concentration had followed the green curve rather than the red curve. Theories built around the false belief that concentration had returned to its pre-bomb test value now had to explain why, after initially falling quickly after atmospheric nuclear testing ended, ^{14}C concentration had since roughly stabilized 30% or more above the pre-1950 plateau that had persisted for centuries. If the ~30% increase does not include lingering bomb carbon as it certainly appears to, what caused it? (Berry 2021) does not address this obvious question, though he drops the many references to ^{14}C data contained in (Berry 2019). (Harde and Salby 2021) recognize their need to address the baseline shift, because (Harde 2019) had used ^{14}C data, wrongly interpreted, to supposedly validate his questionable model.

(Harde and Salby 2021) follows (Harde 2019) in hypothesizing that not only the flow of carbon from atmosphere to oceans, but the fast cycle flow in the other direction, from the oceans to the atmosphere, also depends only on the carbon concentration *in the atmosphere* (!?) They put this into their model through their Equation 6: $e_{R,14} = \beta\ C_{14}/\tau$ This term represents the rate of reemission to the atmosphere of ^{14}C that has been taken up by, say, the ocean. Since β and τ are treated as constants determined from fits in this analysis, equation 6 asserts that reemission is proportional to C_{14}, the concentration *in the atmosphere*. The higher the concentration in the atmosphere, say Harde and Salby, the higher the flow *into it*. This conjecture defies common sense, but its consequences to Harde and Salby's analysis are clear. If the flows both to and from the atmosphere were indeed each proportional to atmospheric concentration, then the net flow would also be proportional to atmospheric concentration, and a single time constant exponential function would of course describe the net exchange, as it does in their model.

(Harde and Salby 2021) treat showing that ^{14}C concentration fell with a simple exponential form

as the crucial empirical question. To transform the red curve in Figure 2 to the green curve, their solution is to postulate new sources of atmospheric ^{14}C that started after about 1964. These are the components of the $e'_{NB,14}(t)$ term in their Equation 10. From their fits to the concentration data assuming an effective time constant of 10 years, they arrive at an evaluation of its magnitude:

$$e'_{NB,14(t)} = 123\ ‰/yr + .3\ ‰/yr^2 \times (year - 1990) \quad \text{valid after 1964} \qquad (2)$$

They chose to express concentration as a dimensionless variable showing deviation from a standard, analogous to the definition $\Delta^{14}C$. We will put this into a more transparent form for comparison with other studies. Since a $\Delta^{14}C$ standard is 1.176×10^{-12} (moles ^{14}C)/ (moles of total C) and taking 315.8 ppm as the total CO_2 abundance in 1959 (Harde and Salby's chosen year to define a standard) their ^{14}C concentration standard is 371.4×10^{-12} ppm. Taking the total atmosphere to contain 1.77×10^{20} moles, then this standard can also be expressed as 65.71 kmoles of ^{14}C. The emission rate in (2) is then equivalent to:

$$e'_{NB,14(t)} = 8.08\ kmoles/yr + .0197\ kmoles/yr^2 \times (year - 1990) \quad \text{valid after 1964} \qquad (3)$$

From Figure 2 we see that prior to 1950, the atmospheric abundance of ^{14}C was approximately constant around 355×10^{-12} ppm. If it is removed with an effective time constant of 10 years, as Harde and Salby argue, then its production rate needs to be 35.5×10^{-12} ppm/year, or 6.28 kmoles/year. (The equilibrium level equals the time constant times the emission rate.) So Harde and Salby would say:

$$e'_{NB,14(t)} = 6.28\ kmoles/yr \quad \text{before 1964 (assumes their 10 yr time constant)} \qquad (4)$$

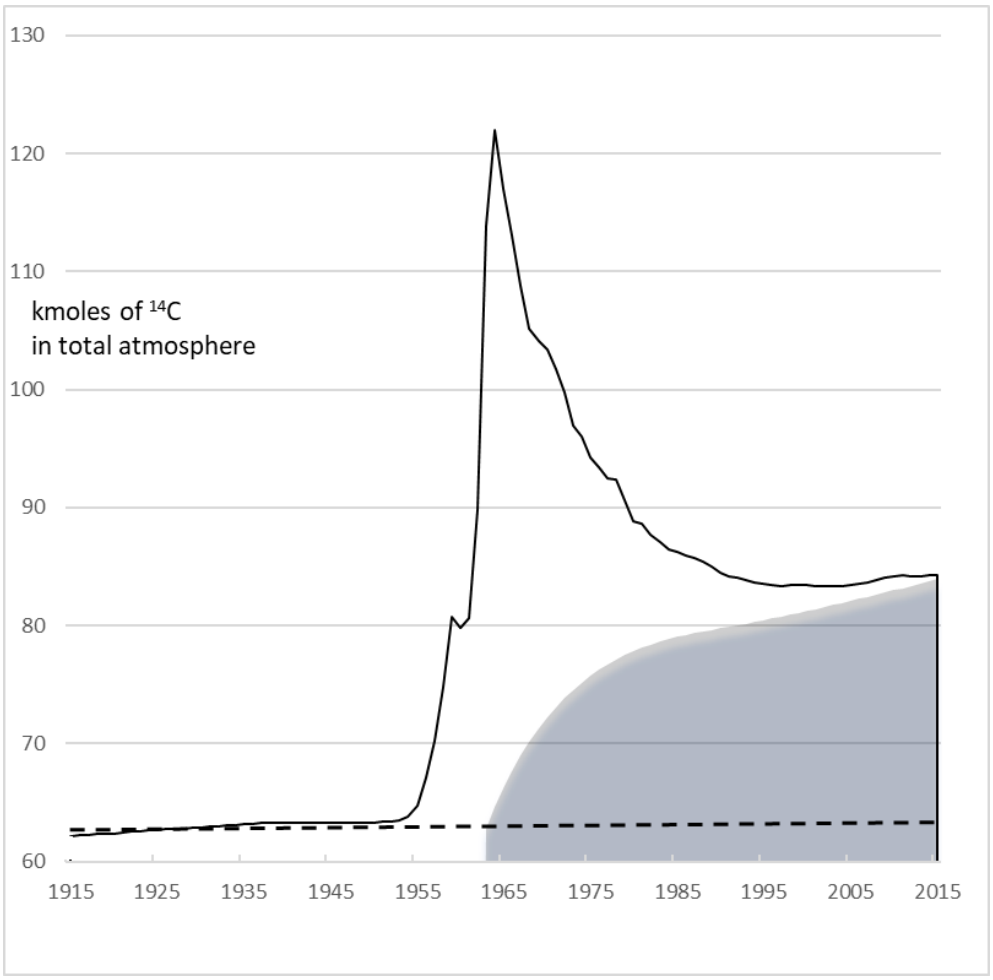

Fig 3 The Engineered Background of Harde and Salby

Figure 3 shows the now familiar bomb pulse concentration curve. This is the same data as in Figure 2, but with the y axis now converted to kmoles in the total atmosphere, and with the background generated by Harde and Salby's emission function (3) shown as the shaded areas. The dashed line is the background level generated by emission function (4), based on the pre-test data. As in Harde and Salby's model, the background is being depleted with a 10-year time constant. It is maintained at the emission rate (4) until (3) switches on in 1964. The new postulated sources increase the background towards a new equilibrium level of 80.8 kmoles. Then in 1990 the linearly increasing "cosmic ray term" in (3) switches on.

To defend their model, Harde and Salby needed to show that the bomb pulse abundance had fallen to near 0 by 2015, some 4 of their 10-year time constants after cessation of testing. They did this by engineering the background to be essentially the same as the data in 2015, as shown. The difference between the solid line and the shaded area is, they say, the real signal, not the difference between the solid line and the dashed line. But (Harde 2019) used the dashed curve as the background. (Harde and Salby 2021) say that the new background accounts for nuclear power plant emissions, continued nuclear testing, and a change in the natural background. *Their justification is only qualitative, yet the size of this engineered background is completely responsible for their claimed "success" in showing that the bomb carbon had gone away by 2020. Their method simply assumed this result. It did not determine it.*

Even though Harde and Salby provide no quantitative estimates of ^{14}C released by nuclear power plants, this has been studied and documented. Figure 1 in (Zazzeri et al. 2018) shows the estimated global ^{14}C emissions of nuclear power plants from 1972 through 2016, by year and by country. Rough integration of that plot through 2012 shows about 3920 TBq of ^{14}C had been emitted globally, some as $^{14}CO_2$ and some as $^{14}CH_4$. One mole of ^{14}C has an activity of 2.31 TBq, so about 1.7 kmoles of ^{14}C have been released into the atmosphere from nuclear power activities by this estimate *in 44 years.* This is slightly less than the 1.8 kmoles (8.08 -1.68) that Harde and Salby's model needs to have emitted above the pre-test baseline *every year*. Nuclear power plant emissions cannot save their model.

(Naegler and Levin 2006) estimate a combined total of about 8 kmoles of ^{14}C released from nuclear testing, nuclear plant operations, and other industrial activities between 1970 and 2005, i.e, a rate of .23 kmoles/year. (See their Figure 4). This would account for about 14% of the background Harde and Salby got by forcing it to rise to the data.

Nuclear testing and nuclear power plants do not come close to accounting for the baseline shift. Let us finally consider the possibility that changes to the incoming flux of cosmic rays can explain it. ^{14}C dating started with the assumption of a constant historical value for atmospheric $\Delta^{14}C$, i.e., a constant production rate produced by a constant flux of cosmic rays. But that assumption has been refined. Samples whose age is known, say from counting tree rings, have been used to investigate the history of atmospheric $\Delta^{14}C$ and calibrate the age vs specific activity curve (Damon and Peristykh 2000). Detailed plots of historical values of $\Delta^{14}C$ over the last 11,000 years do show some variations that are possibly cyclic. But the *maximum* short-term excursions from a constant are about 20 parts per thousand, or two percent. (See their Figure 2.) Harde and Salby, on the other hand, propose a step change in cosmic ray flux close to 30 %. For this to have happened without being noticed elsewhere is highly unlikely.

There is another reason to eliminate cosmic ray increases as an explanation for the failure of the ^{14}C concentration to return to its pre-test level. Fluctuations in the historical cosmic ray flux have been inferred from fluctuations in $\Delta^{14}C$, not fluctuations in concentration. But $\Delta^{14}C$ has not done anything unexpected in recent decades. Has the new ^{14}C from more cosmic rays been precisely balanced by a flux of ^{14}C devoid carbon from somewhere? Again, this is hardly likely.

Note that Harde and Salby's model's need to invent so much background anomalous ^{14}C arises from their belief that it is continually removed on a 10-year time scale. Since the observed ^{14}C

concentration has not declined since 2000, they must keep adding more to explain the data. Of course, if they were to acknowledge that the relatively short time constant observed in the original bomb pulse corresponds only to the initial mixing of bomb carbon into the "fast cycle", and that longer time scales are needed to describe the subsequent exchange of atmospheric ^{14}C with other sinks, their problem would be solved.

Putting in their postulated backgrounds, Harde and Salby go on to label a curve "theory" in their Figure 5. It is a most impotent "theory" that must invent an implausible, ad hoc background to salvage their model's need for a simple exponential decay of atmospheric ^{14}C. This was done to "establish" an hypothesis that never made sense in the first place. Harde and Salby's "fits" to the data are meaningless. Any curve can be transformed into any other curve if one is free to engineer the background. No one who has taken the time to understand the details of what Harde and Salby's did can take their model seriously.

Funding

The author received no financial support for this work.

Editor: Jan-Erik Solheim; Reviewers: anonymous.

Acknowledgements

The author gained insights from multiple sources that are cited, in particular from (Ballantyne et al. 2012), (Caldeira et al.1998), (Graven et al.2020), and (Schwartz et al 2021). The author thanks an anonymous reviewer for pointing out which parts of the argument needed to be strengthened.

References

Andrews, D.E.,2020: *Correcting an Error in Some Interpretations of Atmospheric ^{14}C*, Earth Sciences. Vol. 9, No. 4, pp. 126-129. doi: 10.11648/j.earth.20200904.12.

Andrews, D.E., 2023: *Comments on "Components of CO_2 in 1750 through 2018 Corrected for the Perturbation of the $^{14}CO_2$ Bomb Spike*", Health Physics, vol 124, issue 3, pp 223-225.

Ballantyne, A. P. Alden, C.B., Miller, J.B., Tans, P.P., 2012: *Increase in observed net carbon dioxide uptake by land and oceans during the past 50 years,* Nature, vol 488 pp 70-72. doi:10.1038/nature11299

Beck, E.-G., 2022: *Reconstruction of Atmospheric CO_2 Background Levels since 1826 from Direct Measurements near Ground*, Science of Climate Change vol. 2, no. 2, pp 148-211.

Berry, E. X., 2019: *Human CO_2 emissions have little effect on atmospheric CO_2* International Journal of Atmospheric and Oceanic Sciences, 3(1), 13-26. doi: 10.11648/j.ijaos.20190301.13

Berry, E.X., 2021: *The Impact of Human CO_2 on Atmospheric CO_2*, Science of Climate Change, vol. 1, no.2, pp 1-46.

Caldeira, K., Raul,G. H., and Duffy,P. B.,1998: *Predicted net efflux of radiocarbon from the ocean and increase in atmospheric radiocarbon content*. Geophysical Research Letters, 25(20), 3811-3814.

Cawley, G. C., 2011: *On the atmospheric residence time of anthropogenically sourced CO_2.*" Energy Fuels 25, 5503–5513, http://dx.doi.org/10.1021/ef200914u.

Damon, P.E and Peristykh, A.N. ,2000: *Radiocarbon Calibration and Application to Geophysics, Solar Physics, and Astrophysics, Radiocarbon* Vol 42, Nr 1, pp 137-150.

Denning, A,S, 2022: *Where has all the Carbon Gone?* Annual Review of Earth and Planetary

Sciences, Vol 50, pp 55-78.

EIA. US Energy Information Administration. http://www.eia.gov/energyexplained/energy-and-the-environment/greenhouse-gases-and-the-climate.php. Accessed 20 January 2022.

Graven, H., Allison, C. E., Etheridge, D. M., Hammer, S., Keeling, R. F., Levin, I., et al. ,2017: *Compiled records of carbon isotopes in atmospheric CO_2 for historical simulations in CMIP6*, Geosci. Model Dev., 10, 4405–4417, https://doi.org/10.5194/gmd-10-4405-2017.

Graven, H., Keeling, R.F., & Rogelj, J. ,2020: *Changes to carbon isotopes in atmospheric CO_2 over the industrial era and into the future* Global Biochemical Cycles, 34, e2019GB006170. https://doi.org/10.1029/2019GB006170

Harde, H., 2017: *Scrutinizing the carbon cycle and CO_2 residence time in the atmosphere*. Global and Planetary Change, 152,19-26.

Harde, H., 2019: *What humans contribute to atmospheric CO2: Comparison of carbon cycle models with observations*, Earth Sciences. 8(3), 139-159. doi: 10.11648/j.earth.20190803.13

Harde H., and Salby,M, 2021:*What Controls the Atmospheric CO_2 Level"*, Science of Climate Change vol. 1, no. 1, pp 54-69.

Levin, I., Naegler,T., Kromer, T.B., Diehl, M., Francey, R., Gomez-Pelaez,A., Steele,P., Wagenbach, D., Weller, R. & Worthy. D, 2010: *Observations and modelling of the global distribution and long-term trend of atmospheric $^{14}CO_2$*, Tellus B: Chemical and Physical Meteorology, 62:1, 26-46, DOI: 10.1111/j.1600-0889.2009.00446.x

Naegler, T, Levin, I., 2006: *Closing the global radiocarbon budget 1945–2005*, Journal of Geophysical Research 111:D12311. doi: 10.1029/2005JD006758

Richardson, M., 2013: *Comment on "The phase relation between atmospheric carbon dioxide and global temperature, by Humlum, Stordahl, and Solheim",* Global and Planetary Change, vol 107, pp 226-228.

Salby, M and Harde, H, 2022: *Theory of Increasing Greenhouse Gases*, Science of Climate Change, vol.2, no.3, pp212-238.

Schroder, H,. 2022: *Less than half of the increase in atmospheric CO2 is due to the burning of fossil fuels* Science of Climate Change vol. 2, no. 3, pp 1-19.

Schwartz, Stephen E; Keeling, RF; Meijer, Harro, AJ; Turnbull, JC., 2022: *Comment on "World Atmospheric CO2, Its 14C* Specific *Activity, Non-fossil Component, Anthropogenic Fossil Component, and Emissions (1750–2018)" by Kenneth Skrable, George Chabot, and Clayton French.* Health Physics 122(6):717-719.

Segalstad, T. V. 1992: *The amount of non-fossil-fuel CO_2 in the atmosphere.* AGU Chapman Conference on Climate, Volcanism, and Global Change. March 23-27, 1992. *Hilo, Hawaii.* Abstracts, p. 25, and poster 10 pp. http://www.co2web.info/hawaii.pdf

Skrable, K., Chabot, G., French, C., 2022a: *World Atmospheric CO_2, Its ^{14}C Specific Activity, Non-fossil Component, Anthropogenic Fossil Component, and Emissions (1750-2018),* Health Physics: February 2022 - Volume 122 - Issue 2 - p 291-305 doi: 10.1097/HP.0000000000001485

Skrable, K., Chabot, G., French, C., 2022b: *Components of CO_2 in 1750 through 2018 Corrected for the Perturbation of the 14CO2 Bomb Spike",* Health Physics: November 2022 - Volume 123 - Issue 5 - p 392 doi: 10.1097/HP.0000000000001606.

Stenstrom, K. E., Skog, G., Gerogiadou, Genberg. J., Johansson, A., 2011: "*A guide to radiocarbon units and calculations".* Lund University, LUNFD6(NFFR-3111)/1-17/(2011). https://www.hic.ch.ntu.edu.tw/AMS/A%20guide%20to%20radiocarbon%20units%20and%20calculations.pdf

Stuiver, M. and Polach, H., 1977: *Discussion: Reporting of ^{14}C data*. Radiocarbon, 19(3), 355-363. https://journals.uair.arizona.edu/index.php/radiocarbon/article/viewFile/493/498

Suess, H. E., 1955: *Radiocarbon concentration in modern wood*, Science, 122, 415-417.

Voosen, P., 2022: *Hidden Carbon Layer Sparked Ancient Bout of Global Warming*, Science, Vol 377, Issue 6601, 12-13.

Zazzeri, G., Acuña Yeomans, E., & Graven, H. D., 2018: *Global and regional emissions of radiocarbon from nuclear power plants from 1972 to 2016,* Radiocarbon, 60, 1067–1081. https://doi.org/10.1017/RDC.2018.42

Correspondence to
harde@hsu-hh.de
Vol. 3.1 (2023)
pp. 46-67

Understanding Increasing Atmospheric CO_2

Hermann Harde

Helmut-Schmidt-University Hamburg, Germany

Abstract

The carbon cycle is of fundamental importance to estimate the influence of anthropogenic emissions on the atmospheric CO_2 concentration, and thus, to classify the impact of these emissions on global warming. Different models have been developed, which under simplified assumptions can well reproduce the observed CO_2 concentration over recent years, but they also lead to contradictory interpretations of the human impact. Here we consider, how far such suppositions are substantiated or must be made responsible for significant misinterpretations. We present detailed own calculations based on the Conservation Law, which reproduce all details of the measured atmospheric CO_2 concentration over the Mauna Loa Era. In particular, they allow to deduce an upper limit of 35% for the anthropogenic contribution to the observed increase of CO_2 over the Mauna Loa Era, and a more likely value of 14%. Under non-equilibrium conditions between the Earth's surface and troposphere this even gives a lower bound of only 3.5%. The importance of only one unitary time scale for the removal of anthropogenic and natural CO_2 emissions from the atmosphere, characterized by an effective absorption time, is discussed.

Keywords: Carbon cycle; absorption time; anthropogenic emissions; natural emissions

Submitted 06-01-2023, Accepted 17-02-2023. https://doi.org/10.53234/scc202301/23

1. Introduction

In climate sciences too often half-truths and politically driven illusions are spreading around at lightning speed and are presented on social media or blogs as facts. Deviating findings from the mainstream or from the own conviction of bloggers are dismissed as errors or misconceptions without justification. Often this goes along with unqualified or ad hominem attacks.

A Comment (Andrews 2023) on three recently published papers in this journal (Harde & Salby 2021; Berry 2022, Schrøder 2022) and in another journal (Skrable et al. 2022a, 2022b), apparently tries to imitate this style of social media by attacking these authors without presenting serious arguments against their findings. Instead, superficial considerations are used to persuade other laymen that only human activities such as burning of fossil fuels have caused the rise of atmospheric CO_2 concentration during the Industrial Era.

The Comment is titled "Clear Thinking about Atmospheric CO_2", and obviously this means:

- to embezzle any temperature dependent native emissions, although already from paleoclimatic data it is well known that without any human impact the concentration of greenhouse gases in the atmosphere is changing with the surface temperature (e.g., Petit et al. 1999),
- to ignore any actual studies, which clearly show that the partial pressure of dissolved CO_2 in seawater, the respiration of the biosphere, soil emission and thaw of permafrost are significantly controlled by the temperature (e.g., Lloyd & Taylor 1994; Savage & Davidson 2001; Wood et al. 2013; Nottingham et al. 2018; Brechet et al. 2017; Palmer et al. 2019),
- to ignore any volcanic activities, although from global estimate of about one million submarine volcanoes perhaps many thousands of these volcanoes are active (Oregon State University 2023),

- and to consider only anthropogenic emissions, this on the grounds that the observed CO_2 increase is lower than the estimated fossil fuel emissions (FFE) and land use change (LUC), from which *clear thinkers* follow that nature must be a net sink and therefore cannot be responsible for any increasing CO_2 concentration.

Andrews (2023) alleges, all the papers cited above would present misconceptions and "the errors need to be clearly spelled out in front of those same lay audiences, to ensure that the development of public policy is based on sound science".

In one aspect Andrews is right: His Comment is only for a lay audience and not for readers of this journal, who are interested in serious science. Referring to a consensus among climate scientists as an argument for the validity of his thinking and the anthropogenic global warming hypothesis, is more than questionable, knowing the fraudulent consensus papers of Cook et al. (2013) and Powell (2016), which are meanwhile refuted (Legates et al. 2013, 2015; Fiedler 2020). Science advances not by consensus but by questioning the established paradigms.

It is not the intention of this contribution to reply to all of Andrews' allegations, who apparently is more interested in provoking and inciting statements than exchanging factual arguments. But we use this occasion, to clarify some main misinterpretations and misleading arguments in connection with the thesis that nature is a net sink. This will be considered in Section 2, and in Section 3 further discussed, how nature responds to emissions. Based on the Conservation Law for atmospheric CO_2, we study in Section 4 the influence of anthropogenic and natural emissions on the CO_2 concentration in the atmosphere and compare this with observations over the Mauna Loa Era. Particularly the dependence on the absorption processes at the Earth's surface, characterized by the effective absorption time, is investigated. For the anthropogenic contribution to the observed CO_2 increase over the Mauna Loa Era we derive an upper limit of 35%, a lower bound of 3.5% and a more conservative value of 14% in agreement with previous studies (Harde 2017; Harde 2019; Harde & Salby 2021). We conclude with a summary in Section 5.

2. Is Nature a Net Sink?

From estimates of the anthropogenic emission rate e_A (see, Global Carbon Budget - GCB 2022) and the observed increase ΔC_{CO2} of the atmospheric CO_2 concentration C_{CO2} per time Δt at Mauna Loa (Carbon Dioxide Information Analysis Center - CDIAC 2022) it is widely inferred that about 44% of these emissions (or an equivalent mass) as so-called Airborne Fraction AF remains in the atmosphere, while the rest is ostensibly absorbed by extraneous reservoirs (IPCC, Sixth Assessment Report - AR6 2021, Chap. 5, Fig 5.7). But does this also mean that nature cannot additionally contribute to the observed increasing atmospheric CO_2 concentration?

According to the Conservation Law of atmospheric CO_2 any concentration changes are controlled by a competition between the total emission rate e_{Tot} and its removal through a native absorption rate a_N (up to now artificial uptake does not make any difference):

$$\frac{dC_{CO2}}{dt} = e_{Tot} - a_N = e_A + e_N - a_N, \tag{1}$$

with e_{Tot} as integral of all anthropogenic emissions e_A and all native emissions e_N. Under equilibrium conditions with $dC_{CO2}/dt = 0$ and with a constant emission rate e_{T0}, generally of native origin, $e_{T0} = e_{N0}$, also a constant absorption rate a_{N0} is expected:

$$\frac{dC_{CO2}}{dt} = 0 = e_{T0} - a_{N0} = e_{N0} - a_{N0}. \tag{2}$$

In this context we note that unfortunately some people confuse absorption and emission at the surface with simple mixing of two liquids. CO_2 is mixing in the atmosphere with the other gases but at the surface it is absorbed, partially even changing its compound in seawater or in the bio-

sphere and is again released decades to thousands of years later, strongly dependent on chemical and biological reactions, which on their part are controlled by temperature and humidity.

With an additional perturbation e_P, of natural or anthropogenic origin or both, (1) can also be written as:

$$\frac{dC_{CO2}}{dt} = e_{T0} + e_P - a_N = e_{N0} + e_P - a_{N0} - a_P = e_P - a_P, \tag{3a}$$

or

$$\frac{dC_{CO2}}{dt} - e_P = e_{N0} - a_N = -a_P. \tag{3b}$$

It is obvious that in a linearly responding system without some virtual amplification the changes dC_{CO2}/dt cannot be greater than the perturbation itself, and that these changes are responding with some time delay to the emissions. So, with the left-hand side of (3b) negative, also the right-hand side is negative, and compared to the previous equilibrium the environmental uptake must have increased by an amount a_P. From this right statement, so-called *clear thinkers* deduce that the environment must have acted as a net sink throughout the Industrial Era, and thus, nature could not have been the reason for any observed CO_2 increase (see also Annotations).

As justification reference is made to the IPCC reports AR5 (2013) and AR6 (2021):

- presupposing steady state conditions before 1750 (in first approximation also before 1850) with a CO_2-concentration of $C_{CO2}(1750) \approx 280$ ppm and with constant natural emission and absorption rates $e_{N0} = a_{N0}$ of about 93 ppmv/yr (AR5, Chap.6-Fig.6.1),
- also, assuming steady state conditions for natural emissions over the Industrial Era,
- almost exclusively considering a balance for the anthropogenic emissions with a fractional absorption, proportional to the emission rate $e_A(t)$ with a proportionality factor (1-AF), and
- a cumulating contribution in the atmosphere, the airborne fraction AF, alone responsible for the increasing CO_2-concentration.

Under such hypotheses, when nature is explicitly excluded as additional emitter, it is clear that it cannot be the reason for any observed CO_2 increase. The Conservation Law then reduces to:

$$\frac{dC_{CO2}}{dt} = e_A(t) - (1 - AF) \cdot e_A(t) = AF \cdot e_A(t) \tag{4a}$$

with the solution:

$$C_{CO2}(t) = C_{CO2}(1750) + AF \cdot \int_{1750}^{t} e_A(t) \cdot dt. \tag{4b}$$

As already previously demonstrated (Harde 2019), can the annually averaged Mauna Loa series well be reproduced, only considering these anthropogenic emissions $e_A(t)$ (GCB 2022). Plotted in Fig. 1 is a simulation of the atmospheric CO_2-concentration for AF = 46% (Magenta Diamonds) together with the monthly Mauna Loa measurement (CDIAC 2022, Blue Triangles). Also plotted is $AF(t)$ over time (Green Squares) as increase $\Delta C_{CO2}/\Delta t$ relative to $e_A(t)$. The concentration in 1960 was assumed to be 314 ppmv.

Indeed, can this good agreement be seen as confirmation of only human emissions being responsible for the increasing CO_2-concentration. But a high correlation is no evidence, particularly not, when in advance native sources are excluded and some basic physical principles (see below) are ignored.

Apparently, some experts are not aware that nature is always responding to increased emissions, independent of the *origin*. As long as the perturbation e_P is larger than the additional uptake a_P, the concentration is ascending, till a new quasi equilibrium has established. An observed increasing absorption a_P per se is not equivalent with a net sink. Following the argument of the

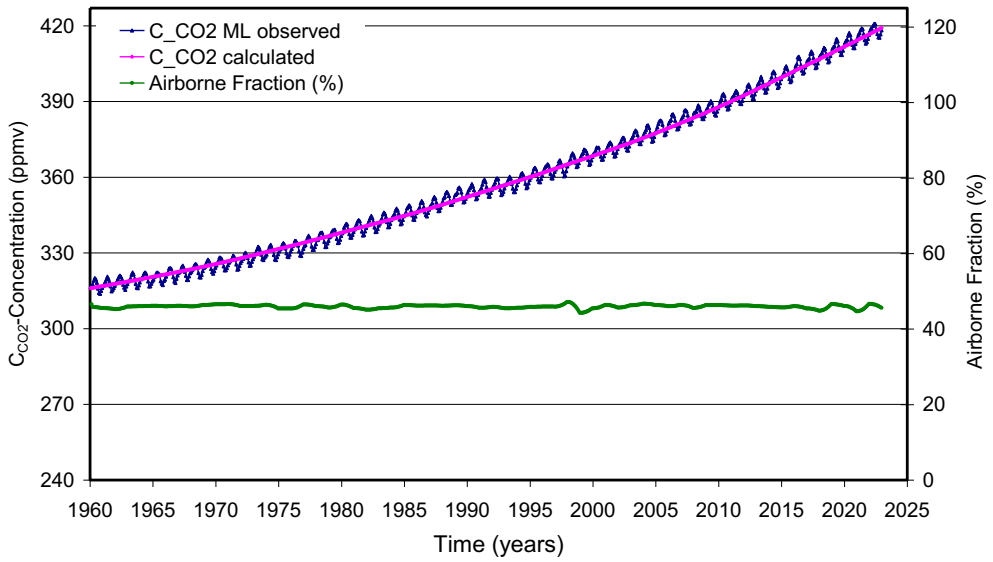

Figure 1: Observed monthly CO_2 concentration at Mauna Loa (Blue Triangles) together with a calculation, only considering anthropogenic emissions $e_A(t)$ and a concentration C_{CO2} *(1960) = 314 ppmv (Magenta Diamonds). Also plotted is the airborne fraction AF (Green Squares).*

clear thinkers, even a net emission caused by a volcanic eruption or an El Niño as pure native events, nevertheless would classify nature as a net sink, since the absorption was increasing.

We have also to remind that emission and absorption are largely independent processes. In tropical areas we find a stronger net emission, in polar regions we have a net absorption, both controlled by the temperature (see, Salby & Harde Part II 2021 and Part III 2022, hereafter SH2 and SH3). Numerical simulations based on the observed tropical temperature reproduce the observed evolution of atmospheric CO_2, including its annual cycle.

This also follows empirically from the observed covariance and high correlation between tropical temperature and *net* emission of CO_2, the component of emission that actually changes CO_2. With a correlation of 0.78 the correspondence holds for interannual fluctuations of net emission, notably during the El Niños of 1973, 1997, and 2016, as well as for its long-term intensification, wherein net emission intensified from ~ 0.7 ppmv/yr to almost 2.5 ppmv/yr (see: SH3, Fig. 8).

The robust coherence between those observed features is also no evidence, but it is in agreement with fundamental physical laws, and this coherence establishes that the changes of tropical temperature do not follow from changes of CO_2, but rather produce them.

An actual study about freshwater CO_2 emissions (Pollard 2022) confirms our results of stronger natural emissions. From in situ measurements at freshwater lakes and rivers this study found a slightly exponential increase of the emissions with temperature, and even more important, that global freshwater lakes are outgassing CO_2 at a rate of 27.5 ppmv/yr, which is of the same size as the mean seasonal emissions with 27.3 ppmv/yr and five times larger than actual anthropogenic emissions with 5.5 ppmv/yr.

These observations are supported by other authors (Ward et al. 2017; Tanentzap et al. 2019), while the IPCC in its preliminary report (AR6-Chap.5, Figure 5.12) specified a mere 0.14 ppmv/yr. This is 200 times less than the estimates from the in-situ measurements. After all, in the final IPCC report a few months later this value has now been increased by a factor of 5, but is still a factor of 40 lower than the actual measurements.

So, obviously it is too *simple thinking* to infer from an increased absorption, relative to a previous level at lower emission, that nature cannot simultaneously be a stronger emitter. With such theses spreading around the globe, together with catastrophic scenarios, how human emissions would endanger our planet, it is indeed high time, that some *dissenters* try to stop such *confused thinking.*

3. Response of Nature to Emissions

A fundamental prerequisite for a consistent description of the emission and absorption processes at the Earth's surface is to rely on well-established physical principles and to integrate them in the Conservation Law. But apparently *clear thinkers* are applying their own principles, which we have to contemplate briefly and to oppose to scientific standards.

1. *Absorption Assumed Proportional to Emission*

   Carbon-cycle models favored by the IPCC rest upon the premise that absorption of anthropogenic CO_2 is proportional, not to its instantaneous abundance, but to its instantaneous emission rate (see eq.(4a) and, e.g., Joos et al., 1988) – irrespective of how much CO_2 is actually in the atmosphere. It is presumed that only some part of the emissions is absorbed, the rest as airborne fraction *AF*, remains in the atmosphere. A consequence of this premise is that CO_2 continuously accumulates in the atmosphere almost for ever, regardless of its actual abundance.

   How could nature have stabilized to any natural emissions with continuous seasonal cycles or glacial periods over millions of years assuming such an absorption? In the presence of real absorption, such behavior is impossible. For constant emission, CO_2 would eventually reach an equilibrium level, at which it is removed through absorption as fast as it is introduced by emission (Essenhigh 2009; Salby 2016; Harde 2017; Harde 2019; Berry 2019; Harde & Salby 2021; Salby & Harde Part I 2021 (SH1); SH2; SH3; Berry 2021; Schrøder 2022). Such equilibrium is only possible with an absorption rate proportional to the instantaneous atmospheric concentration C_{CO2}, as this is confirmed by the exponential decay of radioactive carbon after the stop of the bomb tests (Levin et al. 2013, Harde & Salby 2021).

2. *Division in Anthropogenic and Natural Parts*

   Another physical inconsistency of carbon cycle models is its arbitrary division of the carbon budget into a native part, which is presumed to have remained constant before the Industrial Era, and an anthropogenic part, which is presumed to be solely responsible for increasing CO_2 (see above). The two arbitrarily-defined components are presumed to be independent and, somehow, distinguished by separate absorption processes. A consequence of the different treatment of these arbitrarily-defined components is that, when recombined, they no longer satisfy the Equivalence Principle of physics and the Conservation Law of atmospheric CO_2 - physical laws that *are* satisfied by CO_2 in the real atmosphere (Salby 2018; Harde 2019).

   A division into a constant natural part and a separate anthropogenic part, the latter alone considered to be responsible for increasing CO_2, is circular reasoning. Obviously, Andrews (2023) did not read our previous papers, how otherwise can he allege that we would focus on anthropogenic and natural carbon separately.

3. *Different Time Scales*

   Generally different extraneous reservoirs like the oceans, soil or the vegetation are characterized by significantly different absorption rates, distinguished by different absorptivities α_i or their reciprocals, the absorption times τ_i.

   Some models (e.g., Bern-Model, Joos et al. 1988) even consider up to five individual time scales with separate absorption and decay processes. They distinguish between a shorter residence or turnover time of about 4 yrs, mainly controlling the pre-industrial carbon cycle, and on the other hand between different adjustment times - one even lasting infinite - for the additional uptake caused by the anthropogenic emissions. These adjustments are considered to work essentially in series, where the final absorption is determined by the slowest process. However, as discussed previously (Harde 2017; Harde 2019; Harde & Salby 2021), the different absorption channels at the Earth's surface operate in parallel. Their collective impact on atmospheric CO_2 is represented in the total absorptivity:

$$\alpha = \alpha_1 + \alpha_2 + ... + \alpha_k. \tag{5a}$$

Its inverse is the *direct absorption time* of atmospheric CO_2, τ, which characterizes its direct removal from the atmosphere:

$$\tau = \alpha^{-1} = \left(\alpha_1 + \alpha_2 + ... + \alpha_k\right)^{-1} = \left(1/\tau_1 + 1/\tau_2 + ... + 1/\tau_k\right)^{-1}. \tag{5b}$$

Because CO_2 is virtually conserved in the atmosphere, it is produced and destroyed only at the Earth's surface. The direct absorption time of CO_2 is therefore equal to its *residence time*, and different adjustment times, invented by the IPCC, are incongruous with the physics that controls atmospheric CO_2.

After these annotations on *clear thinking* we derive, based on the physical principles, an absorption rate that is determined by the instantaneous concentration C_{CO2} and the direct absorption time τ:

$$a_N = \frac{C_{CO2}}{\tau}. \tag{6}$$

Then the Conservation Law (3a) converts to:

$$\frac{dC_{CO2}}{dt} = e_{N0} + e_P - \frac{C_{CO2}}{\tau}. \tag{7}$$

This equation is valid for describing the natural carbon cycle in pre-industrial times in the same way as a cycle with additional human emissions. Common in physical systems, the dependence of CO_2 removal on CO_2 abundance by one unitary absorption time is an empirical feature of atmospheric carbon dioxide. It is documented in the monotonic decline of nuclear-perturbed carbon 14 (Salby 2013). Following the 1963 Limited Test Ban Treaty, $^{14}CO_2$ declined exponentially with a single absorption time of about 10 yrs (Levin et al. 2013; Harde & Salby 2021).

For the further considerations it is helpful to distinguish between a direct absorption, which can take place on a time scale even as short as one year, and on the other hand an effective absorption, which can slow down the observed uptake up to one decade (see also: Annotations as reply to some devious comments of Andrews concerning this effective absorption and the ^{14}C-decay).

Generally, we distinguish between a constant, primarily native emission term e_{N0} and the perturbation term e_P. But in addition or in combination with these emissions some fraction, β, of directly absorbed and already removed CO_2 is returned to the atmosphere through re-emission from the Earth's surface (e.g., via outgassing and decomposition of vegetation). This re-emission can be integrated in the other terms or separately considered as an additional source term in the total balance. It is proportional to the instantaneous direct absorption:

$$e_R = \beta \cdot \frac{C_{CO2}}{\tau}, \tag{8}$$

and in this way partially compensating direct absorption. This opposing influence gives a net absorption, which operates with an effective absorption time τ_{eff} and is slowing down the direct absorption from τ to τ_{eff}. Particularly for radiocarbon, which due its radioactivity, can separately be traced in observations, it is necessary for the right interpretation of the carbon cycle to distinguish between re-emission from a temporary reservoir (before sequestration or a further dilution takes place) and a constant basic emission rate e_{N0} from long time storage reservoirs.

This re-emission can well be compared with an induced photonic emission between different excited molecular states, causing transitions and a repopulation between these states, before transitions to a lower state take place and stop this interaction. Such system is generally described by a coupled balance equation system.

With (8) integrated in the total balance, (7) finally becomes:

$$\frac{dC_{CO2}}{dt} = e_{N0} + e_P + \beta\frac{C_{CO2}}{\tau} - \frac{C_{CO2}}{\tau} = e_{N0} + e_P - (1-\beta)\frac{C_{CO2}}{\tau} \tag{9a}$$

or

$$\frac{dC_{CO2}}{dt} = e_{N0} + e_P - \frac{C_{CO2}}{\tau_{eff}}, \tag{9b}$$

with $\tau_{eff} = \tau/(1-\beta)$ and a respectively adapted native emission term e_{N0}.

For a constant perturbation e_P, natural or anthropogenic origin or both, the general solution of (9) is:

$$C_{CO2}(t) = C_{CO2}(0)\cdot e^{-t/\tau_{eff}} + (e_{N0} + e_P)\cdot\tau_{eff}\cdot\left(1 - e^{-t/\tau_{eff}}\right), \tag{10}$$

and with $C_{CO2}(0) = e_{N0}\cdot\tau_{eff}$ as the equilibrium concentration at constant emission e_{N0}, the excess concentration $\Delta C_{CO2}(t) = C_{CO2}(t) - C_{CO2}(0)$ becomes

$$\Delta C_{CO2}(t) = e_P\cdot\tau_{eff}\cdot\left(1 - e^{-t/\tau_{eff}}\right). \tag{11}$$

4. Anthropogenic versus Natural Emissions over the Mauna Loa Era

In general e_P is a function of time and consists of a combination of anthropogenic and native emissions:

$$e_P(t) = e_A(t) + e_S(t) + e_T(\Delta T, t)\,. \tag{12}$$

Anthropogenic emissions $e_A(t)$ are prescribed from the time-varying record of FFE and LUC (GCB 2022).

The seasonal emissions $e_S(t)$ can well be represented by (see Harde & Salby 2021):

$$e_S(t) = \frac{e_{S0}}{2}\cdot\left\{1 + cos\left(\omega(t-t_0) + \varphi_e + m\cdot sin\,\omega(t-t_0)\right)\right\}, \tag{13}$$

where e_{S0} is the amplitude of the seasonal modulation, φ_e is its constant background phase and $m\cdot\sin\omega\cdot(t\text{-}t_0)$ a phase modulation term that recovers the asymmetric shape of the observed seasonality.

The temperature dependence of emission is defined to be slightly nonlinear (see, Harde 2019):

$$e_T(\Delta T, t) = \beta_e\cdot\Delta T(t)^{1.35}, \tag{14}$$

with β_e as the coefficient of temperature response. For anomalous temperature, $\Delta T(t)$, we rely on the record of annual-mean tropical temperature observed at Hawaii (NOAA 2020), which underwent systematic warming (trend) during the Mauna Loa era of 0.13°C/decade.

We note that the time and temperature dependent net emission as derived from tropical temperatures (see: SH3), including seasonal cycles, is in close agreement with this approach.

Together with the basic emission rate e_{N0}, (13) and (14) define the direct native emissions:

$$e_N(t) = e_{N0} + e_S(t) + e_T(\Delta T, t). \tag{15}$$

Inserting (12) in (9b) the numerical integration then can directly be compared with the observed monthly CO_2-concentration series at Mauna Loa (CDIAC 2022) (see also Harde & Salby 2021).

4.1 Stepwise Approach to Reality

As already demonstrated in Section 2, can the annually averaged Mauna Loa series well be reproduced, considering only the anthropogenic emissions $e_A(t)$. In a first step, again we only re-

gard FFE and LUC emissions, but now for an absorption rate proportional to the instantaneous concentration and controlled by an effective absorption time $\tau_{eff} \leq 210$ yrs. Plotted in Fig. 2a is a simulation of the atmospheric CO_2-concentration for $e_{N0} = e_{S0} = e_T = 0$ and $\tau_{eff} = 210$ yrs (Magenta Diamonds) together with the monthly Mauna Loa measurements (Blue Triangles). Larger deviations only become apparent after 2010, which to some smaller part may be explained by the less accurate estimates of LUC. Additionally shown is the airborne fraction *AF* as calculated atmospheric CO_2 increase relative to the anthropogenic emissions per year (Green Dots).

Nearly perfect agreement with the general trend of the Mauna Loa measurement is found for a simulation with an effective absorption time $\tau_{eff} = 50$ yrs (Fig. 2b), again assuming anthropogenic emissions $e_A(t)$ and $e_{N0} = e_T = 0$ with a start concentration $C_{CO2}(1960) = 314$ ppmv, but an additional seasonal modulation amplitude $e_{S0} = 7.6$ ppmv/yr (Magenta Diamonds). The *AF*-graph (Green) with smaller variations around 45% shows also close coincidence with observations. Different to Fig. 1, this simulation does not differentiate between anthropogenic and natural contributions, and it uses a first order absorption term with one single timescale for all emissions.

The same good agreement can be obtained with an amplitude $e_{S0} = 0$, but $e_{N0} = 5.22$ ppmv/yr, equivalent to an annual mean emission $\langle e_S(t) \rangle = 5.22$ ppmv/yr at an amplitude $e_{S0} = 7.6$ ppmv/yr

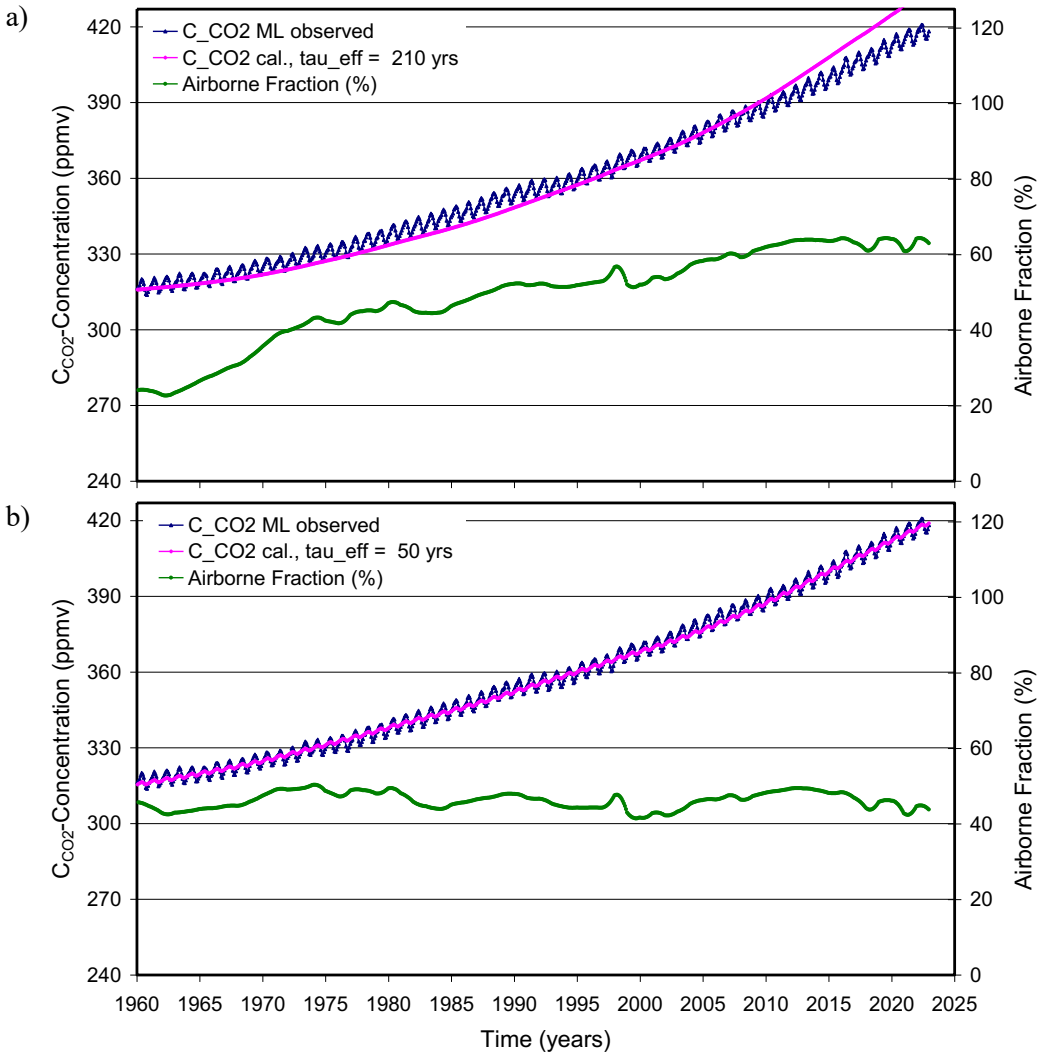

Figure 2: a) Observed monthly CO_2 concentration at Mauna Loa (Blue Triangles) together with a calculation for $\tau_{eff} = 210$ yrs, only anthropogenic emissions $e_A(t)$ and a concentration $C_{CO2}(1960) = 314$ ppmv (Magenta Diamonds). Also plotted is the airborne fraction (Green Dots). b) Respective calculations for $\tau_{eff} = 50$ yrs, $e_A(t)$ and $e_{S0} = 7.5$ ppmv/yr.

and in its size directly comparable to the anthropogenic fraction with a mean $\langle e_A(t)\rangle \approx 3.4$ ppmv/yr (over the Mauna Loa Era) and an actual emission of $e_A \approx 5.5$ ppmv/yr. Also, assuming a slightly larger or lower τ_{eff} and then a respectively smaller or larger seasonal modulation amplitude or basic emission rate e_{N0} gives this good agreement.

However, with these emission rates there exists a significant discrepancy to the emission rates specified in (AR6, Fig.5.12). The mean rates of natural and anthropogenic emissions over the period from 2010-2019 are estimated as $e_{Tot} \approx 226.9$ PgC/yr ≈ 832.7 $PgCO_2$/yr ≈ 106.8 ppmv/yr, while under the conditions of Fig. 2b we obtain not more than $\langle e_A(t)\rangle \approx 5.2$ ppmv/yr over this period, and together with $\langle e_S(t)\rangle = 5.2$ ppmv/yr not more than ≈ 10.4 ppmv/yr, an order of magnitude less. Accordingly, also the respective residence time of CO_2 in the atmosphere, as derived from AR6, and the effective absorption time from Fig. 2b, differ by about one order of magnitude.

Pragmatically this dilemma is solved in some hybrid models by introducing a two-box model, one for the natural cycle as in pre-industrial times with a residence time of 3 to 4 yrs, and an anthropogenic box with an adjustment time between 50 yrs and more than 100 yrs (e.g.: Siegenthaler & Sarmiento 1993; Dietze 2001; Cawley 2011; Lüdecke & Weiss 2016). At least this results again in different timescales and an effectively separate treatment of natural and anthropogenic emissions in these models (see: Harde 2019, Subsec. 5.1).

And there exist three further significant discrepancies with observations:

- From the exponential decay of radioactive carbon after the stop of the bomb tests in 1963 we know that τ_{eff} cannot be larger than 10 yrs (Harde & Salby 2021).
- The monthly Mauna Loa data with the typical seasonal oscillations can only be reproduced with a modulation amplitude $e_{S0} = 40$ ppmv/yr and an effective absorption time $\tau_{eff} \leq 11$ yrs (Harde & Salby 2021).
- The strong correlation between CO_2 emissions and temperature changes, as found on shorter and longer time scales, particularly in the tropics, indicates a systematic variation of the atmospheric CO_2 level with temperature (Palmer et al. 2019; SH2 and SH3; Pollard 2022).

4.2 Consistent Replication of Growing Atmospheric CO_2

A comprehensive analysis and reproduction of the atmospheric CO_2 evolution requires to include these observations and to treat all emissions in a consistent manner.

Plotted in Fig. 3a is the simulated atmospheric CO_2-concentration over the Mauna Loa Era for an effective absorption time $\tau_{eff} = 10$ yrs, a constant background emission $e_{N0} = 3$ ppmv/yr, a seasonal modulation amplitude $e_{S0} = 40$ ppmv/yr, and a temperature coefficient $\beta_e = 10.3$ ppmv/yr/°C$^{1.35}$ (Magenta Diamonds). It tracks almost exactly the observed evolution of CO_2, which is superimposed (Blue Triangles). Different to Fig. 2b this calculation reproduces precisely the seasonal oscillations in amplitude and shape, this with a single absorption or residence time, which is controlling the long-time variations in the same way as the seasonal oscillations, and which does not differentiate between human or native emissions. The asymmetric shape of the oscillations is recovered by a phase modulation with a background phase $\varphi_e = \pi$ and a phase modulation amplitude of $m = 0.8$.

Also shown in Fig. 3a is the airborne fraction $AF(t) = (\Delta C_{CO2}(t)/\Delta t):e_A(t)$ as calculated concentration changes per year relative to the published FFE and LUC data (Green Dots), which despite of increasing anthropogenic and native emissions is slightly declining and by far does not reveal any saturation of the sinks; just opposite it indicates a faster growing uptake of the extraneous reservoirs with rising human and natural emissions. As fraction of the concentration changes to the total varying emissions $(\Delta C_{CO2}(t)/\Delta t):(e_A(t)+e_T(t))$, including the thermal emissions, it even declines to 17.3% in 2022 (not shown).

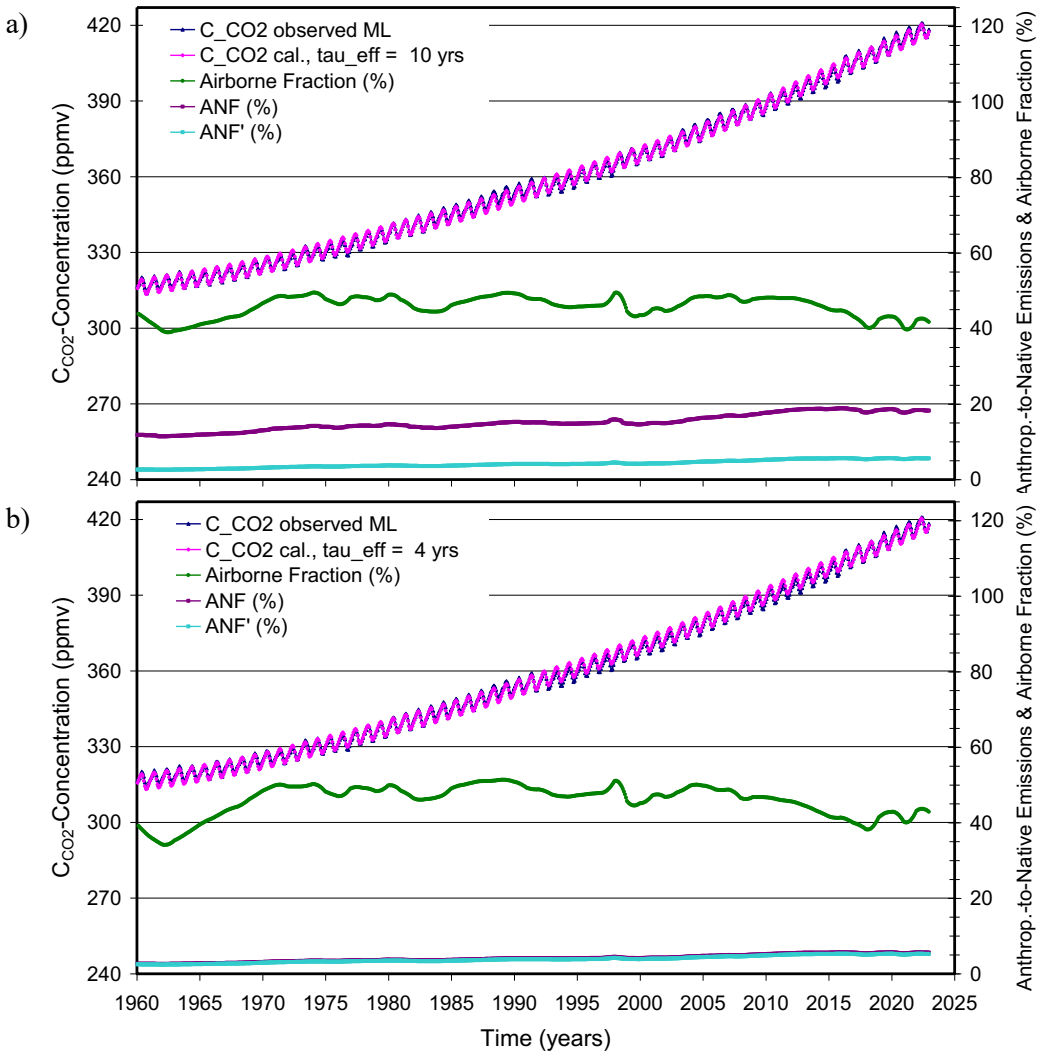

Figure 3: a) Observed monthly CO_2 concentration at Mauna Loa (Blue Triangles) together with a calculation for τ_{eff} = 10 yrs with natural and anthropogenic emissions (Magenta Diamonds). Also plotted is the airborne fraction (Green Dots) and the anthropogenic to natural emissions ANF (Violet Squares) and ANF'(Aqua Squares). b) Respective calculations for τ_{eff} = 4 yrs.

The fraction of anthropogenic to natural emissions $ANF\ (\%) = e_A(t)/e_N(t) \cdot 100$ with $e_N(t) = e_{N0} + e_S(t) + e_T(t)$, see (15), directly reflects the human contribution relative to the natural emissions (Violet Squares). It is slightly increasing over the Mauna Loa Era from 12 to 18%, as the anthropogenic emissions are rising faster than the respective native emissions.

We note that the re-emission of absorbed CO_2, mostly emitted by natural sources, is implicitly included in the effective absorption time, see (8) and (9). With $\beta = 0.6$ ($\tau = 4.0$ yrs) and $\langle C_{CO2} \rangle \approx$ 400 ppm over the last decade, mean re-emission is then $\langle e_R \rangle = \beta \cdot \langle C_{CO2} \rangle / \tau = 60$ ppmv/yr.

The seasonal oscillations with its asymmetric form contribute to an annual-mean emission of $\langle e_S(t) \rangle = 27.3$ ppmv/yr, and the temperature dependence increases emission by 6.9 ppmv/yr, with an average of $\langle e_T \rangle = 6.8$ ppmv/yr from 2010 - 2019. Collective emission from all natural and anthropogenic sources then even adds up to: $\langle e_{N0} \rangle + \langle e_S \rangle + \langle e_T \rangle + \langle e_R \rangle + \langle e_A \rangle \cong 3+27.3+6.8+60+5.2 \cong$ 102.3 ppmv/yr. It corresponds to a total emission of 106.8 ppmv/yr that was estimated by the IPCC (AR6 2021, Fig. 5.12) over the period 2010 - 2019; and in contrast to any temperature and time dependence is the native portion presumed to have been constant.

The respective fraction of anthropogenic to natural emissions $ANF'(\%) = e_A(t)/\{e_N(t)+e_R(t)\} \cdot 100$, including re-emissions, is also plotted over the Mauna Loa Era for $\beta = 0.6$, respectively $\tau = 4$ yrs

(Aquamarine Squares). It increases monotonically from 2.6 to 5.6%, and the anthropogenic to total emissions as

$$ATF'(\%) = \frac{e_A}{e_A + e_N + e_R} \cdot 100 = \frac{ANF'}{ANF' + 100} \cdot 100 \tag{16}$$

is varying from 2.5 to 5.2%. So, the actual human emissions of $e_A \approx 5.5$ ppmv/yr contribute less than 6% to the total emissions, and as average over the Mauna Loa Era with $\langle e_A \rangle = 3.4$ ppmv/yr less than 4%.

The observed evolution of the CO_2-concentration in Fig. 3a can, within bounds, also be recovered for other values of emission. This is a direct consequence of the local mean of CO_2 being determined by the product of total emission and the absorption time (see Eq. (10)). A change in one can therefore be compensated by a change in the other. However, the observed evolution of CO_2 is recovered only for τ_{eff} *shorter than 11 yrs*, regardless of temperature dependence or seasonal emission, slower absorption ($\tau_{eff} >$ 11 yrs) does not recover the long-term increase and the seasonality of observed CO_2 (see, e.g., Figs 2a and 2b). Such calculations provide an upper bound on the absorption time, independent of but consistent with the value revealed by the decline of anomalous $^{14}CO_2$. Together, they provide an upper bound on the anthropogenic perturbation of atmospheric CO_2.

However, absorption can be faster than this limiting absorption. Fig. 3b displays a simulation of the atmospheric CO_2-concentration for an effective absorption time of $\tau_{eff} = 4$ yrs, with a larger undisturbed emission rate $e_{N0} = 50$ ppm/yr and larger thermal coefficient $\beta_e = 30.1$ ppmv/yr/°C[1.35], but an identical seasonal modulation amplitude of $e_{S0} = 40$ ppmv/yr (Magenta Diamonds). Again, it tracks almost exactly the observed evolution of CO_2 (Blue Triangles). Also, the airborne fraction *AF* (Green) reflects similar behavior as in Fig. 3a. With thermal emissions included it even declines to 8.3% in 2022.

While the average seasonal emissions with $\langle e_S(t) \rangle = 27.3$ ppmv/yr are the same as in the previous case, is the basic emission rate with $e_{N0} = 50$ ppmv/yr significantly larger and also the average thermal emission over the period 2010 - 2019 increases to $\langle e_T \rangle = 20.0$ ppmv/yr. Together this adds up to $\langle e_{N0} \rangle + \langle e_S \rangle + \langle e_T \rangle + \langle e_A \rangle \cong 50 + 27.3 + 20.0 + 5.2 = 102.5$ ppmv/yr, and is almost identical with the previous simulation for $\tau_{eff} = 10$ yrs and $\beta = 0.6$ ($\tau = 4$ yrs).

Under these conditions the anthropogenic-to-native fractions *ANF* (Violet Squares) and *ANF'* (Aquamarine Squares) coincide, slightly increasing from 2.5 to 5.3% over the Mauna Loa Era.

But it should also be clear that the total emission rate of approximately 107 ppmv/yr, as specified in AR6, is generally the most uncertain parameter of the guessed rates. When the total rate can be assumed to be even larger, the effective and direct absorption times are further reducing, and in the same way is the anthropogenic to natural fraction further declining.

4.3 Impact of Anthropogenic Emissions on Atmospheric CO_2-Concentration

From the Conservation Law (9) or its solution (10) we see that the anthropogenic and natural emissions are adding up linearly to a total rate, and thus, at least under equilibrium conditions also their relative impacts on atmospheric CO_2 will essentially respond linearly to these rates.

Relative Concentration: For a constant perturbation $\bar{e}_P$ the CO_2-concentration achieves an equilibrium level

$$C_{CO2}^{eq} = \left(e_{N0} + \bar{e}_P\right) \cdot \tau_{eff}, \tag{17a}$$

and with the definitions (12) and (15) for constant rates $\bar{e}_A$ and $\bar{e}_N$ this gives:

$$C_{CO2}^{eq} = C_{A,CO2}^{eq} + C_{N,CO2}^{eq} = \left(\bar{e}_A + \bar{e}_N\right) \cdot \tau_{eff} = \bar{e}_N \cdot \left(\bar{e}_A / \bar{e}_N + 1\right) \cdot \tau_{eff}. \tag{17b}$$

Then, at equilibrium, the relative concentration, caused by anthropogenic emissions to the total concentration, is equivalent to the emission rate $\bar{e}_A$ relative to the total rate $\bar{e}_A + \bar{e}_N$, independent of the absorption time, and in analogy to (16) can be expressed as:

$$\frac{C^{eq}_{A,CO2}}{C^{eq}_{CO2}}(\%) = \frac{\bar{e}_A \cdot \tau_{eff}}{(\bar{e}_A + \bar{e}_N)\cdot \tau_{eff}} \cdot 100 = \frac{\bar{e}_A/\bar{e}_N}{\bar{e}_A/\bar{e}_N + 1} \cdot 100 \approx ATF(\%)\cdot \qquad (17c)$$

In this context we emphasize that the concentrations, $C_{A,CO2}$ and $C_{N,CO2}$, represent the respective fractions to the total concentration in mass or mol units per volume, caused by these emissions and their impact on the total balance. This is independent from any dilution or exchange of molecules from anthropogenic emissions by molecules from natural emissions or vice versa. So, when we consider an anthropogenic fraction $C_{A,CO2}$ to the CO_2-concentration in the atmosphere, here and elsewhere, this is the repercussion on the total concentration and has nothing to do with any isofluxes between reservoirs, as considered by Andrews (2023) in his Comment and his analogy in Subsection 3.5.

Absolute Concentrations: At equilibrium the absolute contributions to the CO_2-concentration are determined by the emission rates and the absorption time (see Eq.(17b)). For conditions as assumed in Fig. 3a with $\tau_{eff} = 10$ yrs we find for constant rates

$$in\ \ 1960: \ C^{eq}_{A,CO2} = 19.8\,ppmv;\ \ C^{eq}_{N,CO2} = 303.4\,ppmv \Rightarrow C^{eq}_{CO2} = 323.2\,ppmv,$$
$$in\ \ 2022: \ C^{eq}_{A,CO2} = 55.5\,ppmv;\ \ C^{eq}_{N,CO2} = 384.5\,ppmv \Rightarrow C^{eq}_{CO2} = 440.0\,ppmv\cdot$$

In 1960 this is 8 ppmv more, and in 2022 about 25 ppmv more than actually observed. These differences represent the additional increase, which still has to be expected till equilibrium has established, i.e., for emissions on the same level as in 2022 the CO_2 concentration will have stabilized within about two decades at 440 ppmv. The calculated temporal increase is plotted in Fig. 4 (Magenta Diamonds) together with the observations (Blue Triangles), the latter till 2022. This calculation differs significantly from the IPCC Representative Concentration Pathways (AR5-Chap6, p.468), prognosticating a further strong CO_2 and temperature increase even for constant future emission rates.

For Fig. 3b with $\tau_{eff} = 4$ yrs we get:

$$in\ \ 1960: \ C^{eq}_{A,CO2} = \ 7.9\,ppmv;\ \ C^{eq}_{N,CO2} = 309.4\,ppmv \Rightarrow C^{eq}_{CO2} = 317.3\,ppmv,$$
$$in\ \ 2022: \ C^{eq}_{A,CO2} = 22.2\,ppmv;\ \ C^{eq}_{N,CO2} = 403.1\,ppmv \Rightarrow C^{eq}_{CO2} = 425.3\,ppmv,$$

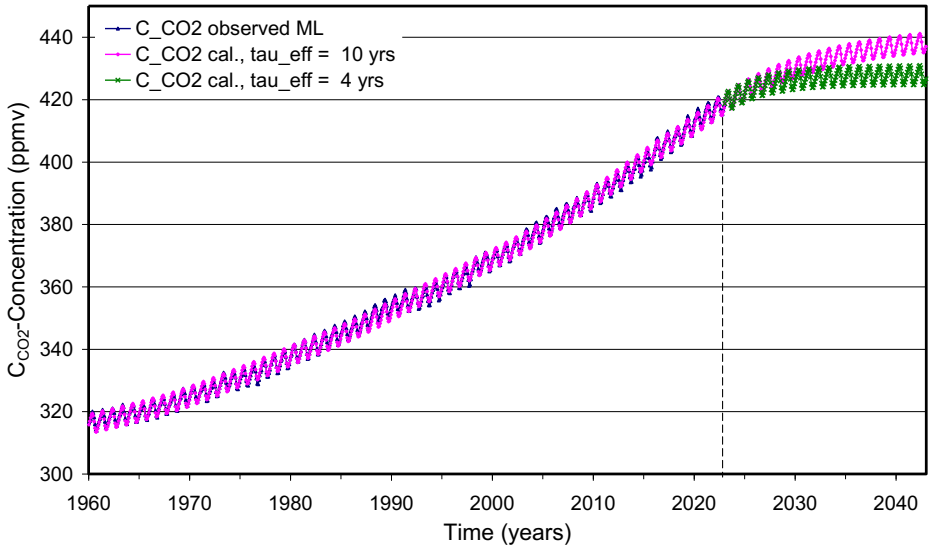

Figure 4: Observed CO_2 concentration at Mauna Loa (Blue Triangles) together with a calculation for $\tau_{eff} = 10$ yrs at constant anthropogenic and thermal emissions after 2022 (Magenta Diamonds) and respective calculation for $\tau_{eff} = 4$ yrs (Green Crosses).

which is 2 ppmv more in 1960 and 10 ppmv more in 2022 than observed. In this case, with emission rates like 2022, the total CO_2-concentration will have stabilized within one decade at about 425 ppmv (Green Crosses).

Due to the larger absorption time in Fig. 3a also the deviations to the observed concentrations are larger. Nevertheless, give these calculations already a good estimation for the absolute and relative fraction of anthropogenic emissions. So, for the limiting case with an effective absorption time of τ_{eff} = 10 yrs, in 1960 the anthropogenic fraction to the total concentration was 6.2% or 19.8 ppmv and in 2022 it doubled to 12.6% or 55.5 ppmv.

With an absorption time τ_{eff} = 4 yrs this further reduces to 2.5% or 7.9 ppmv in 1960 and to 5.2% or 22.2 ppmv in 2022 and is already well represented by the anthropogenic to natural emission fraction $ANF = ANF'$ in Fig. 3b. For still shorter absorption times (see SH3 and Subsec. 4.3.2) this further drops to about 2%.

4.4 Anthropogenic and Natural Contribution to Atmospheric CO_2 Increase

An analysis considering the dynamic evolution of atmospheric CO_2, before equilibrium can be established, requires a direct comparison of simulations with and without anthropogenic emissions. This is plotted in Fig. 5a for τ_{eff} = 10 yrs. The calculation with FFE+LUC emissions included (Magenta Diamonds) is identical with Fig. 3a. It exactly traces the Mauna Loa measurement (Blue Triangles). Additionally plotted is the calculation without anthropogenic emissions (Green Dots), representing the fraction $C_{N,CO2}$ caused only by natural emissions (left axis). The difference of both calculations is the CO_2 increase $C_{A,CO2}$ (Aquamarine Triangles, right axis) caused by the additional anthropogenic emissions (Violet Squares) to the atmosphere. $C_{A,CO2}$ continually increases from 14.1 ppmv to 49.8 ppmv and is in 2022 still 6 ppmv smaller than the equilibrium case.

The difference $\Delta C_{A,CO2} = C_{A,CO2}(2022) - C_{A,CO2}(1960)$ = 35.7 ppmv can directly be compared with the growth of the total concentration over this period: $\Delta C_{CO2} = C_{CO2}(2022) - C_{CO2}(1960)$ = 417.1 - 315.6 = 101.5 ppmv. The ratio $\Delta C_{A,CO2}/\Delta C_{CO2}$ then represents the relative anthropogenic fraction to the observed CO_2 increase over the Mauna Loa Era with:

$$\Delta F_A = \frac{\Delta C_{A,CO2}}{\Delta C_{CO2}} \cdot 100 = \frac{C_{A,CO2}(2022) - C_{A,CO2}(1960)}{C_{CO2}(2022) - C_{CO2}(1960)} \cdot 100 = 35\,\%. \qquad (18)$$

This is in full agreement with our previous estimate for an upper limit of the anthropogenic fraction to the increase (Harde & Salby 2021, eq. (18) and Appendix).

The respective plots for an effective absorption time τ_{eff} = 4 yrs are displayed in Fig. 5b and can again be compared with the Mauna Loa measurement (Blue Triangles). The calculations for the CO_2-concentrations with anthropogenic emissions (Magenta Diamonds) and without these emissions (Green Dots) move closer together, and the difference $C_{A,CO2}$ as anthropogenic fraction shrinks to 7.0 ppmv in 1960 and to 21.5 ppmv in 2022 (note the increased scale versus Fig. 5a).

$C_{A,CO2}$ follows closely the anthropogenic emission rate (Violet Squares). With a difference $\Delta C_{A,CO2}$ = 14.5 ppmv now the respective anthropogenic fraction, causing the CO_2 growth over the Mauna Loa Era, reduces to ΔF_A = 14.3%.

Comparison of Figs 5a and 5b illustrates, how the anthropogenic emissions contribute to the atmospheric CO_2-concentration and how this increase is controlled by the effective absorption time. While Fig. 5a displays the limiting case with τ_{eff} = 10 yrs, and thus, a maximum anthropogenic fraction to the CO_2 incline of ΔF_A = 35%, from the total budget of natural and anthropogenic emissions and absorptions, as compiled in AR6, Fig. 5.12, the residence time of atmospheric CO_2 can be estimated between 3 and 4 yrs (Harde 2017). Therefore, we expect that the simulation in Fig. 5b with a common absorption time τ_{eff} = 4 yrs for natural and anthropogenic

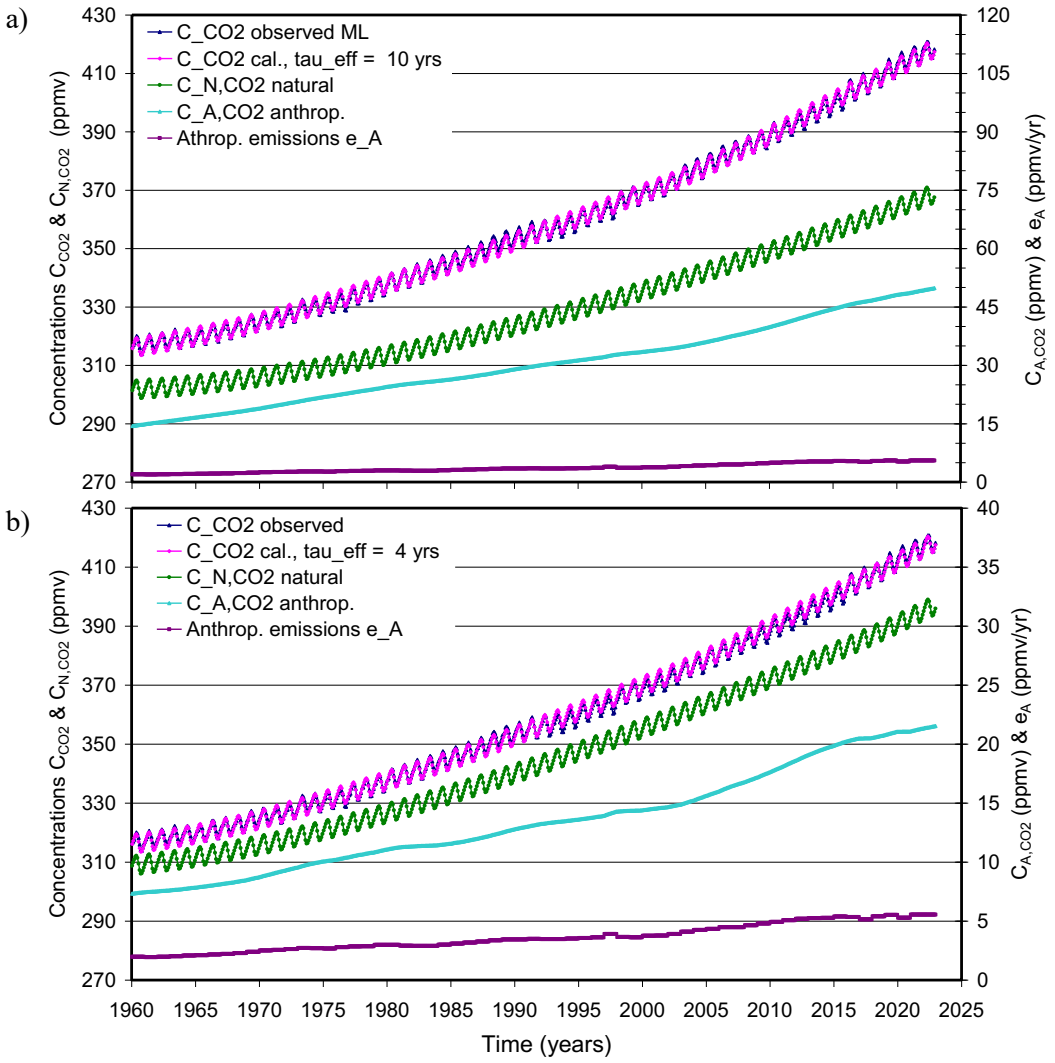

Figure 5: a) Observed monthly CO_2 concentration at Mauna Loa (Blue Triangles) together with a calculation for τ_{eff} = 10 yrs, including anthropogenic and natural emissions (Magenta Diamonds). Also plotted is the concentration $C_{N,CO2}$ (Green Dots) only caused by natural emissions $e_N(t)$, and $C_{A,CO2}$ (Aqua Triangles) caused by the anthropogenic emissions $e_A(t)$ (Violet Squares). b) Respective calculations for τ_{eff} = 4 yrs.

emissions, and $\Delta F_A = 14\%$, provides quite realistic conditions of effective absorption.

The preceding considerations are intended to make clear that obviously it is too simple thinking to surmise from an atmospheric CO_2 growth, which is smaller than the anthropogenic emission rates, that nature is not contributing to any increase. Although in both examples, for $\tau_{eff} = 10$ yrs and 4 yrs, the airborne fraction, generally understood as CO_2 increase only related to anthropogenic emissions, is varying around 45% (see Fig. 3), in Fig. 5a nature contributes with 65 ppmv twice as much to the incline (Green Dots) and in Fig. 5b with 86 ppmv even six times more than human emissions. So, despite a larger uptake than 1960 it would be strange to designate nature as a net sink, when it significantly amplifies the CO_2 increase over the Mauna Loa Era. Altogether, the natural emissions are growing faster than the absorption, and together with the anthropogenic emissions they pretend an almost constant airborne fraction.

4.5 Fast Absorption of Anthropogenic Emissions

From faster oscillations on the $^{14}CO_2$ decay (SH1) and a cross-correlation analysis of interannual CO_2 and temperature fluctuations (Humlum et al. 2013; Salby 2013) it even follows that the direct absorption time τ can be as short as about 1 yr, which under respective conditions also

ties down the effective absorption time.

Unlike thermally-induced emission from the surface, anthropogenic emission operates directly in the atmosphere. For re-emission of CO_2 to amplify and slow effective absorption of CO_2, anthropogenic emission must enrich CO_2 in the surface layer relative to that in the atmosphere. As detailed in SH1 and SH3, however, a slightly growing and continuous re-supply of anomalous CO_2 in the atmosphere maintains the troposphere and surface layer out of equilibrium. Thereby, it limits re-emission and its offset of direct absorption, leaving τ_{eff} fast.

A simulation of the monthly Mauna Loa curve with an effective absorption time for the natural emissions of $\tau_{eff} = 3.8$ yrs and for the human emissions of $\tau = 1$ yr is displayed in Fig. 6 (Magenta Diamonds), which again completely covers the measurement (Blue Triangles).

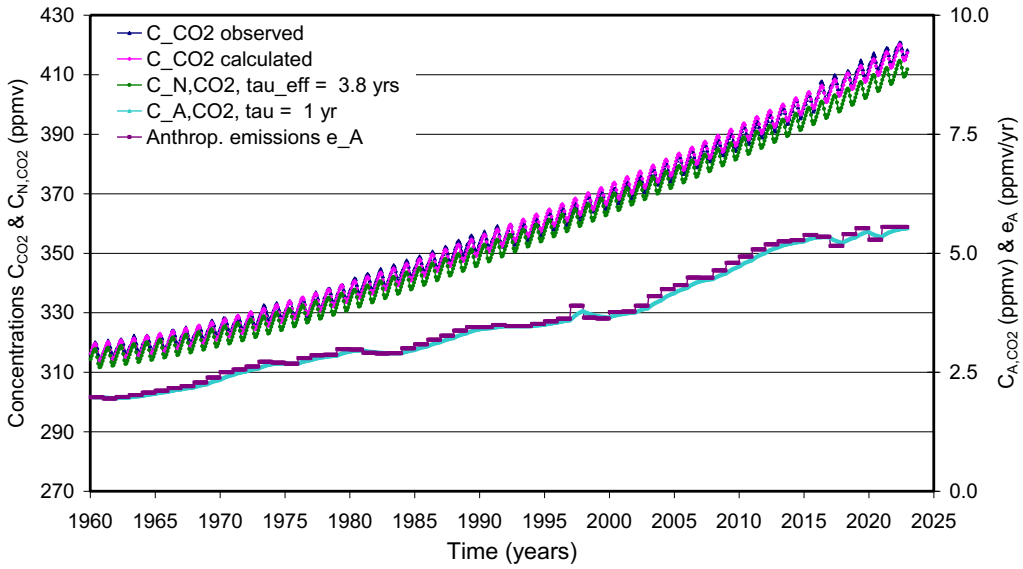

Figure 6: Observed monthly CO_2 concentration at Mauna Loa (Blue Triangles), almost completely covered by a calculation for the natural and anthropogenic emissions together (Magenta Diamonds). Also plotted is the concentration $C_{N,CO2}$ (Green Dots) for $\tau_{eff} = 3.8$ yrs, caused by natural emissions $e_N(t)$ alone, and $C_{A,CO2}$ (Aquamarine Triangles) for $\tau = 1$ yr, caused only by the anthropogenic emissions $e_A(t)$ (Violet Squares).

Almost as closely is the natural component $C_{N,CO2}$ tracking the observed CO_2 concentration (Green Dots). The effective absorption time of $\tau_{eff} = 3.8$ yrs represents a combination of the slower temperature induced CO_2 changes over one decade, and on the other hand the faster interannual fluctuations with an absorption time less than 1 year (SH3). The anthropogenic component $C_{A,CO2}$ (Aquamarine Triangles) with a direct absorption time $\tau = 1$ yr exactly tracks the anthropogenic emission rate $e_A(t)$ (Violet Squares).

The basic natural emission with $e_{N0} = 55.6$ ppmv/yr and the temperature dependent emission over 2010 - 2019 with $\langle e_T \rangle = 23.4$ ppmv/yr ($\beta_e = 33.3$ ppmv/yr/°C$^{1.35}$) are only slightly larger than in Fig. 5b, while the average seasonal emission with $\langle e_S \rangle = 27.3$ ppmv/yr is the same. Together with the human fraction these emissions are causing an average of 111.5 ppmv/yr, in close agreement with the IPCC estimates of total emissions.

The anthropogenic part $C_{A,CO2}$ increases from 2 ppmv in 1960 to 5.5 ppmv in 2022 and under these conditions only contributes to the CO_2 increase over the Mauna Loa Era the fraction $\Delta F_A = 3.5\%$, declining almost proportional with τ (see also SH3, Fig. 11). The respective fraction $C_{A,CO2} / C_{CO2}$ in 2022 reduces to less than 1.5%.

5. Conclusion

The carbon cycle is of fundamental importance to estimate the influence of anthropogenic emissions on the atmospheric CO_2 concentration, and from this to derive the impact of these emissions on global warming. Different models of the carbon cycle, using quite different approaches, can well reproduce the observed CO_2 concentration over recent years, but they also lead to contradictory interpretations of the human impact. Therefore, in this contribution we consider, how far some of these suppositions are substantiated or must be made responsible for significant misinterpretations. We compare these different approaches with own calculations.

Motivation for this study was a critical Comment (Andrews 2023) titled "Clear Thinking about Atmospheric CO_2", in which the author of this article and some other scientists are addressed as *dissenters* or even as *mavericks*, and are accused to distribute misconceptions and errors when publishing an only moderate contribution of anthropogenic emissions to the increasing concentration of atmospheric CO_2. It is not worth to respond to all the strange allegations and inciting statements in this Comment, but to clarify some main misinterpretations and misleading arguments, spreading around in this important discussion.

We present detailed calculations based on the Conservation Law, which reproduce all details of the measured atmospheric CO_2 concentration over the Mauna Loa Era. They clearly demonstrate that nature can be a net emitter, this in contradiction to some *confused thinking* that the environment could not be responsible for any increased CO_2 concentration in the atmosphere. Our studies show the direct influence of the absorption processes at the Earth's surface, which are characterized by a unitary time scale and can be represented by an effective absorption time τ_{eff}, including re-emissions from extraneous reservoirs back to the atmosphere.

In particular, they allow to deduce an upper limit of 35% for the anthropogenic contribution to the observed increase of CO_2 over the Mauna Loa Era, but also a lower bound with 3.5%, one order of magnitude smaller, which has to be explained by a continuous re-supply of anomalous CO_2 in the atmosphere, maintaining the troposphere and surface layer out of equilibrium. This limits re-emission and its offset of direct absorption, leaving τ_{eff} fast (SH3).

But even a more conservative consideration allowing stronger re-emission and thus a larger absorption time $\tau_{eff} \approx 4$ yrs - this also based on the actually estimated CO_2 fluxes in and out of the atmosphere -, gives an anthropogenic fraction to the CO_2 growth over the Mauna Loa Era of about 14%, in agreement with our previous studies.

The calculations reveal that the presented approach is in full agreement with all observations, including the seasonal cycles and temperature induced emissions. It is based on well-known physical principles, and in this aspect, indeed differs from nebulous expositions of so-called *clear thinking*, which try to convince laymen with misleading conceptions that nature is a net sink, or the emission and absorption processes at the Earth's surface would be a simple mixing process like liquids with different alcoholic concentrations.

Would be illuminating to see how *clear thinkers* can explain the whole dynamic of emission and absorption, including all anthropogenic and natural fluxes with the seasonal cycles and observed temperature dependent emissions, this without violating basic physical principles.

Our analysis of the carbon cycle, which uses data for the CO_2 concentrations and fluxes as published in AR6, shows that also a completely different interpretation of these data than favored by the IPCC is possible, this in complete conformity with all observations and natural causalities. Science advances not by consensus but by questioning the established paradigm.

Annotations

This article is no Reply to Andrews' attacks and his Comment (2022), which is more a feat of hubris fuelled by vanity and political delusion and has far removed from any serious disputa-

tion. Otherwise he would have taken a closer look at the arguments made in our previous papers, where we have extensively discussed what speaks against an interpretation of the carbon cycle as favored by the IPCC. It is not worth to comment on all of Andrews' false claims and misinterpretations, but his most unqualified assertions cannot be left unchallenged and, although to some part already addressed above, they are here briefly summarized with some additional annotations.

Net Global Uptake

In his summary Andrews writes: "*Like the other papers critiqued, Salby & Harde (2022) ignore the well-established fact that Net Global Uptake is solidly positive in the current era as the authors should know. All credible models need to be constrained by this simple observation*".

The answer to this false assertion is given in Section 2 and further demonstrated by the calculations in Subsection 4.4. Already in a preceding paper (Harde 2019, Subsection 5.3) this has been discussed extensively. *Clear thinkers* overlook that an increasing emission causes a delayed increase of the atmospheric CO_2 concentration. They derive from this increase, relative to the anthropogenic emissions, an increased absorption of nature. But independent of the fact that also the actual absorption is responding with some delay, from an increasing absorption relative to a previous level at lower emissions, we cannot automatically follow that nature is a net sink, particularly not when in forehand only anthropogenic emissions are considered and native contributions, often not well known, have been neglected. This is an obvious case of circular reasoning. A complete balance requires to include all emissions and absorption.

Isoflux-Model

Andrews writes: "*Isoflux effects can change carbon isotope distributions without changing total carbon distributions. These authors ignore them and mistakenly believe that total carbon changes mimic isotope changes. See the appendix for further criticism of the radiocarbon model of these authors*".

Obviously, Andrews did not realize that his isoflux model is a bad copy of our description of effective absorption, which considers re-emission from previously absorbed CO_2. In distinction to a simple mixing effect like liquids of different concentration (a bad and misleading comparison) we consider real absorption and emission processes at the Earth's surface, as they are authentically observed and which include a partial and/or delayed sequestration of CO_2. These processes determine the actual exchange of CO_2 with the oceans or the biosphere.

For this uptake and release of CO_2 it is reasonable to distinguish between direct absorption processes on a timescale even as short as about one year, as this follows from observations of the faster oscillations on the $^{14}CO_2$ decay (SH1) and also from cross-correlation analyses of interannual CO_2 and temperature fluctuations (Humlum et al. 2013; Salby 2013), and on the other hand between an effective absorption on an extended timescale, which is determined by re-emission from extraneous reservoirs. This re-emission is assumed to be proportional to a previous absorption by these reservoirs and represents a good approximation for a coupled balance scheme of adjacent reservoirs with the atmosphere.

Our description in no way ignores any two-way exchanges between different carbon inventories, which can happen without real changes of these reservoirs, as the total concentration and also the composition of the different CO_2 isotopologues in the atmosphere is completely controlled by these processes. So, the $^{14}CO_2$-decay after the stop of the bomb tests in 1963 is the result of real absorption and emission cycles, this indeed without net concentration change, from which we can learn, on which timescale they are taking place.

Radiocarbon is an ideal tracer, which obeys the same rules as the main isotopologues, and thus can be well used to study temporal carbon mixing and exchange processes. Of course, indicates this $^{14}CO_2$-decay curve that the absorption rate of all CO_2 is proportional to the instantaneous

concentration in the atmosphere and reciprocal to an effective absorption time (e-folding time) of $\tau_{eff} \approx 10$ yrs, which simultaneously defines an upper limit for the direct absorption time τ. Independently this also follows from an analysis of the seasonal cycles (Harde & Salby 2021).

A more serious study of our approach and clear thinking about coupled systems would have shown Andrews that our description does not ignore, what he simply explains as mixing, but includes such processes and quantifies them on a scientifically confirmed basis. Instead, Andrews apparently ignores real science and tries to explain everything by isofluxes in his artificial universe.

Interpretation of the ^{14}C-decay

The Appendix of Andrews' Comment is only aimed at defaming without any new content. It is a repeat of his earlier unqualified claims, to which we were already responding elaborately (Harde & Salby, 2021). Continuously he stresses that we and others have misinterpreted the ^{14}C-decay, and that it required his enlightenment to point out the correct interpretation of this decay together with the right description of the carbon cycle.

He writes: "*As an example of authors' clinging to old and discredited ideas, we will describe (Harde and Salby 2021)'s attempt to salvage Harde's model by designing (inventing?) a background to transform the true concentration curve (red in Figure 2) to the curve they originally thought was the concentration (green in Figure 2)*".

Here only a few additional remarks for clarification. First of all, we never thought or were anywhere writing that the fractionation corrected ‰-deviation $\Delta^{14}C$ from the International Standard activity (green graph in Andrews' Fig. 2) would be the concentration of ^{14}C in the atmosphere. But indeed, can we derive from such data the residence time, respectively the effective absorption time of $^{14}CO_2$. The only question is, under which conditions such data were collected and evaluated.

The $\Delta^{14}C$-measurements of Levin et al. (1980 and 1994), we were using for our analyses, were performed by taking air samples of 15 m^3, and after an extraction and cleaning procedure the activity of the samples was recorded by conventional counting techniques. Over the first two decades after the bomb test stop it was standard to normalize the measured activities to the sampling volume or the air density (see also Stuiver & Polach 1977). Under such condition the measured activity directly reflects the $^{14}CO_2$-concentration changes over time. Since the 80s many groups are using additionally or parallel accelerator mass spectrometry (AMS), which relies on counting the relative abundance of the carbon isotopes directly in terms of the isotope ratios $^{14}C/^{12}C$. In this case, due to the increased $^{12}CO_2$-concentration in the atmosphere over the observation period a further correction is necessary, to determine the correct decline of ^{14}C. The publications (Levin et al. 1980 and 1994) give no hint of using AMS or applying additional corrections. Nevertheless, Andrews (2020) states:

"*Unconventional models motivated by a misinterpretation of the isotope ratio variable "$\Delta^{14}C$" are excluded when the error is corrected ... Harde and Berry erroneously concluded that after atmospheric nuclear testing ceased, the "pulse" of extra ^{14}C introduced by the tests exponentially disappeared from the atmosphere with a time constant of approximately 16 years*".

In Harde & Salby (2021) we explicitly show that the increasing CO_2 concentration in the analysis of the $\Delta^{14}C$-data, either based on the original activity measurements or using AMS with or without further correction of the increased $^{12}CO_2$-concentration, only results in a marginal correction for the decay time. In both cases we deduce for $^{14}CO_2$ an effective absorption time of about 10 yrs, only on a different background, which for several reasons cannot be assumed to be the same today as before the Test Ban Treaty (see also Levin et al., 2010). In any way, the artificially constructed background in Andrews' Fig. 3 has nothing to do with our calculation and explanation, which unambiguously confirms our previous conclusion that the observed exponential decay of ^{14}C represents an upper limit for the absorption time of CO_2 in the atmosphere.

Funding

This research did not receive any specific grant from funding agencies in the public, commercial, or not-for-profit sectors.

Chief-Editor: Prof. Jan-Erik Solheim; Reviewers were anonymous.

Acknowledgements

We thank *Science of Climate Change* for the opportunity to provide a counterstatement to a Comment published in this journal that unqualifiedly constructs misrepresentations and aims to discredit previous publications of the author in this journal.

In particular, we thank the chief-editor Prof. Jan-Erik Solheim for his support of this publication and the anonymous reviewers for their constructive reports.

References

Andrews, D. E., 2020: *Correcting an Error in Some Interpretations of Atmospheric ^{14}C Data*, Earth Sciences, Vol. 9, No. 4, pp. 126-129, http://www.sciencepublishinggroup.com/j/earth, doi: 10.11648/j.earth.20200904.12.

Andrews, D. E., 2023: *Clear Thinking about Atmospheric CO_2*, Science of Climate Change, Vol. 3, No. 1, pp.33-45, https://doi.org/10.53234/scc202301/20

Berry, E., 2019: *Human CO_2 Emissions Have Little Effect on Atmospheric CO_2*, Intern. J. Atmospheric and Oceanic Sciences, Vol. 3(1), pp. 13-26, https://doi:10.11648/j.ijaos.20190301.13.

Berry, E., 2021: *The Impact of Human CO_2 on Atmospheric CO_2,* Science of Climate Change, Vol. 1, No. 2, pp. 213 - 249, https://doi.org/10.53234/scc202112/13

Brechet, L., Lopez-Sangil, L., George, C., Birkett, A., Baxendale, C., Trujillo, B., and E. Sayer, 2018: *Distinct responses of soil respiration to experimental litter manipulation in temperatue woodland and tropical forest*, Ecol and Evolution, 8, 3787-3796.

Carbon Dioxide Information Analysis Center (CDIAC), 2022: https://cdiac.ess-dive.lbl.gov/trends/co2/recent_mauna_loa_co2.html

Cawley, G. C., 2011: *On the Atmospheric Residence Time of Anthropogenically Sourced Carbon Dioxide*, Energy Fuels, Vol. 25, pp. 5503–5513, dx.doi.org/10.1021/ef200914u

Cook, J., et al., 2013: *Quantifying the consensus on anthropogenic global warming in the scientific literature*, Environ. Res. Lett. 8 024024 (7pp), doi:10.1088/1748-9326/8/2/024024

Dietze, P., 2001: *IPCC's Most Essential Model Errors*, Carbon Model Calculations, http://www.john-daly.com/dietze/cmodcalc.htm.

Essenhigh, R. E., 2009: *Potential dependence of global warming on the residence time (RT) in the atmosphere of anthropogenically sourced carbon dioxide*, Energy Fuel 23, pp. 2773–2784, http://pubs.acs.org/doi/abs/10.1021/ef800581r.

Fiedler, M. 2020: *Die 97% Einigkeit unter Wissenschaftlern, die es nie gegeben hat,* https://markus-fiedler.de/2020/01/02/die-97-einigkeit-unter-wissenschaftlern-die-es-nie-gegeben-hat/

Global Carbon Budget (GCB) 2022: https://www.carbonbrief.org/analysis-global-co2-emissions-from-fossil-fuels-hit-record-high-in-2022/

Harde, H., 2017: *Scrutinizing the carbon cycle and CO_2 residence time in the atmosphere*,

Global and Planetary Change 152, pp. 19-26, http://dx.doi.org/10.1016/j.gloplacha.2017.02.009.

Harde, H., 2019: *What Humans Contribute to Atmospheric CO_2: Comparison of Carbon Cycle Models with Observations*. Earth Sciences, Vol. 8, No. 3, pp. 139-158, doi: 10.11648/j.earth.20190803.13.

Harde, H., M. L. Salby, 2021: *What Controls the Atmospheric CO_2 Level?*, Science of Climate Change, Vol. 1, No.1, pp. 54 - 69, https://doi.org/10.53234/scc202111/28.

Humlum, O., K. Stordahl, and J.-E. Solheim, 2013: *The phase relation between atmospheric carbon dioxide and global temperature*, Global and Planetary Change, vol. 100, pp. 51–69.

IPCC Fifth Assessment Report (AR5), 2013: T. F. Stocker, D. Qin, G.-K. Plattner, M. Tignor, S. K. Allen, J. Boschung, A. Nauels, Y. Xia, V. Bex, P. M. Midgley (Eds.): *Climate Change 2013: The Physical Science Basis. Contribution of Working Group I to the Fifth Assessment Report of the Inter-governmental Panel on Climate Change*, Cambridge University Press, Cambridge, United Kingdom and New York, NY, USA.

IPCC Sixth Assessment Report (AR6), 2021: V. Masson-Delmotte, P. Zhai, A. Pirani et al.: Climate Change 2021: *The Physical Science Basis. Contribution of Working Group I to the Sixth Assessment Report of the Intergovernmental Panel on Climate Change*, Cambridge University Press.

Joos, F., M. Bruno, R. Fink, U. Siegenthaler, T. F. Stocker, C. Le Quéré, J. L. Sarmiento, 1996: *An efficient and accurate representation of complex oceanic and biospheric models of anthropogenic carbon uptake*, Tellus B 48, pp. 397–417, https://doi.org/10.1034/j.1600-0889.1996.t01-2-00006.x

Legates, D. R., W. Soon, W. M Briggs, 2013: *Learning and Teaching Climate Science: The Perils of Consensus Knowledge Using Agnotology,* Science & Education **22**, 2007–2017, https://doi.org/10.1007/s11191-013-9588-3

Legates, D. R., W. Soon, W. M. Briggs, et al., 2015: *Climate Consensus and 'Misinformation': A Rejoinder to Agnotology, Scientific Consensus, and the Teaching and Learning of Climate Change,* Science & Education 24, 299–318, https://doi.org/10.1007/s11191-013-9647-9

Levin, I., K. 0. Münnich, W. Weiss, 1980: *The Effect of Anthropogenic CO_2 and ^{14}C Sources on the Distribution of ^{14}C in the Atmosphere*, Radiocarbon, Vol. 22, No. 2, pp. 379-391.

Levin, I., B. Krömer, H. Schoch-Fischer, M. Bruns, M. Münnich, D. Berdau, J.C. Vogel, K.O. Münnich, 1994: *Atmospheric $^{14}CO_2$ measurements from Vermunt, Austria, extended data up to 1983*, https://cdiac.ess-dive.lbl.gov/ftp/trends/co2/vermunt.c14

Levin, I., T. Naegler, B. Krömer, M. Diehl, R. J. Francey, A. J. Gomes-Pelaez, L. Paul Steele, D. Wagenbach, R. Weller, D. E. Worthy, 2010: *Observations and modelling of the global distribution and long-term trend of atmospheric $^{14}CO_2$,* Tellus B: Chemical and Physical Meteorology, 62:1, pp. 26-46, DOI: 10.1111/j.1600-0889.2009.00446.x

Levin, I., B. Krömer, and S. Hammer, 2013: *Atmospheric $\Delta^{14}CO_2$ trend in Western European background air from 2000 to 2012*, Tellus B: Chemical and Physical Meteorology, 65(1), p. 20092, http://doi.org/10.3402/tellusb.v65i0.20092

Lloyd, J. and J. Taylor, 1994: *On the temperature dependence of soil respiration*, Functional Ecology, 8 315-323.

Lüdecke, H.-J., C. O. Weiss, 2016: *Simple Model for the Anthropogenically Forced CO_2 Cycle Tested on Measured Quantities*, JGEESI, Vol. 8, No. 4, pp. 1-12, doi: 10.9734/JGEESI/2016/30532.

Nottingham, A., Baath, E., Reischke, S., Salinas, N., and P. Meir, 2018: *Adaptation of soil microbial growth to temperature: Using a tropical elevation gradient to predict future changes*,

Glob. Change Biol., 25, 827-838.

Oregon State University, 2023: https://volcano.oregonstate.edu/submarine-eruptions

Palmer, P., L. Eng, D. Baker, F. Chevallier, H. Bosch and P. Somkuti, 2019: *Net carbon emissions from African biosphere dominate pan-tropical atmospheric CO_2 signal*, Nature Comm., https://doi.org/10.1038/s41467-019-11097-w.

Petit, J.-R., J. Jouzel, D. Raynaud, N. I. Barkov, J.-M. Barnola, I. Basile, M. Bender, J. Chappellaz, M. Davis, G. Delaygue, et al., *Climate and Atmospheric History of the past 420,000 Years from the Vostok Ice Core, Antarctica,* Nature, vol. 399, no. 6735, pp. 429–436 (1999).

Pollard, P. C., 2022: *Globally, Freshwater Ecosystems Emit More CO_2 Than the Burning of Fossil Fuels*, Front. Environ. Sci., Vol. 10, p. 904955, doi: 10.3389/fenvs.2022.904955

Powell, J. L., 2016: *The Consensus on Anthropogenic Global Warming Matters*, Bulletin of Science, Technology & Society, Vol. 36, issue 3, pp 157-163, https://journals.sagepub.com/doi/10.1177/0270467617707079

Salby, M. L., 2013: *Relationship Between Greenhouse Gases and Global Temperature*, Video Presentation, April 18, 2013, Helmut-Schmidt-University Hamburg https://www.youtube.com/watch?v=2ROw_cDKwc0.

Salby, M. L., 2016: *Atmospheric Carbon: Why It's Not Pollution and Why Humans Cannot Regulate It*, Video presentation, 18 July, University College London, https://youtu.be/3q-M_uYkpT0?t=1330.

Salby, M. L., 2018: What is Really Behind the Increase of Atmospheric CO_2? Helmut-Schmidt-University Hamburg, 10. October 2018, https://youtu.be/rohF6K2avtY

Salby, M. L., H. Harde, 2021 (SH1): *Control of Atmospheric CO_2 - Part I: Relation of Carbon 14 to Removal of CO_2*, Science of Climate Change, Vol. 1, No.2, pp. 177 - 195, https://doi.org/10.53234/SCC202112/30

Salby, M. L., H. Harde, 2021 (SH2): *Control of Atmospheric CO_2 - Part II: Influence of Tropical Warming*, Science of Climate Change, Vol. 1, No.2, pp. 196 - 212, https://doi.org/10.53234/scc202112/12

Salby, M. L., H. Harde, 2022 (SH3): *Theory of Increasing Greenhouse Gases*, Science of Climate Change, Vol. 2, No.3, pp 212 - 238, https://doi.org/10.53234/scc202212/17.

Savage, K. and E. Davidson, 2001: *Interannual variation of soil respiration in two New England forests*, Glob. Biogeochem. Cycles, 15, 337-350.

Schrøder, H., 2022: *Less than half of the increase in atmospheric CO_2 is due to the burning of fossil fuels*, Science of Climate Change, Vol. 2, No.3, pp 1 - 19, https://doi.org/10.53234/scc202111/17

Siegenthaler, U., J. L. Sarmiento, 1993: *Atmospheric carbon dioxide and the ocean*, Nature 365, pp. 119-125,.

Skrable, K., Chabot, G., French, C., 2022a: *World Atmospheric CO_2, Its ^{14}C Specific Activity, Non-fossil Component, Anthropogenic Fossil Component, and Emissions (1750-2018),* Health Physics, Vol. 122, No. 2 - pp. 291-305, doi: 10.1097/HP.0000000000001485

Skrable, K., Chabot, G., French, C., 2022b: *Components of CO_2 in 1750 through 2018 Corrected for the Perturbation of the $^{14}CO_2$ Bomb Spike",* Health Physics, Vol. 123, No. 5, p. 392, doi: 10.1097/HP.0000000000001606.

Stuiver, M. and H. Polach, 1977: *Discussion: Reporting of ^{14}C data*, Radiocarbon, Vol. 19, No. 3, pp. 355-363.

Tanentzap, A. J., A. Fitch, O. Cole, 2019: *Chemical and Microbial Diversity Covary in Fresh*

Water to Influence Ecosystem Functioning, Proc. Natl. Acad. Sci., Vol. 116, p. 24689, doi:10.1073/pnas.1904896116

Ward, N. D., T. Bianchi, M. Seidel, 2017: *Where Carbon Goes when Water Flow: Carbon Cycling across the Aquatic Continuum,* Front. Mar. Sci., Vol. 4, pp. 1-27, doi:10.3389/fmars.2017.00007

Wood, T., Detto, M., and W. Silver, 2013: *Sensitivity of soil respiration to variability in soil moisture and temperature in a humid tropical forest*, *PLOS ONE*, 8, https://doi.org/10.1371/journal.pone.0080965.

Nature Controls the CO_2 Increase

Correspond to
ed@edberry.com

Edwin X Berry

Ed Berry LLC, Bigfork, Montana 59911, USA

Vol. 3.1 (2023)
pp. 68-91

Abstract

Climate alarmism and politics are based on the invalid United Nations (UN) assumption that human CO_2 is the dominant cause of the CO_2 increase above 280 ppm, or since 1750. This assumption conflicts with UN's own data, is derived from invalid circular reasoning, and violates physics. UN data show human carbon emissions have added only 33 ppm to atmospheric CO_2 as of 2020 while natural CO_2 emissions added 100 ppm. This predicted human-caused increase of 33 ppm is 8% of the total carbon in the atmosphere as of 2020, not 33% as the invalid assumption claims..

Also, $\delta^{14}C$ data prove nature is the overwhelming cause of the CO_2 increase since 1750, and lower the 8% of human carbon in the atmosphere calculated from the UN data to less than 4 percent.

The relative equilibrium percentage levels of available natural carbon in land, air, surface ocean, and deep ocean is the strongest predictor of the effect of human carbon on atmospheric CO_2 because the independent human carbon cycle seeks the same percentage levels as the equilibrium natural carbon cycle. For example, if the carbon levels of land, surface ocean, and deep ocean were each doubled, the effect of human carbon emissions on atmospheric CO2 would be reduced by about half, to 18 ppm.

The bomb-caused increase in ^{14}C and $\delta^{14}C$ has now depleted as $\delta^{14}C$ has returned to its balance level of zero. Yet the ^{14}C level is now higher than in 1950. To explain this ^{14}C increase, we propose a theory that nature keeps the $\delta^{14}C$ balance level equal to zero. This theory predicts the non-bomb ^{14}C increase since 1950 is caused by the ^{12}C increase while the $\delta^{14}C$ balance level stayed at zero. This is the simplest (Occam's Razor) explanation for the non-bomb ^{14}C increase since 1950.

Keywords: CO_2; carbon cycle; climate change; climate emergency; climate alarmism; climate fraud; climate crisis; human emissions.

Submitted 15-02-2023. Revised version 20-03-2023. Accepted 21-03-2023.

https://doi.org/10.53234/scc202301/21

1. Introduction

The *Intergovernmental Panel on Climate Change* (IPCC, 2013, p. 467, Executive Summary, selected paragraphs) say incorrectly and without scientific basis,

> The Human-Caused Perturbation in the Industrial Era CO_2 increased by 40% from 278 ppm about 1750 to 390.5 ppm in 2011.
>
> With a very-high-level of confidence, the increase in CO_2 emissions from fossil fuel burning and those arising from land use change are the dominant cause of the observed increase in atmospheric CO_2 concentration.
>
> About half of the emissions remained in the atmosphere (240 ± 10 PgC) since 1750.
>
> It is virtually certain that the increased storage of carbon by the ocean will increase acidification in the future, continuing the observed trends of the past decades.
>
> The removal of human-emitted CO_2 from the atmosphere by natural processes will take a few hundred thousand years (high confidence).

> … about 15 to 40% of emitted CO_2 will remain in the atmosphere longer than 1,000 years. This very-long time required by sinks to remove anthropogenic CO_2 makes climate change caused by elevated CO_2 irreversible on a human time scale.
>
> By contrast, since the beginning of the Industrial Era, fossil fuel extraction from geological reservoirs, and their combustion, has resulted in the transfer of significant amount of fossil carbon from the slow domain into the fast domain, thus causing an unprecedented, major human-induced perturbation in the carbon cycle.

IPCC's first sentence above defines what we call IPCC Theory (1), which says that human CO_2 is the overwhelming cause of the measured CO_2 increase since 1750, when according to the IPCC the CO_2 level was 278 ppm, or approximately 280 ppm.

According to the IPCC, the natural CO_2 level remained at about 280 ppm since 1750.

Berry (2021) used IPCC's own natural carbon cycle data to compute IPCC's true human carbon cycle, which shows that nature, not human CO_2 emissions, drives the CO_2 increase. So, while the IPCC claims "with a very-high-level of confidence" that human CO_2 emissions caused the CO_2 increase, IPCC's own data say with a very-high-level of confidence that natural CO_2 caused the CO_2 increase.

Thus, IPCC's own data prove its Theory (1) is false. This conclusion cannot be ignored. According to the scientific method, data prevails over theory and over votes by scientists. Therefore, Berry's (2021) proof that IPCC's Theory (1) is false based on IPCC's own data is the new default truth that must be proved wrong before anyone can legitimately claim or believe that Theory (1) is true.

Using a different method, Harde and Salby (2021) and Harde (2019, 2017) also prove IPCC's Theory (1) is false. These proofs that Theory (1) is false undermine IPCC's claims about human-caused climate change. Murry Salby passed away in 2022, leaving Hermann Harde to support and defend their proofs that the IPCC Theory (1) is false.

Salby and Harde (2022) is a research masterpiece that shows how increasing temperatures are the true cause of increasing CO_2.

Science progresses when we prove theories are wrong. A correct prediction does not prove a theory is true, but one bad prediction proves a theory is false. That is the key to science.

2. This is the first open debate of Theory (1)

Andrews (2023) is the first formal public challenge to Berry (2021). Andrews represents all scientists who still claim Theory (1) is true. He stands for scientists in the IPCC, America's National Academy of Scientists (Pickering, 2016), the American Meteorological Society, American Physical Society, and in universities from the University of Montana to MIT and Caltech who still incorrectly assume Theory (1) is true. Andrews also stands for the Heartland Institute and the CO_2 Coalition (Burton and Wrightstone, 2022) whose scientists make the same invalid claims and errors that Andrews presents.

Andrews (2023) makes the same arguments as they do but better than they do. So, thanks to Andrews, the debate on Theory (1) is now on the table.

Andrews writes,

> A cornerstone of the argument that humans are responsible for climate change is the consensus among climate scientists that human activities such as the burning of fossil fuels have caused the rise of atmospheric CO_2 concentration during the Industrial Era, all of it.
>
> This is perhaps the most well-established piece of the case for anthropogenic global warming.

Andrews (2023) says he will provide,

> A simple and compelling argument that human emissions, not natural sources, have caused

the increase.

However, "consensus" is not evidence, and it is fundamentally impossible to prove a theory is true. Yet, according to the scientific method, one contradiction to a theory proves the theory is false.

Top prevail, Andrews (2023) must show Berry (2021) is wrong. This paper replies to Andrews (2023) and shows how he and those he stands for make one big fundamental error that no scientist should ever make. Their argument is based on circular reasoning that even they do not recognize.

Andrews' circular reasoning error invalidates his related criticisms of Berry (2021, 2019), Harde and Salby (2021), Schroder (2022), and Skrable et al. (2022a; 2022b) because all his criticisms derive from his overlooked invalid assumption that Theory (1) is true.

3. Physics carbon cycle model

3.1 Physics carbon cycle model supersedes IPCC's models

This summary is a necessary reference because Andrews and others claim Berry's physics carbon cycle model is wrong.

Berry's (2021) physics carbon cycle model for IPCC's carbon cycle supersedes earlier IPCC carbon cycle models in its simplicity, versatility, and accuracy. The IPCC and its authors should have used this physics model.

Berry derives his carbon cycle model for one reservoir in only 8 equations. Then he expands his single reservoir model to multiple reservoirs to simulate IPCC's full carbon cycle. His model exactly replicates IPCC's natural carbon cycle at equilibrium using only one simple hypothesis that the IPCC itself approves. His model can be easily expanded to more than 4 reservoirs.

Berry's physics model is a valid systems-engineering model where levels set outflows and flows set new levels. This is the same formulation and computational method used by Kemeny and Snell (1960) for Markov Chains, Forrester (1968) for systems models, and many systems engineering books. Berry follows Scarborough (1966) to guide his numerical integrations.

Berry used the same systems formulation and numerical methods in his PhD thesis to calculate cloud droplet growth by stochastic collection. See Berry (1967, 1969) and Berry and Reinhardt (1974a, b, c, d) which revolutionized the way scientists now calculate particle growth.

The physics model has only one hypothesis – outflow equals level divided by an outflow time (that we call "e-time") – that the IPCC itself recommends but does not always follow. The physics model is not a curve fit, but it exactly replicates IPCC's natural carbon cycle data. The IPCC has no carbon cycle model that makes this replication.

Segalstad (1998) noted that IPCC's models do not allow CO_2 to flow out of the atmosphere in linear proportion to the CO_2 level, which means IPCC's models are not valid. Rather, IPCC's models use a non-linear constraint on the outflow that contradicts physics and chemistry.

IPCC's human carbon cycle models incorrectly assume Theory (1) is true. They use Greens functions to solve core equations, and pulse additions of Greens functions to do annual sums, a method that is not as simple, efficient, and correct as Berry's numerical calculations.

3.2 Berry's physics model for one reservoir

We follow Berry (2019, 2021) for the derivation of the physics model.

Fig. 1 shows the one-level physics model with one inflow and one outflow.

Inflow sets the balance level. Level sets the outflow. Level always moves toward its balance level. The outflow time, or e-time, is set by the data.

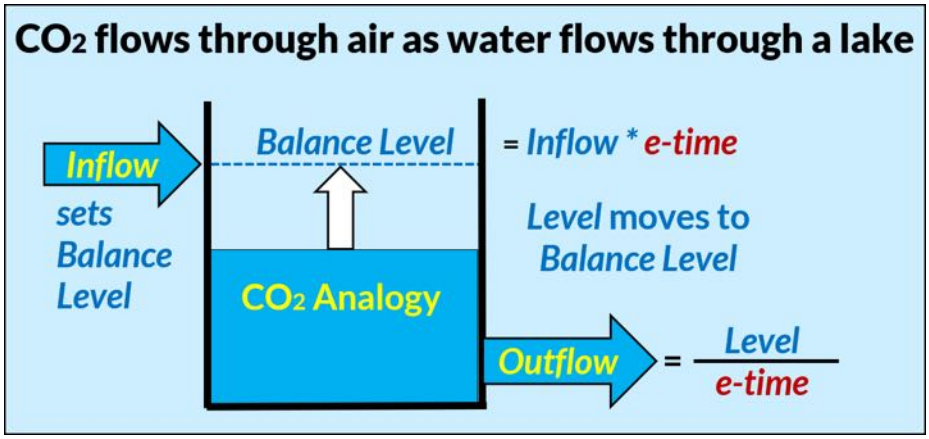

Figure 1. The physics model for one inflow and one outflow node.

Inflow sets the balance level. Level sets the outflow. Level always moves toward its balance level. The outflow time, or e-time, is set by the data.

The physics model derivation begins with the continuity equation (1) that says the rate of change of level is the difference between inflow and outflow,

$$dL / dt = Inflow - Outflow \quad (1)$$

where

L = carbon level (PgC)

t = time (years)

dL / dt = rate of change of L (PgC / year)

Inflow = carbon inflow (PgC / year)

Outflow = carbon outflow (PgC / year)

When *Outflow* = *Inflow*, then $dL/dt = 0$. The flows continue while the level is constant.

The physics model has only one hypothesis, outflow is proportional to level,

$$Outflow = L / T_e \quad (2)$$

where T_e is the "e-time," so defined because it is an exponential time. Equation (2) shows e-time T_e is the same as IPCC's turnover time, T.

e-time is the time for the level to move (1 - 1/e) of the distance from its present level to its balance level.

Substituting (2) into (1) we get,

$$dL / dt = Inflow - L / T_e \quad (3)$$

When dL/dt is zero, the level will be at its balance level, L_b, defined as,

$$L_b = Inflow\ T_e \quad (4)$$

Substitute (4) for *Inflow* into (3) to get,

$$dL / dt = -(L - L_b) / T_e \quad (5)$$

Equation (4) shows how inflow sets the balance level. Equation (5) shows the level always moves toward the balance level set by the inflow. The variables L, L_b, and T_e are functions of time.

In the special case when L_b and T_e are constant, which means *Inflow* is constant according to (4), there is an analytic solution to (5). Rearrange (5) to get,

$$dL / (L - L_b) = - dt / T_e \tag{6}$$

Then integrate (6) from L_0 to L on the left side, and from 0 to t on the right side to get,

$$\ln [(L - L_b) / (L_0 - L_b)] = - t / T_e \tag{7}$$

where

L_0 = Level at time zero ($t = 0$)

L_b = the balance level for a given inflow and T_e

T_e = time for L to move (1 – 1/e) from L to L_b

e = 2.7183

We define half-life, T_h, as the time for the level to fall to half its original level. Then (7) becomes,

$$\ln (1/2) = - T_h / T_e \tag{7a}$$

$$T_h = T_e \ln (2) = 0.6931\ T_e \tag{7b}$$

The original integration of (6) has two absolute values, but they cancel each other because both L and L_0 are always either above or below L_b.

Raise e to the power of each side of (7), to get the level as a function of time,

$$L(t) = L_b + (L_0 - L_b) \exp(- t / T_e) \tag{8}$$

Equation (8) is the analytic solution of (5) when L_b and T_e are constant.

All equations after (2) are deductions from hypothesis (2) and the continuity equation (1). There are no more assumptions and no curve fits.

IPCC (2007, p. 948) defines turnover time to equal our e-time,

> Turnover time (T) is the ratio of the mass M of a reservoir (e.g., a gaseous compound in the atmosphere) and the total rate of removal S from the reservoir: T = M / S. For each removal process, separate turnover times can be defined.

IPCC's turnover time, equal to our e-time, sets how fast carbon flows out of the atmosphere. The same formula, with different e-times, applies to carbon flows out of Land, Surface Ocean, and Deep Ocean.

3.3 Physics model properties

Because (2) is a linear function of level, the physics model applies independently and in total to human and natural carbon and to all definitions of carbon or CO_2. It applies independently to human CO_2, natural CO_2, and to $^{12}CO_2$, $^{13}CO_2$, and $^{14}CO_2$, and their sums.

This *superposition principle* applies to all linear systems. The net response caused by two or more stimuli is the sum of the responses caused by each stimulus individually. So, if input A produces response X and input B produces response Y then input (A + B) produces response (X + Y).

Dalton's law of partial pressures applies to a linear system. It says the total pressure in a mixture of non-reacting gases equals the sum of the partial pressures of the individual gases.

Equation (2) is compatible with all applicable physical and chemical laws. It is the simplest hypothesis for carbon cycle models and it exactly replicates IPCC's natural carbon cycle.

Fig. 2 illustrates how level moves toward its balance level following (8).

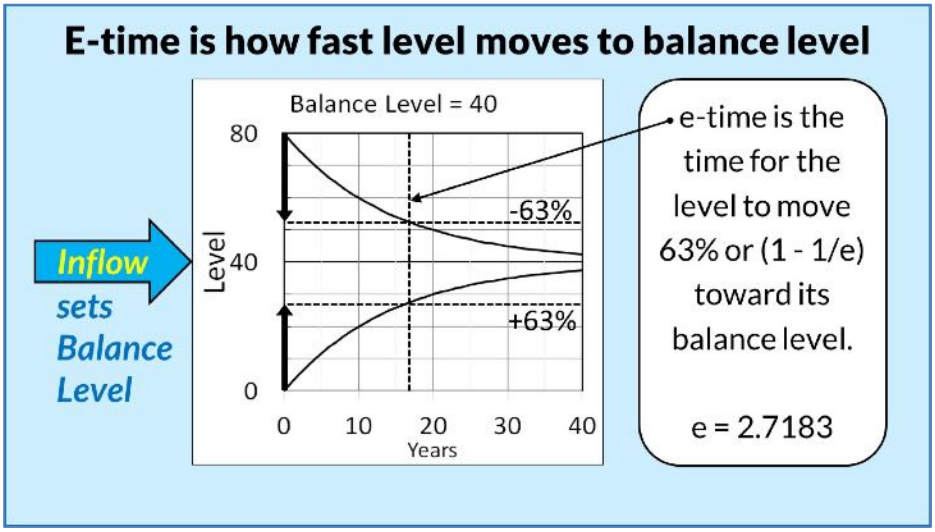

Figure 2. Inflow sets the balance level. The level always moves to its balance level. If Inflow is constant, the balance level stays constant. There is no accumulation.

Systems models calculate outflows as functions of the levels and update the levels according to the inflows and outflows. Talk of uptakes is irrelevant because uptakes are not functions of levels.

Equation (4) shows how inflow sets the balance level. Equation (5) shows how the level moves to its balance level with a speed set by the e-time. When the level equals its balance level, outflow will equal inflow and the level will remain constant.

3.4 Physics carbon-cycle model formulation

We follow Berry (2021) for the derivation of the physics model for multiple reservoirs. A popular version of this subject is in Berry (2020). IPCC's (2013) carbon cycle has four key carbon reservoirs, e.g., land, atmosphere, surface ocean, and deep ocean.

Fig. 3 shows the physics carbon cycle model with IPCC's four reservoirs and six outflows, where the arrows are all positive numbers. The "level" of each reservoir is the mass of carbon in each reservoir. The origin of each arrow is a "node."

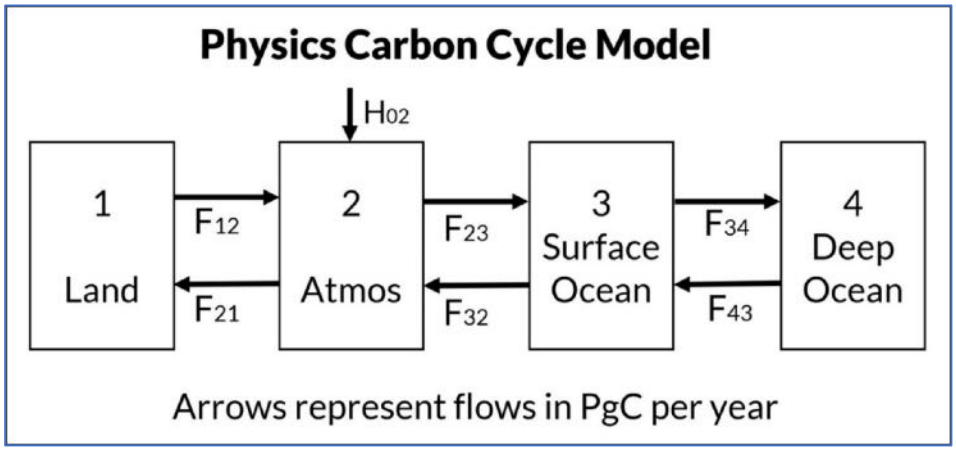

Figure 3. The physics carbon cycle model for IPCC's carbon cycles.

The physics model is a dynamic flow model that accurately computes the evolution of beginning levels and flows as functions of time.

Define the Levels,

L_1 = level of carbon in the land

L_2 = level of carbon in the atmosphere

L_3 = level of carbon in the surface ocean

L_4 = level of carbon in the deep ocean

Define the individual flows out of the six nodes,

F_{12} = flow from land to atmosphere

F_{21} = flow from atmosphere to land

F_{23} = flow from atmosphere to surface ocean

F_{32} = flow from surface ocean to atmosphere

F_{34} = flow from surface ocean to deep ocean

F_{43} = flow from deep ocean to surface ocean

Define other variables,

t = time in years

H_{02} = human carbon flow to atmosphere

H_{12} = land carbon flow to atmosphere

Using (2), the flows out of the six nodes are,

$$\begin{aligned} F_{12} &= L_1 / T_{12} \\ F_{21} &= L_2 / T_{21} \\ F_{23} &= L_2 / T_{23} \\ F_{32} &= L_3 / T_{32} \\ F_{34} &= L_3 / T_{34} \\ F43 &= L_4 / T_{43} \end{aligned} \tag{9}$$

Using (1) and (9), the rate equations for each reservoir are,

$$\begin{aligned} dL_1 / dt &= F_{21} - F_{12} - H_{12} \\ dL_2 / dt &= F_{12} - F_{21} + F_{32} - F_{23} + H_{02} + H_{12} \\ dL_3 / dt &= F_{23} - F_{32} + F_{43} - F_{34} \\ dL_4 / dt &= F_{34} - F_{43} \end{aligned} \tag{10}$$

The physics model uses (9) and (10) to calculate the natural and the human carbon cycles.

Numerical calculations use time steps as follows,

1. Set initial levels.
2. Calculate nodal flows using (9).
3. Calculate level rates of change using (10).
4. Multiply level rates of change by time step to get changes of levels.
5. Add changes of levels to the levels to get new levels.
6. Repeat for next time step.

Berry (2021) shows more of the computational process and supplies an Excel download showing all Berry's calculations.

3.5 IPCC's natural and human carbon cycles

Fig. 4 is IPCC's Figure 6.1 (IPCC, 2013, p. 471, Fig. 6.1). Fig. 4 assumes Theory (1) is true. The natural carbon level in the atmosphere stayed constant at its assumed 1750 level of 589 PgC (278 ppmv) while human carbon caused all the carbon increase above 589 PgC.

This human carbon is 29% (= 240/829) of the carbon in the atmosphere as of about 2010. By 2020, the human percentage increases to 33% (Berry, 2021).

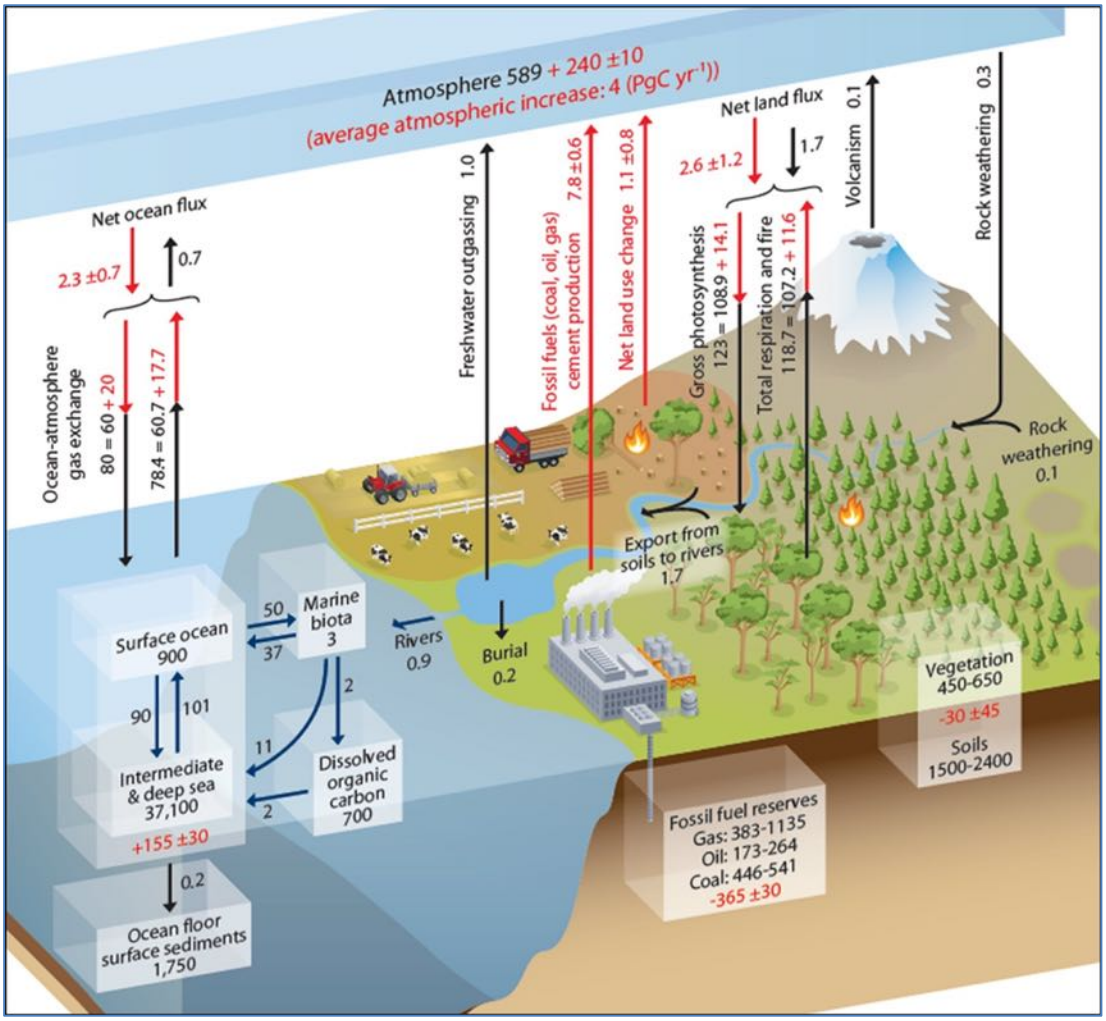

Figure 4. IPCC's Figure 6.1 (IPCC, 2013, p. 471, Fig. 6.1) showing IPCC's data for its shows IPCC's natural carbon cycle (in black) and human carbon cycle (in red) as of about 2010.

Fig. 5 shows IPCC's natural and human carbon cycles at equilibrium. Outflow from all nodes follows (2).

The percentages in each box show the percent of total carbon in each reservoir when IPCC's natural carbon cycle is at equilibrium. Because human and natural carbon atoms are identical, the human carbon cycle has the same equilibrium percentages and e-times as the natural carbon cycle.

Total human carbon emissions as of 2020 added about one percent to the carbon in the natural carbon cycle. So, if we stopped human carbon emissions in 2020, the equilibrium addition of human carbon to the atmosphere would be about one percent of the total carbon in the 2020 atmosphere, or about 4 ppm.

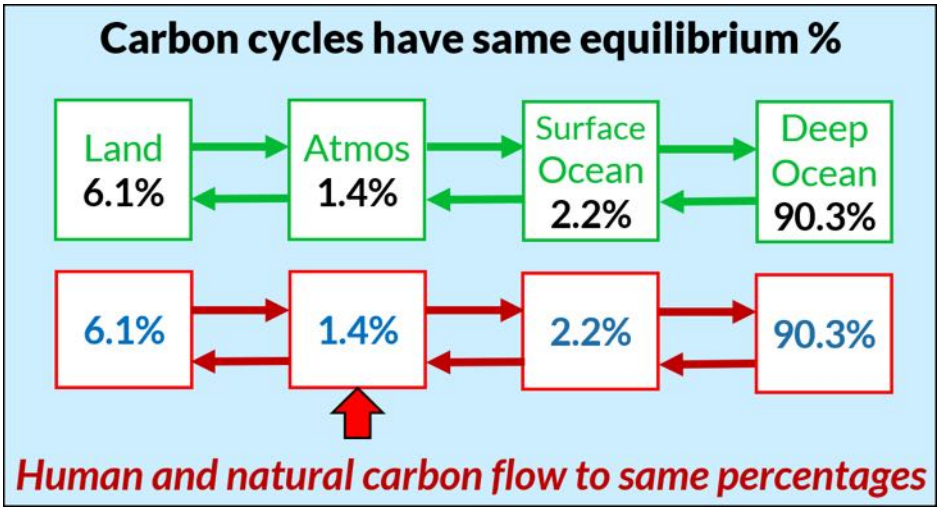

Figure 5. IPCC's natural and human carbon cycles according to IPCC's Figure 6.1. The percentages show the distribution of carbon in the carbon cycle at equilibrium.

IPCC's true human carbon cycle shows nature added about three times more carbon than human carbon to the carbon cycle since 1750. So, human carbon is NOT "causing an unprecedented, major human-induced perturbation in the carbon cycle" as IPCC (2013) claims.

3.6 How to calculate IPCC's true human carbon cycle

IPCC's natural carbon cycle is based on IPCC's data, which may be the best data we have for the natural carbon cycle. But IPCC's human carbon cycle is based on Theory (1) and not upon IPCC's natural carbon cycle data.

Berry's (2021) insight was that IPCC's natural carbon cycle at equilibrium has the level and outflow data necessary to calculate the e-times for each node, and these e-times apply equally to human and natural carbon. So, Berry (2021) uses data from IPCC's natural carbon cycle to calculate IPCC's true human carbon cycle (yellow boxes).

IPCC's natural carbon cycle includes data, but IPCC's Theory (1) human carbon cycle has no data. So, Berry used IPCC's natural carbon cycle data to calculate IPCC's true human carbon cycle.

Berry did what the IPCC should have done. He used IPCC's natural carbon cycle data to calculate IPCC's true human carbon cycle. The calculation is deductive, confirmed, and not complicated.

IPCC's failure to properly calculate its true human carbon cycle has caused false climate alarmism, its costs, and failures to educate students in true physics.

Fig. 6 shows IPCC's two carbon cycles, natural and human.

IPCC's own data predict human CO_2 caused 24% of the CO_2 increase by 2020 and nature caused 76%. But IPCC's Theory (1) predicts human CO_2 caused 100% of the CO_2 increase and nature caused 0%.

Therefore, Theory (1) is false because it conflicts with IPCC's own data.

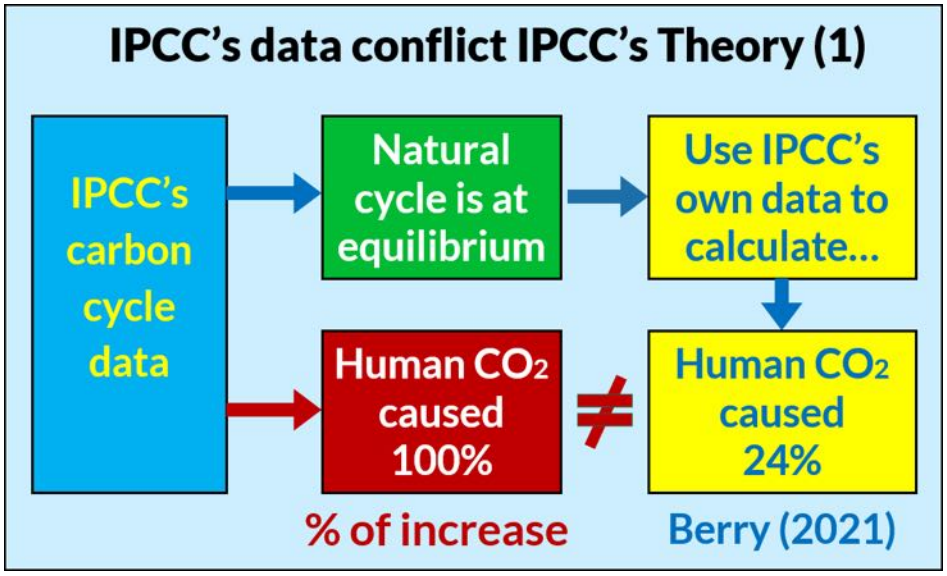

Figure 6. IPCC's natural carbon cycle derives from data. IPCC's Theory (1) human carbon cycle is not derived from data. Berry (2021) used IPCC's natural carbon cycle data to properly.

3.7 Human carbon was too small before 1950

Fig. 7 shows data from 1820 to 2020. IPCC's true human carbon cycle shows human carbon in the atmosphere as of 2020 was about 70 PgC. The measured carbon level was 290 PgC. Therefore, natural carbon added 220 PgC to the atmosphere.

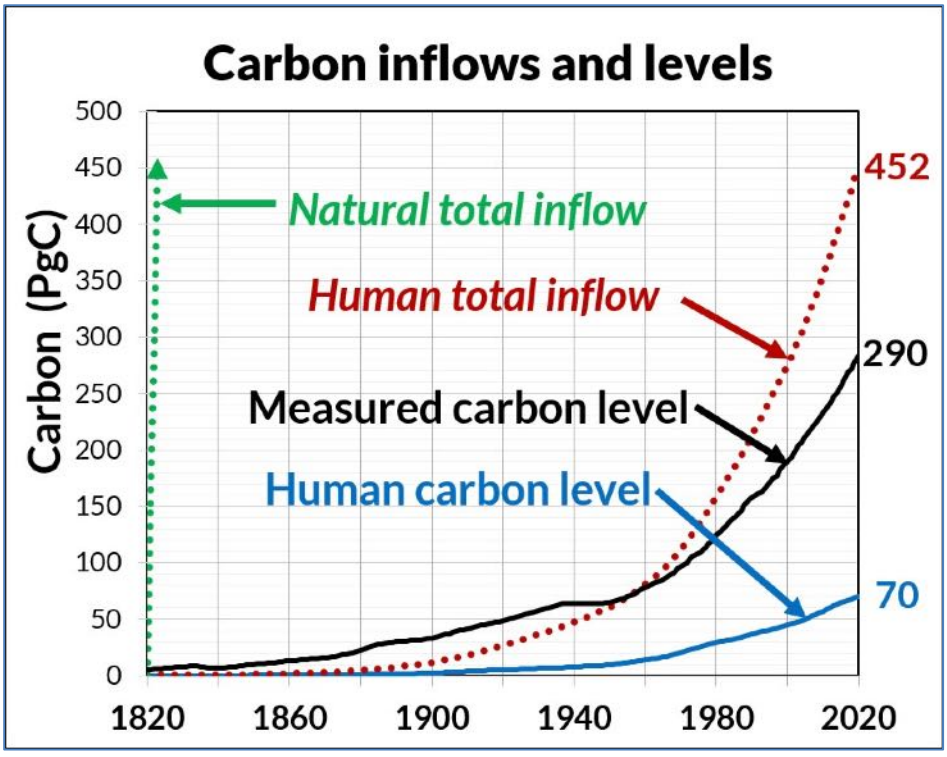

Figure 7. The blue line shows the human CO_2 level of IPCC's true human carbon cycle. The black line is the measured carbon level. The red dotted line is the accumulated human total carbon inflow since 1750 assuming all human emissions remained in the atmosphere. The green dotted line is the accumulated natural inflows.

The accumulated human total inflow reaches 452 in 2020, much greater than the measured total in 2020. IPCC's Theory (1) believers use this difference to claim Theory (1) is true. However, their claim is invalid because they do not subtract outflow.

Before 1950, human total inflow was less than the measured carbon level. So, human carbon emissions were insufficient to have produced the measured carbon level. This alone falsifies IPCC's Theory (1).

Finally, the green dotted line shows the accumulated natural inflow. Yet, no one argues this proves natural carbon caused all the added carbon. This illustrates how arguments that use accumulated inflows do not prove a cause of the increase.

4. Theory (1) argument uses circular reasoning

4.1 Theory (1) believers reject separate carbon-cycles

The IPCC defines two separate carbon cycles, human and natural. Berry (2021) shows why it is better to calculate human and natural carbon cycles independently rather than using their total because two cycles provide more, independent information.

However, Andrews (2023) argues for the true believers,

> In their quest to determine the fraction of anthropogenic carbon in the present atmosphere Harde and Salby, Berry, and Schroder focus on anthropogenic and natural carbon separately. This complicates their analysis, and they miss the simple conclusions made here.
>
> What they do find is natural carbon is accumulating in the atmosphere faster than human carbon, and indeed it is! Nothing in the analysis presented here conflicts with this fact.
>
> Anthropogenic carbon can be the cause of the entire Industrial Age increase without being a large part of the present atmospheric composition.
>
> Of course, it is the *total* atmospheric carbon that impacts climate, and the above analysis leaves no doubt where the increase in the total is coming from.
>
> Tracking anthropogenic carbon separately from natural carbon is a distraction, which is why few papers in the serious peer-reviewed literature do so.

Andrews' every paragraph above is wrong. His arguments fail physics and contradict IPCC's separation of human and natural carbon cycles. It is not a *distraction* to calculate human and natural carbon cycles separately. It is a necessity.

Andrews discards important data and consequently makes an invalid, circular argument.

4.2 Theory (1) believers use circular reasoning

Berry (2021) wrote,

> Another invalid argument used to support the IPCC basic assumption is, because nature absorbs human carbon from the atmosphere, therefore nature cannot add carbon to the atmosphere. This argument neglects the physics model *superposition principle* that explains why the natural carbon cycle is independent of the human carbon cycle.

Andrews argues incorrectly for Theory (1) believers [brackets show Berry's replies],

1. Because the carbon from human emissions during this period exceeds the rise in atmospheric *total carbon*, we know immediately that land and sea reservoirs together have been net sinks, not sources, of *total carbon* during this period. [No, we do not. This is circular reasoning.]
2. We can be sure of this without knowledge of the detailed inventory changes of individual non-atmospheric reservoirs. [No, we cannot.]
3. This is not a model dependent result. It is a simple statement based on carbon conservation,

data on emissions and atmospheric levels, and arithmetic. [No, it is based on circular reasoning.]

4. Note that this conclusion contains no assumption whatsoever about the constancy of natural carbon in this period. [No, it inherently assumes Theory (1) is true.**]**
5. In fact, the primary conclusion of Ballantyne is that non-atmospheric natural reservoirs – during the 50-year period studied – have not only increased their carbon inventory, they have also increased the rate at which they are doing so *in response to the higher atmospheric levels*. [No. Ballantyne and "*in response to the higher atmospheric levels***"** assume Theory (1) is true.]
6. Nor does the conclusion rely on treating "human" and "natural" carbon differently as (Harde and Salby 2021) and (Berry 2021) both allege. [No, because Theory (1) requires different e-times for natural and human CO_2.]
7. Net Global Uptake is simply what is left over after atmospheric accumulation has been subtracted from total emissions. If more carbon was injected into the atmosphere by human activities than stayed there, it had to have gone somewhere else. [No, this claim is based on circular reasoning.]

Let's take this one little baby step at a time because too many potentially smart PhDs are fooled by the argument repeated by Andrews. (If this does not work, we may publish a coloring book.)

Fig. 8 shows a simple spreadsheet. The rows are Inflow, Added, and Outflow totaled from 1750 to 2020. The columns are the Human, Natural, and Total.

For terminology, we use our terms relevant to the atmosphere to replace Andrews' terms as follows:

1. Human Inflow = Cumulative Human Emissions = 452 PgC
2. Human + Natural Added = Atmospheric Accumulation = 290 PgC
3. Total Inflow – Total Added = Net Global Uptake = 162 PgC
4. Total Outflow = Net Global Uptake = 162 PgC

Net Global Uptake is simply Total Outflow. So, why use it? The proper way to view the effects of human and natural carbon inflow is shown in Figs. 8 and 9.

The difference between Berry's numbers and Andrews numbers is not relevant because Andrews totals the data from 1960 to 2010 while Berry totals the data from 1750 to 2020. These differences have no bearing on the logic of this discussion.

Fig. 8 shows the only values derived from data: Human Inflow = 452 PgC and Total Added = 290 PgC (from Fig. 7). These values tell us nothing about the Human Added vs the Natural Added.

To make his argument, Andrews assumes Theory (1) is true (without realizing he made this assumption) and thereby puts zeros in the natural column, forcing Total Inflow to equal Human Inflow.

Then he subtracts the Total Added from his assumed Total Inflow to get 162 for Total Outflow, that he calls Net Global Uptake.

Andrews' argument requires all natural components to be zero, which is the same as assuming Theory (1) is true. To assume the result to prove the result is called circular reasoning.

The only way to separate Human Added from Natural Added is to calculate IPCC's true human carbon cycle. Berry (2021) does this using IPCC's own data.

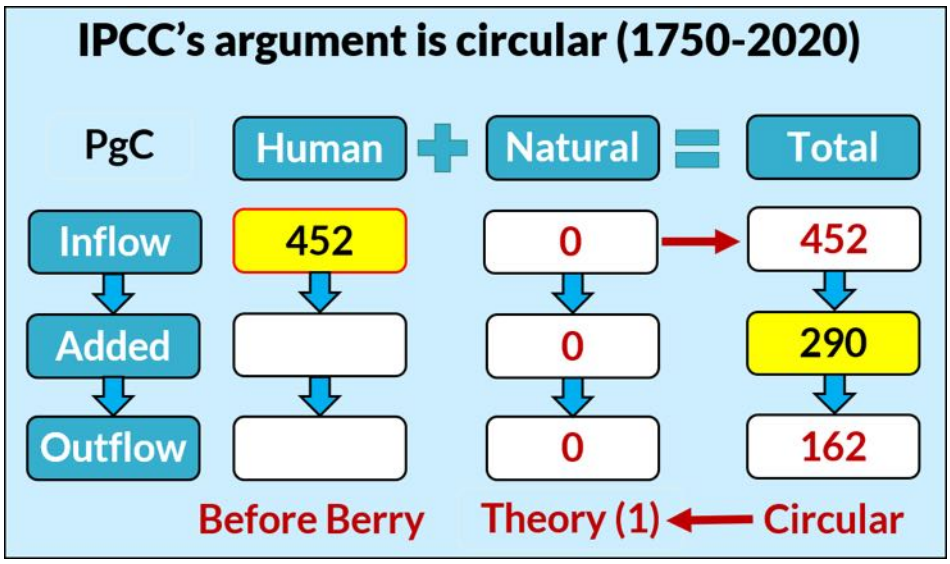

Figure 8. Carbon sums from 1750 to 2020. Carbon cycle overview shows the Inflow, Added, and Outflow for the Human, Natural, and Total carbon cycles.

Fig. 9 updates Fig 8 by including Human Added of 70 PgC according to IPCC's true human carbon cycle.

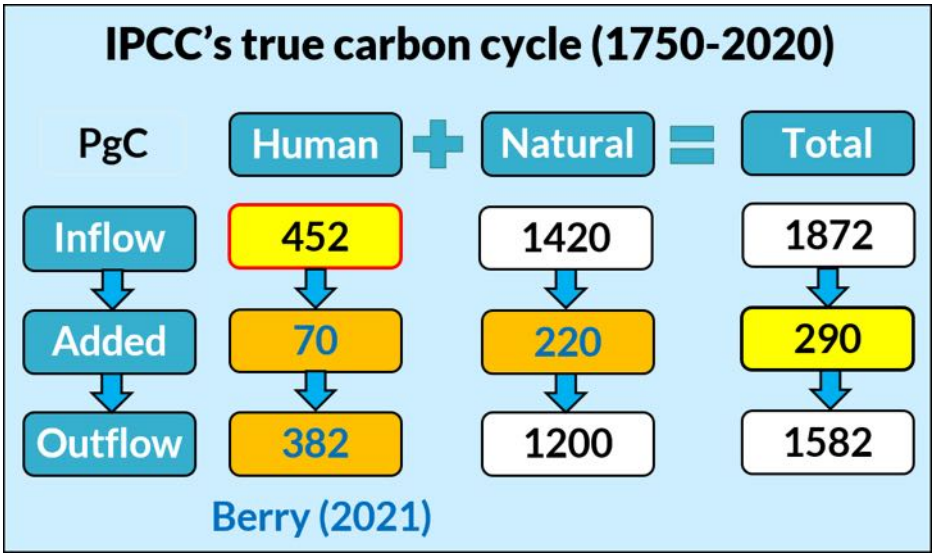

Figure 9. Carbon sums from 1750 to 2020. We insert 70 PgC for Human Added according to IPCC's true human carbon cycle. This Natural Added is 220 PgC and Human Outflow is 382 PgC.

This makes the Natural Added equal to 220 PgC and Human Outflow equal to 382 PgC. The numbers in the white boxes are estimates that keep the human and natural flows proportional.

Fig. 9 contradicts the believers' invalid argument that because "nature" absorbs human carbon (Human Outflow), nature can't also add carbon (Natural Added).

Fig. 10 shows the summary of IPCC's true carbon cycle. As of 2020, human carbon was 24% of the Total Added, and 8% of the Total in the Atmosphere. These results prove IPCC's Theory (1) is false and Andrews (2023) is science fiction.

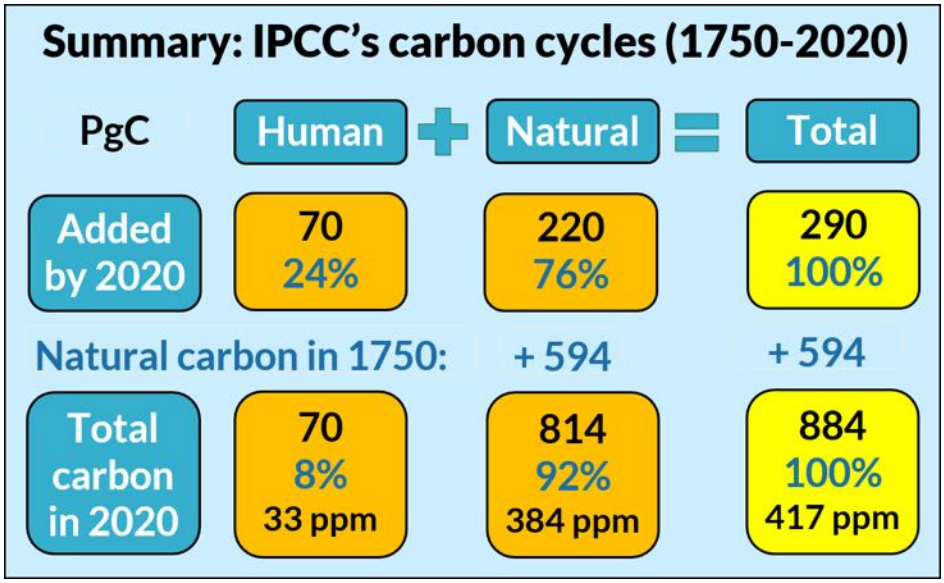

Figure 10. Human carbon is 24% of Total Added and 8% of Total in Atmosphere.

4.3 Cawley's analogy confirms Berry's model

Andrews boldly claims,

> As the disconnect between current inventories and fundamental causes is subtle, an analogy may be helpful for understanding it. Cawley (2011) proposed a good one, worth repeating verbatim here:
>
> *Consider a married couple, who keep their joint savings in a large jar. The husband, who works in Belgium, deposits six euros a week, always in the form of six one-euro coins minted in Belgium but makes no withdrawals.*
>
> *His wife, who works in France, deposits 190 euros a week, always in the form of 190 one-euro coins, all minted in France. Unlike her husband, however, she also takes out 193 euro per week, drawn at random from the coins in the jar.*
>
> *At the outset of their marriage, the couple's savings consisted of the 597 French-minted one-euro coins comprising her savings.*
>
> *Clearly, if this situation continued for some time, the couple's savings would steadily rise by 3 euros per week (the net difference between total deposits and withdrawals).*
>
> *It is equally obvious that the increase in their savings was due solely to the relatively small contributions made by the husband, as the wife consistently spent a little more each week than she saved.*

Andrews adds for emphasis, showing he misunderstands the physics:

> Cawley goes to the trouble of showing with a Monte Carlo simulation that, after some time, Belgian coins make up only 3% of the inventory, even though they accounted completely for the savings increase.
>
> In a like manner human carbon, while a relatively small percentage of carbon in the present atmosphere, is completely responsible for the increase.

If Andrews had read and understood Berry's physics model, he might have understood that Cawley's analogy proves Berry's physics model is valid. Here is why.

Let S = Savings = 597 F

Let B = Belgium Deposits = 6 B per week

Let F = France Deposits = 190 F per week

Let W = Withdrawals = 193 (B or F) per week,

Use physics model (3) with $T_e = 1$ to describe the weekly evolution of B and F in the money jar,

$$dB/dt = 6 - 193\ B / (B+F) \quad (11a)$$

$$dF/dt = 190 - 193\ F / (B+F) \quad (11b)$$

The final terms in (11) represent the probability of selecting either a B or F coin.

In this analogy, the levels of B and F are increasing so there are no fixed balance levels. However, we can calculate the relative balance levels that depend upon their relative inflows.

Use physics model (4) to find their relative balance levels,

$$B_b / (B_b + F_b) = 6 / 196 = 0.0306 \quad (12a)$$

$$F_b / (B_b + F_b) = 190 / 196 = 0.9694 \quad (12b)$$

Equation (12a) shows the final percent of B in the jar is 3.06 percent, which is Cawley's result.

The difference is we don't need no stinkin' Monte Carlo simulation to solve this problem. Berry's physics model gives the answer at once. That is the power of the physics model.

Andrews is fooled by Cawley's analogy.

Andrews incorrectly claims for Theory (1) believers:

> We have seen that the statement "Human carbon in the present atmosphere is only 30% of the Industrial Age increase" is not the same as "Human emissions caused only 30% of the increase."
>
> Anthropogenic carbon can be the cause of the entire Industrial Age increase without being a large part of the present atmospheric composition.

Andrews thinks the B coins represent human carbon emissions, and argues they "accounted completely for the savings increase."

However, the B coins do not account for all the increase, just as human carbon emissions do not account for all the CO_2 increase. The B coins account for only 3.06% of the increase and the F coins account for 96.94% of the increase. The B coins are also responsible for 3.06% of the money in the bank.

It does not matter how many B or F coins were in the jar in the beginning, or who withdraws the coins. The only thing that matters is the ratio (or percentage) of their balance levels which is the ratio (or percentage) of their inflows.

Cawley's analogy proves Berry's (2021) physics model is correct and powerful.

Similarly, the best way to understand the impact of human and natural CO_2 on the CO_2 increase is to calculate IPCC's true human carbon cycle independently as Berry (2021) has done.

Human and natural carbon cycles are independent. Therefore, a calculation that human carbon has produced 25% of the CO_2 increase means it has caused 25% of the CO_2 increase.

Andrews (2023) says incorrectly,

> Ocean acidification has been observed and confirms what Net Global Uptake tells us: the primary reservoir, the oceans, have on balance globally been taking in net carbon, even while outgassing net carbon at some locations.

There are no data that show the net the source of the carbon added to the surface ocean. The data show levels, not flow directions. IPCC reports assume Theory (1) is true to then claim the added carbon comes from the atmosphere.

Berry (2021) shows it is more logical to assume that nature increased the natural carbon in the oceans, and this added ocean carbon flows into the atmosphere.

5. Why IPCC's Theory (1) is false

5.1 IPCC's Theory (1) needs a magic demon

IPCC (2007, p. 948) says the turnover time (T) for natural CO_2 is about four years.

> *Carbon dioxide* (CO_2) is an extreme example. Its turnover time is only about four years because of the rapid exchange between the atmosphere and the ocean and terrestrial biota.

However, IPCC (2013, p. 469) assumes human CO_2 turnover time is much larger than four years,

> The removal of human-emitted CO_2 from the atmosphere by natural processes will take a few hundred thousand years (high confidence).

Fig. 11 compares the two scenarios: IPCC's true human carbon cycle vs IPCC's Theory (1).

- IPCC's true human carbon cycle shows human carbon is 8% of atmospheric carbon as of 2020.
- IPCC's Theory (1) claims human carbon is 33% of atmospheric carbon.

There are no data that show human CO_2 stays in the atmosphere for thousands of years. IPCC makes this claim because Theory (1) requires this claim.

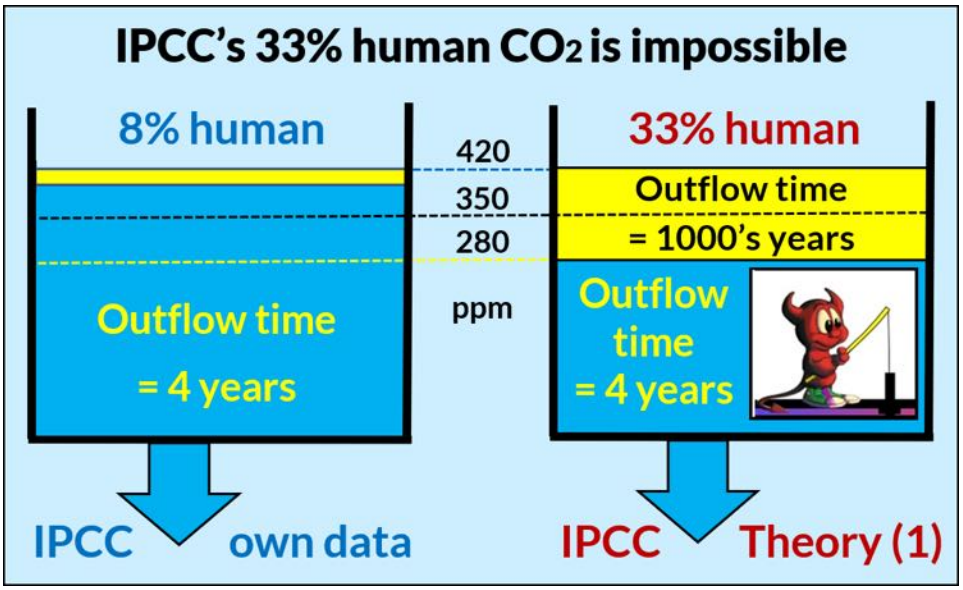

Figure 11. IPCC's true human carbon cycle that says human carbon is 8% of the carbon increase. IPCC's Theory (1) that says human carbon is 33% of the carbon increase.

Levels (like 33%) must be supported by relative inflows. So, the Theory (1) claim that human carbon is 33% of atmospheric carbon requires the inflow of human carbon to be 33% of the total (human plus natural) inflow. IPCC's own data show the inflow of human carbon is about 5% of the total carbon inflow.

To the first order approximation, the relative levels of human to natural CO_2 follow the relative inflows of human to natural CO_2, which produces their relative balance levels. (The second order

approximation includes the human addition of new carbon to the carbon cycle.)

Therefore, to support its Theory (1), the IPCC contradicts physics to claim the human CO_2 e-time is much larger than the natural CO_2 e-time. Andrews and others believe this charade.

So, IPCC's Theory (1) requires a magic demon in the atmosphere to capture human CO_2 and put it in a box with an e-time of 1000's of years, while it lets natural CO_2 flow freely out of the atmosphere with an e-time of 4 years.

But because human and natural CO_2 molecules are identical, human and natural CO_2 must have equal e-times, according to the physics *Equivalence Principle*. Therefore, Theory (1) is false.

5.2 $\delta^{14}C$ data show human emissions are insignificant

We learned in Section 3.2 that inflows set balance levels, and levels always approaches their balance levels.

The balance level of a mixture, like $\delta^{14}C$, is the non-dimensional ratio of the balance levels of its components. We used ratios of balance levels to quickly and accurately solve Cawley's analogy.

Forget Andrews' elaboration on isofluxes. Mixtures do not flow. Their components flow and their mixtures follow. The easiest way to understand components is with their relative balance levels, as we showed with Cawley's analogy.

Fig. 12 shows $\delta^{14}C$ data from 1955 to 2015. Turnbull et al. (2017) processed $\delta^{14}C$ data for Wellington, New Zealand, from 1954 to 2014.

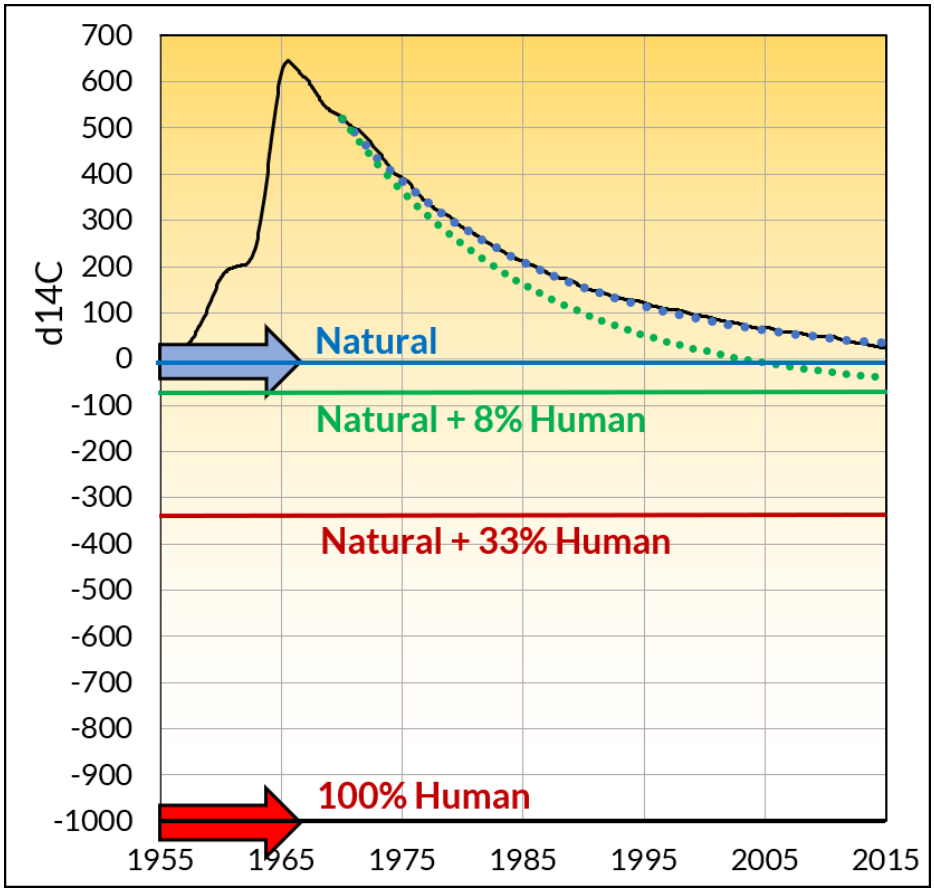

Figure 12. $\delta^{14}C$ data (Turnbull et al., 2017, black line) show it has returned toward its original balance level of zero even as the ^{12}C level increased.

The "natural" $\delta^{14}C$ balance level, defined by the average measured level before 1950, is zero, as shown by the blue horizontal line.

The blue dotted lines that fit the $\delta^{14}C$ decrease are a mathematical fit of (8) with a balance level of zero and an e-time of 16.5 years. The close mathematical fit to the $\delta^{14}C$ data shows the $\delta^{14}C$ natural balance level remained near zero and its e-time has been constant, at least since 1970.

Since 1970, the $\delta^{14}C$ level decreased toward its natural balance level of zero, showing the natural $\delta^{14}C$ balance level has not changed.

So, while the atomic bomb tests in the 1960s added ^{14}C to the atmosphere, thereby increasing $\delta^{14}C$, the bomb tests did not change the $\delta^{14}C$ balance level of zero.

Human carbon has no ^{14}C, so its $\delta^{14}C$ level is -1000, as shown in Fig. 12. Human carbon will dilute $\delta^{14}C$ inflow and thereby lower the $\delta^{14}C$ balance level below zero.

If human CO_2 were truly 33% of atmospheric CO_2 as IPCC's Theory (1) claims, this would lower the $\delta^{14}C$ balance level to -330 as shown by the horizontal red line. Data show this has not happened, so IPCC's Theory (1) is false.

If human CO_2 were 8% of atmospheric CO_2 as Berry (2021) calculates using IPCC's data, this would lower the $\delta^{14}C$ balance level to -80 as shown by the horizontal green line. But even this has not happened. Fig. 12 indicates human carbon in the atmosphere is less than 4%, contradicting IPCC's natural carbon cycle data.

The $\delta^{14}C$ balance level has remained near zero, showing human ^{12}C inflow has not lowered the $\delta^{14}C$ balance level. Graven et al. (2020) agree. Their Figure 6 shows the observed $\delta^{14}C$ is still above zero as of about 2015 and it is not headed toward a negative value.

The Graven et al. plot of $\delta^{14}C$ below zero are not data but are projections after 2020 by an unreferenced model that is likely a climate model. We cannot trust climate models because they assume Theory (1) is true.

The bottom line is $\delta^{14}C$ data prove IPCC's Theory (1) is false.

5.3 A new theory: nature keeps $\delta^{14}C$ balance level constant

Our sections above have proved Theory (1) is false. In this section, we propose a new theory that is open to being proved false.

Berry's calculation of IPCC's true human carbon cycle is deductive and reproducible. By contrast, this $\delta^{14}C$ argument is inductive and a theory subject to being proved wrong.

The first question is, what caused ^{14}C to increase after 2000?

The second question is, what keeps the $\delta^{14}C$ balance level near zero?

Fig. 13, (improved from Berry, 2021) plots the following data:

- $\delta^{14}C$ (solid black line) and its curve fit after 1970 (dotted red line).
- ^{12}C increase scaled to zero (red sawtooth line).
- ^{14}C increase scaled to zero, is identical to the ^{12}C increase.
- ^{14}C total of natural plus bomb (blue sawtooth line).

As in Fig. 12, (8) fits the $\delta^{14}C$ data from 1970 to 2014 with a constant e-time of 16.5 years and constant balance level of zero.

The blue dotted line is a curve fit to the ^{14}C data using (8). This fit shows $^{14}CO_2$ has an e-time of 10.0 years. Harde and Salby (2021) found the same value using a different method.

The ^{12}C increases since 1955 (red sawtooth line) following Graven et al. (2020) and is scaled to fit zero in 1957 by multiplying ppm data by 3.1676.

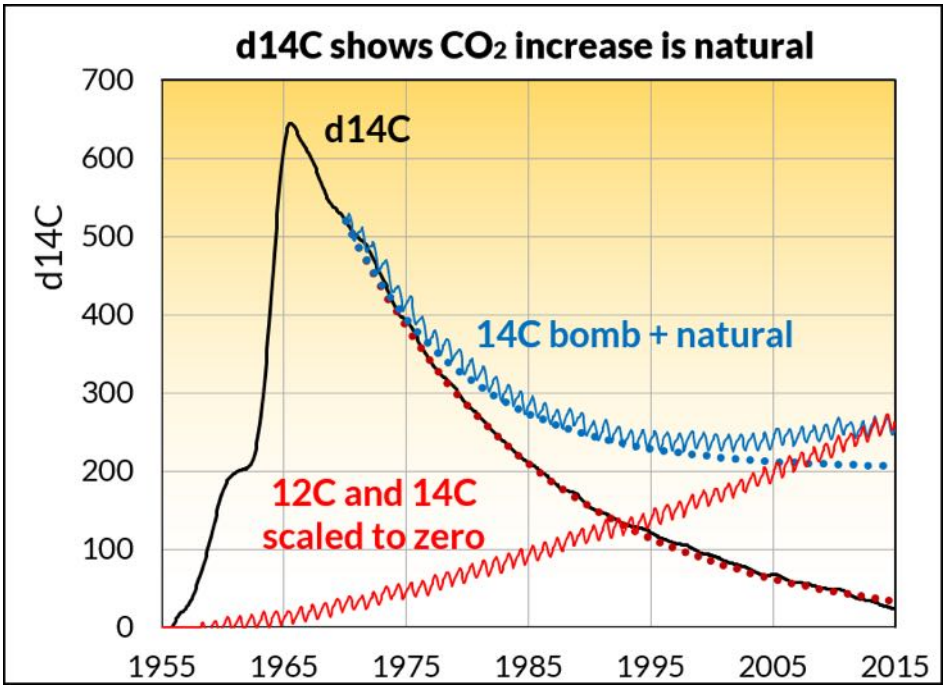

Figure 13. $\delta^{14}C$ data (Turnbull et al., 2017, black line), the physics model fit to $\delta^{14}C$ (red dotted line), ^{12}C scaled to zero (red sawtooth line), and ^{14}C (blue sawtooth line) total of natural plus bomb. The dotted blue line is a curve fit to the ^{14}C data.

$\delta^{14}C$ is a function of the ratio of $^{14}C/^{12}C$. The components, ^{14}C and ^{12}C, flow independently. Yet, $\delta^{14}C$ has kept its balance level near zero for a long time.

Andrews (2023) asks,

> If the ~30% increase [of ^{14}C] does not include lingering bomb carbon as it certainly appears to, what caused it?

Andrews thinks Caldeira et al. (1998) have the correct answer. They say the flow of human carbon from the atmosphere into the oceans drives ^{14}C out of the oceans and into the atmosphere. They predict that ^{14}C will go up after 1990, but they also predict $\delta^{14}C$ will go negative after 2010.

However, the $\delta^{14}C$ balance level has remained at zero which contradicts their predictions, and the Caldeira et al. model assumes Theory (1) is true, which negates their conclusions.

Harde and Salby (2021) present a better model. They assume the $^{14}CO_2$ and $^{12}CO_2$ balance levels have increased in proportion due to the re-emission of ^{12}C and ^{14}C from external reservoirs in proportion to their direct absorption rate, thereby keeping $\delta^{14}C$ close to zero.

We propose another theory for the increase in ^{14}C, that extends Harde and Salby (2021).

Our theory says that, somehow, through rain and shine, nature keeps $\delta^{14}C$ near zero.

Our theory says, the rise in ^{12}C, while keeping $\delta^{14}C = 0$, causes the ^{14}C increase. This correctly predicts the observed increase in ^{14}C.

Our theory is based on the following observations:

1. $\delta^{14}C$ has remained near zero for the last, say, 100,000 years, sufficient to allow carbon dating. It is likely that the $^{12}CO_2$ and $^{14}CO_2$ levels have changed up and down during that time.
2. $\delta^{14}C$ decreased smoothly since 1970 toward its original balance level of zero with a constant e-time of 16.5 years.

3. The $\delta^{14}C$ balance level stayed near zero throughout the bomb pulse.

We cannot explain how nature may have kept the $\delta^{14}C$ balance level and e-time constant. But we cannot accept that these have remained constant by mere coincidence. Somehow, nature must control the $\delta^{14}C$ balance level that has remained unchanged since 1950.

The ^{14}C natural (non-bomb) increase since 1955 is the same line as the ^{12}C increase because the $\delta^{14}C$ balance level remained near zero.

Were it not for the bomb ^{14}C, the natural increase in ^{14}C (blue sawtooth line) would have followed the ^{12}C increase (red sawtooth line) while $\delta^{14}C$ remained at zero.

It may be easier to follow this if we imagine two separate carbon cycles, one for natural ^{14}C and the other for bomb ^{14}C. Then we see that the bomb ^{14}C is depleted by 2015 and the continued ^{14}C increase is caused by the natural ^{12}C increase.

This is the simplest (Occam's Razor) explanation for the increase in ^{14}C. That does not mean it is correct, but it is a theory we can use until someone proves it is false.

5.4 Equilibrium percentage levels sets effect of human CO_2

Pollard (2022) determined the global CO_2 emissions from freshwater ecosystems is some 60 times larger than IPCC's data show. (See Figure 4, Section 3.5.)

To find the significance of this adjustment to IPCC's data for its natural carbon cycle at equilibrium, we inserted this change into the physics carbon cycle program of Berry (2021). Since IPCC's equilibrium natural carbon cycle levels are unchanged, Pollard's new data changes some flows and e-times reported in Berry (2021).

First, it changes the flows between the land and atmosphere reservoirs from 108 PgC per year to 166 PgC per year. Second, it changes the e-times T_{12} from 23.15 years to 12.96 years, and T_{21} from 5.45 years to 3.55 years, as needed to keep IPCC's levels at equilibrium.

The effect of these changes on the (Berry, 2021) predicted human-caused CO_2 increase of 33 ppm as of 2020 is zero.

This result shows the equilibrium reservoir levels, rather than the flows between the reservoirs, determine the effect of human CO_2 emissions on the increase in atmospheric CO_2.

Therefore, research can focus on getting more accurate measurements of the levels of the natural carbon cycle because changes in flows will be compensated by changes in e-times.

To test the model effect of changing the carbon reservoir levels, we doubled the IPCC equilibrium levels in Berry's physics model to 4300 PgC for land, 1800 PgC for surface ocean, and 80,891 PgC for deep ocean. The atmosphere level stayed the same because it is set by good data.

To keep these new levels at equilibrium required setting the following e-times: T_{12} to 7.65 years, T_{21} to 1.05 years, and T_{23} to 4.90 years. The ocean e-times stayed the same, suggesting the carbon level in the land reservoir has the strongest effect on the human increase in the CO_2 level.

These changes reduced the CO_2 increase caused by human emissions as of 2020 from 33 ppm to 18 ppm. So, to the first approximation, doubling the equilibrium levels for land, surface ocean, and deep ocean reduced the human CO_2 effect by about one-half.

6. Conclusions

IPCC's Theory (1) assumes incorrectly that human CO_2 is the dominant cause of the CO_2 increase above 280 ppm, or since 1750. Ardent Theory (1) believers include the American Meteorological Society, American Physical Society, CO_2 Coalition, Heartland Institute, and most schools, universities, and science teachers in America and the world.

IPCC's Theory (1) fails because it is based on invalid physics and circular reasoning. This proof

that Theory (1) is false undermines the whole scientific and political thesis of human-caused climate change.

Until Andrews (2023), Theory (1) believers censored and ignored proofs that Theory (1) is false. Andrews published their best arguments to support IPCC's Theory (1).

Berry's (2021) carbon cycle model supersedes other IPCC carbon cycle models in simplicity and accuracy. It uniquely replicates IPCC's natural carbon cycle.

Berry (2021) used IPCC's own natural carbon cycle data to calculate IPCC's true human carbon cycle. This true human carbon cycle predicts human carbon emissions have added only 33 ppm to atmospheric CO_2 as of 2020 while natural CO_2 emissions added 100 ppm of the CO_2 above 280 ppm, proving Theory (1) is false. This 33 ppm is 8% of the carbon in the atmosphere in 2020.

In addition, $\delta^{14}C$ data show natural CO_2 emissions dominate human CO_2 emissions, proving Theory (1) is false. The $\delta^{14}C$ data further suggest IPCC's natural carbon cycle data overpredict the effect of human CO_2 on atmospheric CO_2, and lower the 8% of human carbon in the atmosphere calculated from IPCC's data to less than 4%.

Pollard's (2022) determination that freshwater systems emit 60 times more CO_2 than IPCC's data show, led us to conclude the equilibrium level percentages of the natural carbon cycle control the effect of human CO_2 emissions on the CO_2 increase.

The relative equilibrium percentage levels of available natural carbon in land, air, surface ocean, and deep ocean is the strongest predictor of the effect of human carbon on atmospheric CO_2 because the independent human carbon cycle seeks the same percentage levels as the natural carbon cycle at equilibrium. For example, if the carbon levels of land, surface ocean, and deep ocean were each doubled, the human-caused CO_2 in the atmospheric would be reduced by about half, or to 18 ppm which would be 4% of the carbon in the atmosphere.

The bomb-caused increase in ^{14}C, and therefore in $\delta^{14}C$, is now almost depleted as $\delta^{14}C$ has returned to its original balance level of zero. Yet the ^{14}C level is now higher than in 1950. To explain this ^{14}C increase, we propose a theory that says nature keeps the $\delta^{14}C$ balance level equal to zero. This theory correctly predicts the non-bomb ^{14}C increase since 1950 is caused by the ^{12}C increase while nature kept the $\delta^{14}C$ balance level equal to zero. This is the simplest (Occam's Razor) explanation for the non-bomb ^{14}C increase since 1950.

Appendix: Andrews' fundamental errors

We all make progress step by step. Berry (2019) made several advancements and Berry (2021) extended the knowledge in Berry (2019).

Andrews (2023) makes the following fundamental, disqualifying errors:

1. Assumes Theory (1) is true when that is the subject under discussion.
2. Uses circular reasoning to argue Theory (1) is true.
3. Omits the natural carbon cycle in his Figure 1 arguments.
4. Does not realize this omission caused his argument to be circular.
5. Does not treat human and natural carbon cycles independently.
6. Does not realize Theory (1) uses different e-times for human and natural CO_2.
7. Uses isoflux arguments where he should have used balance levels.
8. Thinks Cawley's analogy supports Adrews but Cawley's analogy supports Berry (2021).
9. Uses the meaningless term "characteristic time" rather than e-time.
10. Says "characteristic time for the mixing can be seen to be about one decade" without referencing Berry (2021) and Harde and Salby (2021) who were the first to calculate,

independently, the $^{14}CO_2$ e-time is 10.0 years.

11. Says, incorrectly, the increase of $^{14}CO_2$ after 2000 was caused by the bomb $^{14}CO_2$.
12. Says, without proof, "Eventually, around 2000, $^{14}C/Ctot$ in the atmosphere was again less than it was in the oceans for the first time since the early 1950's. This again caused a net flow, an isoflux, of ^{14}C from the oceans to the atmosphere."
13. Says, incorrectly, "... quantitative analyses have been performed by (Caldiera et al.1998), and more recently by (Graven et al. 2020). The Caldeira analysis preceded and anticipated the rise in ^{14}C concentration beginning about 2000."
14. Says, incorrectly, "Isoflux effects explain and dominate the evolution of ^{14}C distributions… over the last 100 years."
15. His bad science includes (a) omitting data available to solve a problem, (b) not recognizing his invalid assumptions, (c) using circular reasoning, and (d) using complicated theories when simpler theories are available.
16. Says "That progress is helped when the originators of the wrong ideas acknowledge their errors and find constructive ways to contribute," but he does not apply his suggestion to himself.
17. Says "Successful predictions are the hallmark of good science," incorrectly suggesting correct predictions prove a theory is true.
18. Says "Scientific progress also relies on the use of empirical data to weed out ideas that may be original but are also just plain wrong," but he cannot prove Berry (2021) is wrong.
19. Says "The unconventional ideas critiqued here have been around for well over a decade. It should not have been necessary for this article to refer to a 2011 paper to, once again, refute them," when he has not proved Berry (2021) is wrong and Cawley (2011) proves Andrews is wrong and Berry is correct.

Guest-Editor: Jan-Erik Solheim; Reviewers: anonymous.

Acknowledgements

My thanks to all who have helped me continue my climate physics research by commenting and challenging me on my website, by reviewing my papers, by encouraging me to pusue excellence, by simply being my friend, and especially to my wife, Valerie, who has been essential to my continuing research work.

Funding

The author received no financial support for this work.

Conflicts of Interest

The Author declares he has no known competing financial interests or personal relationships that could have appeared to influence the work reported in this paper.

References

Andrews, D.E. 2023: *Clear Thinking about Atmospheric* CO_2. Science of Climate Change, vol. 3.1, pp 1-13. https://doi.org/10.53234/scc202301/20

Berry, E.X, 1967: *Cloud droplet growth by collection*. J. Atmos. Sci. 24, 688-701. DOI:

https://doi.org/10.1175/1520-0469(1967)024<0688:CDGBC>2.0.CO;2

Berry, E.X, 1969: *A mathematical framework for cloud models*. J. Atmos. Sci. 26, 109-111. https://moam.info/a-mathematical-framework-for-cloud-models-edberry-com_59a6a1c81723dd0c40321bda.html

Berry, E. X and Reinhardt, R.L. 1974a: *An analysis of cloud drop growth by collection. Part I. Double distributions*. J. Atmos. Sci., **31,** 1814–1824. https://doi.org/10.1175/1520-0469(1974)031<1814:AAOCDG>2.0.CO;2

Berry, E. X and Reinhardt, R.L. 1974b: *An analysis of cloud drop growth by collection. Part II. Single initial distributions.* J. Atmos. Sci., **31,** 1825–1831. https://doi.org/10.1175/1520-0469(1974)031<1825:AAOCDG>2.0.CO;2

Berry, E. X and Reinhardt, R.L. 1974c: *An analysis of cloud drop growth by collection. Part III. Accretion and self-collection*. J. Atmos. Sci., **31,** 2118–2126. https://doi.org/10.1175/1520-0469(1974)031<2118:AAOCDG>2.0.CO;2

Berry, E. X and Reinhardt, R.L. 1974d: *An analysis of cloud drop growth by collection. Part IV. A new parameterization.* J. Atmos. Sci., **31,** 2127–2135. https://doi.org/10.1175/1520-0469(1974)031<2127:AAOCDG>2.0.CO;2

Berry, E.X, 2019: *Human* CO_2 *emissions have little effect on atmospheric* CO_2. International Journal of Atmospheric and Oceanic Sciences. Volume 3, Issue 1, June, pp 13-26. https://doi.org/10.11648/j.ijaos.20190301.13

Berry, E.X, 2020: *Climate Miracle: There is no climate crisis. Nature controls the climate*. Published in the United States by Amazon. 70 pp. https://www.amazon.com/dp/B08LCD1YC3/

Berry, E.X, 2021: *The Impact of Human* CO_2 *on Atmospheric* CO_2, Science of Climate Change, vol. 1, no.2, pp 1-46. https://doi.org/10.53234/scc202112/13

Burton, D. and G. Wrightstone, 2022: *The* CO_2 *Coalition is wrong because its physics is wrong*. CO_2 Coalition and Heartland censor good science. (edberry.com)

Caldeira, K., Raul,G. H., and Duffy,P. B.,1998: *Predicted net efflux of radiocarbon from the ocean and increase in atmospheric radiocarbon content*. Geophysical Research Letters, 25(20), 3811-3814. https://doi.org/10.1029/2001GL014234

Cawley, G. C., 2011: *On the atmospheric residence time of anthropogenically sourced* CO_2." Energy Fuels 25, 5503–5513, https://dx.doi.org/10.1021/ef200914u.

Forrester, J.W., 1968, 2022: *Principles of Systems*. System Dynamics Society. 392 pp. Principles of Systems: Text and Workbook Chapters 1 through 10: Forrester, Jay W: 9781935056188: Amazon.com: Books

Graven, H., Keeling, R.F., & Rogelj, J. ,2020: *Changes to carbon isotopes in atmospheric* CO_2 *over the industrial era and into the future* Global Biochemical Cycles, 34, e2019GB006170. https://doi.org/10.1029/2019GB006170

Harde, H. 2017: *Scrutinizing the carbon cycle and* CO_2 *residence time in the atmosphere*. Global and Planetary Change. 152, 19-26. https://doi.org/10.1016/j.gloplacha.2017.02.009

Harde, H. 2019: *What Humans Contribute to Atmospheric* CO_2*: Comparison of Carbon Cycle Models with Observations.* International Journal of Earth Sciences. Vol. 8, No. 3, pp. 139-159. http://www.sciencepublishinggroup.com/journal/paperinfo?journalid=161& https://doi.org/10.11648/j.earth.20190803.13

Harde, H. and Salby, M. L. 2021: *What Controls the Atmosphere* CO_2 *Level?* Science of Climate Change, Vol. 1, No. 1, August 2021, pp. 54-69. https://doi.org/10.53234/scc202111/28.

IPCC. 2007: *Climate Change 2007 - The Physical Science Basis. Contribution of Working Group 1 to the Fourth Assessment Report of the IPCC***.** Annex 1: Glossary: Lifetime.

https://www.ipcc.ch/site/assets/uploads/2018/02/ar4-wg1-annexes-1.pdf

IPCC, 2013: Ciais, P., Sabine, C., Bala, G., Bopp, L., Brovkin, V., Canadell, J., Chhabra, A., DeFries, R., Galloway, J., Heimann, M., Jones, C., Le Quéré, C., Myneni, R.B., Piao, S., and Thornton, P. 2013: *Carbon and Other Biogeochemical Cycles.* In: Climate Change 2013: The Physical Science Basis. Contribution of Working Group I to the Fifth Assessment Report of the Intergovernmental Panel on Climate Change [Stocker, T.F., Qin, D., Plattner, G.-K., Tignor, M., Allen, S.K. Boschung, J., Nauels, A., Xia, Y., Bex, V., and Midgley, P.M. (eds.)]. Cambridge University Press, Cambridge, United Kingdom and New York, NY, USA. https://www.ipcc.ch/site/assets/uploads/2018/02/WG1AR5_Chapter06_FINAL.pdf

Kemeny, J.G., J.L. Snell, 1960: *Finite Markov Chains*. Springer. 238 pp. Amazon.com: Finite Markov Chains: With a New Appendix "Generalization of a Fundamental Matrix" (Undergraduate Texts in Mathematics): 9780387901923: Kemeny, John G., Snell, J. Laurie: Books

Pickering, K., 2016: *Comment on cause of* CO_2 *increase*. Murry Salby: Atmospheric Carbon, 18 July 2016 (edberry.com)

Pollard, P.C., 2022: *Globally, Freshwater Ecosystems Emit More* CO_2 *Than the Burning of Fossil Fuels*. Environ. Sci., 06 June 2022. https://doi.org/10.3389/fenvs.2022.904955

Salby, M.L. and Harde, H. 2021: *Control of Atmospheric* CO_2*: Part I: Relation of Carbon 14 to the Removal of* CO_2. Science of Climate Change, 1, no.2. https://doi.org/10.53234/scc202112/210

Salby, M.L. and Harde, H. 2022: *Theory of Increasing Greenhouse Gases*. Science of Climate Change, Vol. 2.3, pp 212-238. https://doi.org/10.53234/scc202212/17

Scarborough, J.B. 1966: *Numerical Mathematical Analysis*. Sixth Edition. The John Hopkins Press. 608 pp. Numerical Mathematical Analysis: Scarborough, Dr. William, Scarborough, James B.: 9780801805752: Amazon.com: Books

Segalstad, T.V. 1998: *Carbon cycle modelling and the residence time of natural and anthropogenic atmospheric* CO_2*: on the construction of the Greenhouse Effect Global Warming dogma*. In: Bate, R. (Ed.): Global warming: the continuing debate. ESEF, Cambridge, U.K. (ISBN 0952773422): 184-219. http://www.CO_2web.info/ESEF3VO2.pdf

Schroder, H., 2022: *Less than half of the increase in atmospheric* CO_2 *is due to the burning of fossil fuels* Science of Climate Change vol. 2, no. 3, pp 1-19. https://doi.org/10.53234/scc202112/17

Skrable, K., Chabot, G., French, C., 2022a: *World Atmospheric* CO_2*, Its* ^{14}C *Specific Activity, Non-fossil Component, Anthropogenic Fossil Component, and Emissions* (1750-2018), Health Physics: February 2022 - Volume 122 - Issue 2 - p 291-305 doi: 10.1097/HP.0000000000001485

Skrable, K., Chabot, G., French, C., 2022b: *Components of* CO_2 *in 1750 through 2018 Corrected for the Perturbation of the* $^{14}CO_2$ *Bomb Spike",* Health Physics: November 2022 - Volume 123 - Issue 5 - p 392 https://doi.org/10.1097/HP.0000000000001606.

Turnbull, J.C., Mikaloff Fletcher, S.E., Ansell, I., Brailsford, G.W., Moss, R.C., Norris, M.W., and Steinkamp, K. 2017: *Sixty years of radiocarbon dioxide measurements at Wellington, New Zealand: 1954–2014.* Atmos. Chem. Phys., 17, pp. 14771–14784. https://doi.org/10.5194/acp-17-14771-2017

Analytical Carbon Cycle Impulse Response Function

Correspondence to jonas.w.rosen@gmail.com

Vol. 3.1 (2023)
pp. 92-106

Jonas Rosén, Sandviken, Sweden
Sten Kaijser, Department of mathematics, Uppsala University, Sweden

Abstract

The purpose of this paper is to derive an analytical impulse response function (IRF), for the carbon cycle between atmosphere and sea. The analysis is starting from the Box-Diffusion model (BDM) given by Oeschger et al. The BDM is also the underlying model for the "sum of exponentials – IRF" presently used in many papers to describe the atmosphere/sea carbon cycle.

10 to 100 years is a relevant time scale when discussing the effect of anthropogenic emissions on the atmospheric carbon dioxide. We show that on this time scale there is an analytical IRF. Our view is that this analytical IRF is a better representation of the physics in the system than the presently used "sum of exponentials" IRF.

Another important conclusion is that there is only one characteristic time constant. All physics in the BDM can thus be represented with one characteristic time and an analytical IRF. With the values used in the BDM the characteristic time will be in the interval 80 – 145 years. This value is strongly dependent on assumed values of Revelle factor and eddy diffusion constant.

Keywords: Carbon Cycle Models; Bern model; Impulse response function; Box models; Diffusion;
Submitted 01-02-2022, Accepted 24-03-2023, https://doi.org/10.53234/SCC202301/25

1. Introduction

Carbon cycle models are important tools for understanding the atmospheric concentrations of carbon dioxide.

A central model in this context is the so-called Bern Model. It has gradually been developed over the last 50 years. One can trace the basic ideas behind the model to a paper by Suess and Revelle (1957) [1].

The present foundation for the Bern model is a work by Oeschger et al. (1975) [2]. The model was further developed by Siegenthaler (1983) [3], who included a formalism for direct contact between the atmosphere and the so-called deep sea.

Maier-Reimer et al. (1987) [4] introduce the concept of impulse response function (IRF), "Transport and storage of CO_2 in the ocean". They fitted a five-term exponential sum to the numerically calculated impulse response for the Box Diffusion model.

This five-term exponential impulse response function is commonly referred to in modern articles about Carbon Cycle, e.g Joos et al. (2013) [5]. There have been later modifications to this IRF, but the basic characteristics of Maier-Reimer et al´s IRF are representative for presently used

models.

A very short summary of the evolution of today's carbon cycle models is:

- Suess and Revell, they introduce the so called Revelle factor
- Oeschger et al., developed the Box Diffusion Model
- Maier-Reimer et al., introduced the impulse response function (IRF)

This work will describe a mathematical analysis of the base model – Oeschger et al.´s (1975) [2] Box Diffusion Model which is the foundation for today's Carbon Cycle models.

The aim with this paper is to present an analytically derived IRF, instead of the curve fitted IRF introduced by Maier-Reimer et al. (1987) [4].

We will also show that the IRF of the Box Diffusion Model (BDM) is strongly dependent on the Revelle factor. The Revelle factor describes the solubility of $CO_2(g)$ as function of total dissolved inorganic carbon (DIC). The Revelle factor was first calculated by Bolin and Eriksson (1959) [8]. They reached the conclusion that for a system with sea water and carbon dioxide containing atmosphere the R-value is 12.5. Oeschger et al. use an R-value of 10. Bolin and Eriksson also conclude that the R-value for a system with sea water, limestone (in the sea water), and carbon dioxide containing atmosphere is 2.4.

An R-value equal to 1 means that the carbon outflux from the sea is proportional to the carbon content in the sea.

2. The "Box Diffusion Model"

The BDM (Box Diffusion Model) consists of two boxes, atmosphere, and surface sea (also called mixed layer), the deep sea and the biosphere. The concentration of carbon dioxide in a box is uniform within the box.

Carbon dioxide in the mixed layer is transported to the deep sea by "eddy diffusion", and the transport within the deep sea is also controlled by so called eddy diffusion. Eddy diffusion is modelled by the diffusion equation, with a constant diffusion coefficient.

In this analysis we will omit the biosphere, which is equivalent to set the "biological growth factor" to zero in the BDM.

The reason why we omit the biosphere is that our analytical IRF is compared with Maier-Reimer´s (1987) [4] curve fitted exponential IRF. That IRF is only for the atmosphere-ocean system, why the biosphere is not needed for comparisons of the mathematics.

If one wants a complete carbon cycle model that should of course include the biosphere. Future work may develop models with our analytical IRF (representing the interaction between atmosphere and sea) and the biosphere included.

The BDM uses the following governing equations.

$$\frac{dn_a}{dt} = p + k_{ma}(N_m + R * n_m) - k_{am}(N_a + n_a) \qquad (1)$$

$$\frac{dn_m}{dt} = k_{am}(N_a + n_a) - k_{ma}(N_m + R * n_m) + K * \frac{\partial c_d}{\partial z}(z = 0) \qquad (2)$$

$$\frac{\partial c_d}{\partial t} = K\frac{\partial^2 c_d}{dz^2} \qquad (3)$$

$$\frac{N_m + n_m}{h_m} = C_d + c_d \; för \; z = 0 \qquad (4)$$

Eq. (4) follows from the boundary condition; carbon concentration at the top of deep sea (z=0) equals the concentration in the mixed layer

$$K\frac{\partial c_d}{dz} = 0 \; för \; z = h_d \; ; \;\; no \; flux \; through \; deep \; sea \; floor \qquad (5)$$

The symbols in the equations are:

$$N_i + n_i\,(t) = \frac{total\ amount\ of\ CO_2\ in\ reservoare\ i}{surface\ area}\ , i$$
$$= a\ (atmosphere), m\ (mixed\ layer), d\ (deep\ sea),$$

N *is the preindustrial equlibrium value (constant) and* n *is the deviation* $[\frac{mol}{m^2}]$

$C_d + c_d(t)$

$= CO_2$ *concentration in deep sea,* C_d *is constant and depth independent* $[\frac{mol}{m^3}]$

$p(t) = \frac{(CO_2\ production\ rate)}{surface\ area}\ [\frac{mol}{m^2 y}]$

$h_m = depth\ of\ mixed\ layer = 75\ m$

$h_d = depth\ of\ deep\ sea = 3725\ m$

$k_{am} = exchange\ rate\ atmosphere - mixed\ layer\ = \frac{1}{7.53\ yr}$

$k_{ma} = exchange\ rate\ mixed\ layer - atmosphere = \frac{1}{9.53\ yr}$

$K = eddy\ diffusion\ constant\ \approx 4000\frac{m^2}{yr}$

$R = Revell\ factor\ \approx 10$

$$k_{am} * N_a = k_{ma} * N_m \qquad (6)$$

The notation is the same as in the work of Oeschger et al. (1975) [2].

3. Analysis of the timescales in the Box Diffusion Model

The above are the basic equations of the Bern model. We now turn to our analysis of these equations. The following are thus our calculations, and not described by Oeschger et al. (1975) [2].

Consider only the atmospheric – mixed layer system (i.e., no diffusion to the deep sea). Use Eq. (6) in Eq. (1) and (2).

$$\frac{dn_a}{dt} = p + k_{ma} * R * n_m - k_{am} * n_a \tag{7}$$

$$\frac{dn_m}{dt} = k_{am} * n_a - k_{ma} * R * n_m \tag{8}$$

For p = a pulse with amplitude (area) 1, this equation system has the solution:

$$n_a = \frac{k_{ma} * R}{k_{am} + k_{ma} * R} * \left(1 + \frac{k_{am}}{k_{ma} * R} * e^{-(k_{am}+k_{ma}*R)*t}\right) \tag{9}$$

$$n_m = \frac{k_{am}}{k_{am} + k_{ma} * R} * \left(1 - e^{-(k_{am}+k_{ma}*R)*t}\right) \tag{10}$$

With current values of the constants, the time constant becomes about 1 year. The dynamic of this system is fast, i.e., the equilibrium sets in such a short time that one can consider the atmosphere-mixed layer as equilibrium for the times of interest, i.e., tens of years.

It is a reasonable approximation to set these to their equilibrium levels, i.e., the amount present in the total reservoir atmosphere + mixed layer is distributed according to:

$$n_a = \frac{k_{ma} * R}{k_{am} + k_{ma} * R} \approx 0.89 \tag{11}$$

This means that about 89 % of the total content in the combined reservoir is in the atmosphere.

$$n_m = \frac{k_{am}}{k_{am} + k_{ma} * R} \approx 0.11 \tag{12}$$

About 11 % of the total content in the combined reservoir is in the mixed layer.

The relation between mixed layer and atmosphere is given by:

$$n_m = \frac{k_{am}}{(k_{ma} * R)} * n_a = \alpha * n_a \tag{13}$$

Where $\alpha \approx 0.13$.

Atmosphere – mixed layer now becomes like one reservoir emptied by diffusion from the mixed layer down to the deep sea.

Under the approximation of instant equilibrium between atmosphere and mixed layer we get the following basic equations.

$$\frac{d(n_a + n_m)}{dt} = p + K * \frac{\partial c_d}{dz}(z = 0) \tag{14}$$

Use Eq. (13) in Eq. (14), which gives:

$$\frac{dn_a}{dt} = \frac{k_{ma} * R}{k_{am} + k_{ma} * R} * \left(p + K * \frac{\partial c_d}{dz}(z = 0) \right) = \beta * \left(p + K * \frac{\partial c_d}{\partial z}(z = 0) \right) \tag{15}$$

$$\beta = \frac{k_{ma} * R}{k_{am} + k_{ma} * R} \approx 0.89 \tag{16}$$

$$\frac{\partial c_d}{\partial t} = K * \frac{\partial^2 c_d}{\partial z^2} \tag{17}$$

With the boundary conditions:

$$c_d = \frac{n_m}{h_m}\,, \quad z = 0 \tag{18}$$

The carbon concentration in the deep sea is equal to the concentration in the mixed layer at the boundary.

$$\frac{\partial c_d}{\partial z} = 0\,, \quad z = h_d \tag{19}$$

The implication is that there is no net flow through the seabed.

Since diffusion is relatively slow, i.e., it takes a while for the concentration at the bottom of the deep sea to change, the second boundary condition, Eq. (19), can be ignored when one wants to

get an idea of the system's behavior over a 100-year period. It will be the same as viewing the deep sea as infinite.

Note that the system is now a kind of "1-box model" that is emptied by diffusion. The Bern model is thus a diffusion model.

4. Derivation of an analytical Impulse Response Function

Eq. (15) can be solved analytically, under the assumption that the diffusion time in the deep sea is long compared to the time scale of interest.

Now we apply Laplace transformation of the equations. Denote the Laplace transform by the corresponding capital letter and the transform variable with s. For example, $N_a(s)$ is thus the Laplace transform of $n_a(t)$ given by equation 20, and is not related to the equilibrium value N_a.

$$N_a(s) = \int_0^\infty e^{-st} * n_a(t)\, dt \tag{20}$$

Eq. (17) becomes:

$$s * C_d(s) = K * \frac{\partial^2 C_d(s)}{dz^2} \tag{21}$$

Which has the general solution:

$$C_d(s) = a1(s) * e^{-z*\sqrt{\frac{s}{K}}} + a2(s) * e^{z*\sqrt{\frac{s}{K}}} \tag{22}$$

Since the concentration must go towards zero as the depth moves towards infinity, it follows that a2(s)=0.

Eq. (18) gives $a1(s) = N_m(s)/h_m$. Insert $C_d(s)$ as given by Eq. (22) into the Laplace transform of Eq. (15),

$$s * N_a(s) = \beta * \left(P(s) - \frac{N_m(s)}{h_m} * \sqrt{s * K} \right) = \beta * \left(P(s) - N_a(s) * \frac{\alpha}{h_m} * \sqrt{s * K} \right) \tag{23}$$

Let

$$\gamma = \beta * \alpha * \sqrt{K}/h_m \propto \sqrt{K}/R \tag{24}$$

We now get the equation,

$$N_a\,(s) = \beta * P(s)/(s + \gamma * \sqrt{s}\ ) \tag{25}$$

Consider the case that the carbon dioxide is added as an impulse with area 1. This means that P(s) = 1.

By rewriting the expression:

$$N_a(s) = \frac{\beta * 1}{\gamma} * \left(\frac{1}{\sqrt{s}} - \frac{1}{\sqrt{s} + \gamma}\right) \tag{26}$$

Now, define a time constant $\varphi = 1/\gamma^2$, or

$$\varphi = \left(\frac{h_m * (k_{am} + k_{ma} * R)}{k_{am} * \sqrt{K}}\right)^2 \tag{27}$$

The expression can now be inverse transformed using tables. The solution is:

$$n_a(t) = \beta * e^{t/\varphi} * erfc(\sqrt{t/\varphi}\ ) \tag{28}$$

This is thus the impulse response function of the Bern model, under the assumption of an infinite deep sea and an instant equilibrium between atmosphere and mixed layer. It represents the dynamics of the BDM on a time scale ten to hundreds of years.

It is this expression that in later articles is approximated with a sum of exponential functions.

Using the values given in Oeschger et al´s (1975) [2] paper, φ will have a value in the range of 80 – 145 years, with an expected value of 111 years. It should however be noted that Oeschger et al. assume that the Revelle factor has a value about 10 with high certainty. A lower value of the Revelle factor will have a significant effect on the φ – value.

Limit values can be checked:

When t=0, $n_a = \beta$ which is the pulse distribution between atmosphere and mixed layer.

When t becomes large, the approximate expression of complementary error function can be used, $erfc(\gamma\sqrt{t}) \approx \frac{e^{-\gamma^2 t}}{\gamma\sqrt{\pi t}}$

From this one can see that the carbon dioxide content of the atmosphere will go towards zero as $1/\sqrt{time}$ (assuming infinite deep sea!) which is consistent with a diffusion process.

4.1 How long does the "infinite deep-sea approximation" apply?

A rough estimate is to take the "diffusion distance" $2 * \sqrt{K * t}$ and compare with the sea depth of 3725 m. It takes about 1800 years for the "diffusion distance" to be comparable to the depth of the sea. When looking at a period of about 100 years, "infinite deep sea" is a good description of the dynamics of the system.

4.2 Equilibrium

If one considers that the sea is not infinite, a balance will of course occur where the residual value of the atmosphere's carbon dioxide content is greater than zero.

This equilibrium can be easily calculated:

From the boundary condition that the carbon dioxide flow at the bottom of the sea should be zero, it follows that the concentration c_d must be a constant at equilibrium.

The equilibrium atmospheric content can be calculated by inserting Eq. (13) and Eq. (18) into Eq. (29) below (the sum of the reservoir´s content must equal the injected pulse).

$$c_d * h_d + n_m + n_a = 1 \tag{29}$$

After a pulse injection (of area 1) in the atmosphere,

$$n_{a_{eq}} = \frac{1}{1 + \alpha * \left(1 + \frac{h_d}{h_m}\right)} \approx 0.13 \tag{30}$$

The perpetual contribution to the atmosphere is reinforced by the Revelle factor. Instead of about 2 % remaining (current equilibrium distribution atmosphere – ocean), about 13 % will stay forever.

At a first glance at Eq. (30), it looks as if the equilibrium atmospheric content is dependent on the depth of the mixed layer. This is however not really the case.

$k_{ma} = 1/residence\ time\ in\ the\ mixed\ layer = 1/\tau_m$

It is reasonable to assume that the residence time is proportional to volume, meaning:

$\tau_m = \mu * h_m$, $where\ \mu\ is\ a\ constant$

Inserting this into Eq. (30) gives:

$$n_{a_{eq}} = \frac{1}{1 + \alpha * \left(1 + \frac{h_d}{h_m}\right)} = \frac{R}{R + k_{am} * \mu * (h_m + h_d)} \quad (31)$$

This equation is independent of where one chooses to end mixed layer and start deep sea.

4.3 The biosphere

The biosphere is included in the BDM. The full equation for the atmosphere in Oeschger et al.´s work (1975) [2] is:

$$\frac{dn_a}{dt} = p + k_{ma}(N_m + R * n_m) - k_{am}(N_a + n_a) - \varepsilon * F * \left(\frac{n_a(t)}{N_a} - \frac{n_a(t-\tau)}{N_a}\right) \quad (32)$$

where

$\varepsilon = biological\ growth\ factor$
$F = flux\ to\ biosphere\ [moles/year]$
$\tau = biospheric\ time\ delay\ for\ CO_2$

In the derivation of the analytical IRF we set $\varepsilon = 0$, which is Eq (1) and is equivalent to a constant biosphere.

The purpose with this paper is to derive an analytical IRF for the system atmosphere – sea. This analytical IRF is comparable to the curve fitted exponential IRF derived by Maier-Reimer (1987) [4], which is frequently used in present carbon cycle models, e.g., Joos et al. (2013) [5]. The curve fitted IRF is calculated from numerical simulations with $\varepsilon = 0$. This means that the curve fitted IRF and the analytical IRF are based on the same governing equations.

The biosphere (as modelled in Oeschger et al´s work) can easily be included in the analytical IRF if we do either of the following approximations:

1- assume that $n_a(t) - n_a(t-\tau) \approx constant * \tau$ $(atmospheric\ increase\ is\ linear)$

2- assume that $(n_a(t) - n_a(t-\tau))/\tau \approx \frac{dn_a}{dt}(t)$

5. The development of the exponential IRF

Maier-Reimer et al. (1987) [4] introduced the Impulse Response Function (IRF) concept for carbon cycle models.

They fitted a sum of exponential functions to a numerical calculated impulse response of the Bern model. The idea was to get an expression that could be used in analytical analysis.

They obtain the following expression for the IRF (for small disturbances):

$$IRF = 0.131 + \ 0.201 * e^{-\frac{t}{363}} + \ 0.321 * e^{-\frac{t}{74}} + 0.249 * e^{-\frac{t}{17.3}} + 0.098 * e^{-\frac{t}{1.9}} \quad (33)$$

Following their article, they comment that this expression is in good agreement with numerically calculated IRF based on Siegenthaler's work (1983) [3].

Siegenthaler (1983) [3] use the same basic equations as Oeschger et al.(1975) [2], but includes a direct contact between the deep see and the atmosphere in the model.

The above IRF is compared to Siegenthaler's reference case with zero direct contact between deep sea and atmosphere, which is equivalent to Oeschger´s model (Bern model).

It can thus be concluded that the IRF derived by Maier-Reimer et al. (1987) [4] is based on the governing equations developed in Oeschger et al.´s work.

Figure 1 shows the impulse response based on Eq. (28) compared to the IRF given by Eq. (33) The agreement is good.

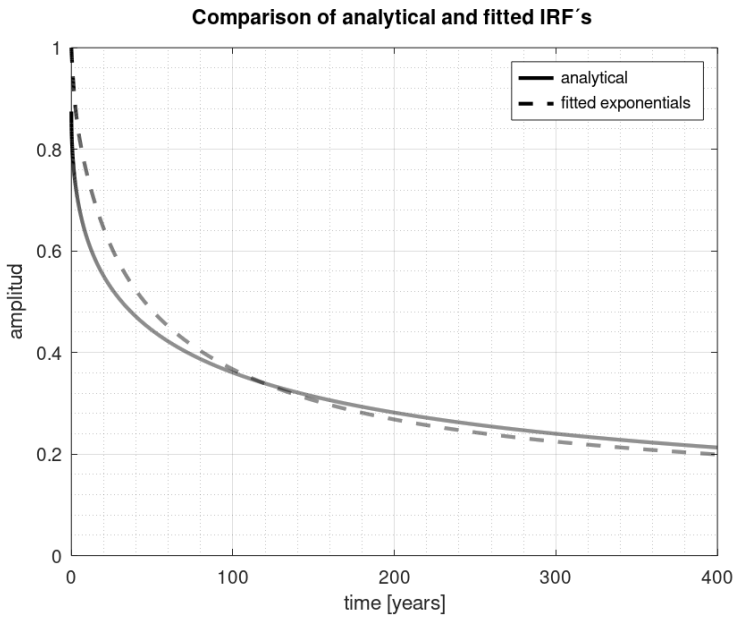

Figure 1 – Impulse response according to equation 28 compared to IRF derived by Maier-Reimer et. al {4}.

Figure 2 shows how the analytical impulse response given by Eq. (28) depends on the Revelle factor.

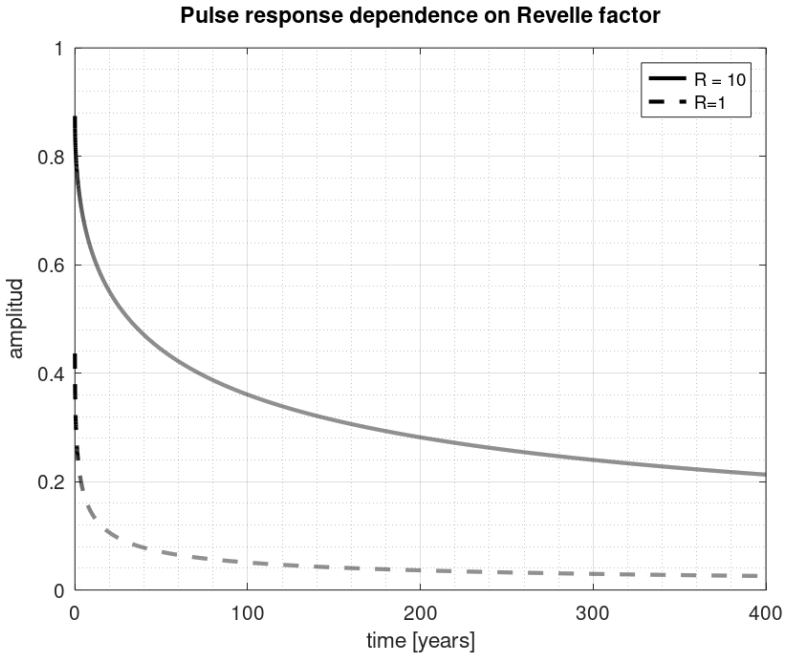

Figure 2 – Impulse response according to Eq. (28), with different Revelle values.

The IRF derived by Reimer-Maier is very similar to IRF´s used in later articles/ models. E.g., ACC2, Tanaka et al. (2007) [6], use an IRF of the form:

$$IRF = 0.132 + 0.311 * e^{-\frac{t}{236.5}} + 0.253 * e^{-\frac{t}{59.5}} + 0.209 * e^{-\frac{t}{12.2}} + 0.095 * e^{-\frac{t}{1.27}} \quad (34)$$

There is no direct exchange between deep sea and the atmosphere in the ACC2 model, which means that it is consistent with Oeschger et al.´s Box-Diffusion model.

The wording in the ACC2 paper is "ACC2 accounts for the influence of the solubility pump from the temperature change by calculating the thermodynamic equilibria explicitly, but it cannot resolve the influence from the thermohaline circulation and the ocean ventilation (Falkowski et al., 2000)"

It is clear that presently used IRF´s are based on Oeschger et al´s work, and that there is no direct contact between atmosphere and deep see included in the IRF´s.

6. Anthropogenic contribution to atmospheric carbon dioxide level

The analytical IRF derived in the previous section, Eq. (28), can be used to calculate the anthropogenic contribution to the increased carbon dioxide content in the atmosphere.

The accumulated atmospheric carbon dioxide is given by the convolution.

$$C_{atm}(t) = C_{atm0} + \int_{to}^{t} IRF(t-\tau) * H(\tau)\, d\tau \quad (35)$$

$C_{atm} = atmospheric\ CO_2\ content\ in\ ppm$

$C_{atm0} = 280\ ppm = \ reference\ level\ at\ year\ 1750$

$H(t) = anthropogenic\ contribution$

According to Harde (2019) [7] the anthropogenic contribution can be described by the following expression.

$$H(t) = h_0 * \left(e^{\frac{t-t0}{\delta}} + h_1\right) \quad (36)$$

Where:

$h_0 = 0.026\ ppm/yr$
$\delta = 50\ yr$
$t0 = 1750$
$h_1 = 4$

Inserting the analytical IRF given by Eq. (28), and Eq. (36) into Eq. (35) makes it possible to calculate how much human emissions has added to the atmospheric concentration as function of the Revelle factor.

Eq. (35) must be numerically integrated. The value is 160 ppm, using the data in the BDM. This is higher than the observed atmospheric increase. The reason can be that the BDM underestimates sea absorption, or that there are other sinks than the ocean. E.g., the biosphere. If one assumes that the emission from land/biosphere has increased due to increased temperature, then it is likely that the BDM underestimates the sea absorption.

Eq. (35) is strongly dependent on the Revelle factor (R-value).

Since it is possible to assume different R-values, Eq. (35) is analyzed with respect to this parameter.

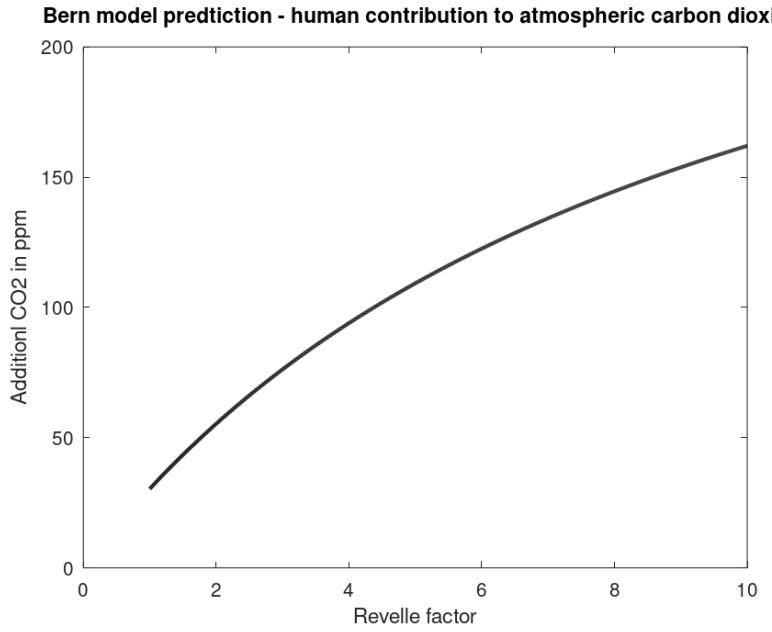

Figure 3. Atmospheric carbon dioxide increases due to human emissions, from 1750 – 2020, as function of the Revelle factor.

Figure 3 shows the increase in atmospheric carbon dioxide concentration (due to anthropogenic emissions) year 2020 as function of the Revelle factor (R-value).

The calculation is based on:

- Oeschger et al.´s Box-Diffusion model (Bern model)

- Harde´s equation for human emissions (36)

7. Summary and Discussion

We have developed an analytical expression for the Bern model impulse response function (IRF). The derivation is based on two assumptions:

- neglect the time to establish equilibrium between the atmosphere and mixed layer. The argument is that the timescale for equilibrium atmosphere – mixed layer is short (about 1 year) compared to the timescale of interest.
- the deep sea has infinite depth. This approximation should be reasonable for times up to several hundreds of years.

The derived IRF is consistent for a system dominated by diffusion.

The analytical IRF also has a physical meaning. Our view is that this is an advantage since it is difficult to give a physical interpretation of a curve fitted equation.

The present use of the curve fitted exponential IRF is somewhat misleading. Since this type of IRF is correct for a box model, it is easy to view the underlying model as a box model. It is not. It is a diffusion model. Oeschger et al. comment that box models do not agree with observations,

why they propose a diffusion model instead of a box model. When one fits a box model IRF to the BDM it lacks physical meaning.

The exponential IRF gives the impression that there are some outflows which are very slow (exponentials with long time constant) and that a certain fraction of the outflow must pass through those "slow" outflows. That is of course not the case.

The analytical IRF derived in this paper reflects what actually is going on in the BDM. There is a fast but limited uptake in the surface sea (restricted by the Revelle factor). The additional CO_2 in the surface sea is transported away by a rather slow diffusion process. Since only a small fraction of the excess CO_2 is in the surface sea – only a small part of the addition is exposed to the downward diffusion.

One important feature is that the derived IRF only has one characteristic time constant, Eq. (27). That makes it possible to easily evaluate the effect of the parameters on the system dynamics.

It is a fact that the biosphere has a significant impact on the atmospheres CO_2 level, and the assumption about $\varepsilon = 0$ is a simplification. The same assumption is, however, done in Maier-Reimer et al.´s work when they introduce the exponential IRF.

The biosphere can rather easily be included in the present work if one assumes that the biosphere reacts to the change rate of atmospheric CO_2 (the time derivative). In the BDM they assume that the reaction is proportional to the present CO_2 minus the CO_2 some years ago (τ).

Funding

This research did not receive any specific grant from funding agencies in the public, commercial, or not-for-profit sectors.

Guest-Editor: Stein Bergsmark; Reviewers: anonymous.

Acknowledgments

We thank the editor as well as the reviewers for critical reading the manuscript and important advice.
.

References:

1. Revelle, R., Suess, H.E., 1957: *Carbon Dioxide Exchange Between Atmosphere and Ocean and the Question of an Increase of Atmospheric CO, during the Past Decades*, Tellus, 9:1, 18-27.
https://doi.org/10.3402/tellusa.v9i1.9075

2. Oeschger, H., Siegenthaler, U., Schtterer, U., Gugelmann, A., 1975: *A box diffusion model to study the carbon dioxide exchange in nature*, Tellus A, vol 27, pp. 168-192
https://doi.org/10.3402/tellusa.v27i2.9900

3. Siegenthaler, U., 1983: *Uptake of Excess C02 by an Outcrop-Diffusion Model of the Ocean*, Journal of Geophysical Research, vol 88, No. C6, pp. 3599-3608
https://doi.org/10.1029/JC088iC06p03599

4. Maier-Reimer, E., Hasselmann, K., 1987: *Transport and storage of CO_2 in the ocean ——an inorganic ocean-circulation carbon cycle model*, Climate Dynamics **2**, pp. 63–90
https://doi.org/10.1007/BF01054491

5. Joos, F., Roth, R., Fuglestvedt, J.S., Peters, G.P., Enting, I.G., von Bloh, W., Brovkin, V., Burke, E.J., Eby, M., Edwards, N.R., Friedrich, T., Frolicher, T.L., Halloran, P.R., Holden, P.B., Jones, C., Kleinen, T., Mackenzie, F.T., Matsumoto, K., Meinshausen, M., Plattner, G.-K., Reisinger, A., Segschneider, J., Shaffer, G., Steinacher, M., Strassmann, K., Tanaka, K., Timmermann, A., and Weaver, A.J., 2013: *Carbon dioxide and climate impulse response functions for the computation of greenhouse gas metrics: A multi-model analysis.*, Atmospheric Chemistry and Physics, vol 13, pp. 2793-2825
https://doi.org/10.5194/acp-13-2793-2013

6. Tanaka, K., Kriegler, E., Bruckner, T., Hooss, G., Knorr, W., Raddatz, T., et al., 2007: *Aggregated Carbon cycle, atmospheric chemistry and climate model (ACC2): description of forward and inverse mode.*, Reports on Earth System Science, Max Planck Institute for Meteorology
http://doi.org/10.17617/2.994422

7. Harde, H., 2019: *What Humans Contribute to Atmospheric CO2: Comparison of Carbon Cycle models with Observations*, Earth Sciences, vol 8(3), s.p. 139

http://dx.doi.org/10.11648/j.earth.20190803.13

8. Bolin, B., Eriksson, E., 1959: *Changes in the Carbon Dioxide Content of the Atmosphere and Sea due to Fossil Fuel Combustion*, The atmosphere and the sea in motion, Rossby memorial volume (ed B. Bolin), pp. 130-142. Rockefeller Inst. Press, New York.

https://geosci.uchicago.edu/~archer/warming_papers/bolin.1958.carbon_uptake.pdf

Correspondence to Ferdinand.engel-been@telenet.be

Vol. 3.1 (2023)
pp. 107-113

Comment on Understanding Increasing Atmospheric CO_2 by Hermann Harde

Ferdinand Engelbeen

Antwerp, Belgium

Abstract

While many of the points made by Harde (2023) [1] are right, a few points are not right and need correction. That includes allegations of certain statements of the IPCC they never did or intended in the way that Harde interpretated.

Keywords: CO_2 levels

Submitted 05-03-2023. Accepted 20-03-2023. https://doi.org/10.53234/SCC202301/26

1. **Introduction.**

I was preparing a large comment on the paper by Harde and Salby (2022) [2], but the comment by Andrews (2023) [3] was published before mine was finished. Most points I was preparing were already given by Andrews, so I don't need to repeat them here.

Even if Andrews did mention several items in a simple way, that doesn't mean that these remarks are wrong, neither is a more technical explanation right if the reasoning behind it is wrong…

2. The mass balance.

Whatever the CO_2 sources and sinks in the atmosphere, the carbon mass balance must be closed at any moment of time. No carbon can created from nothing, no carbon destroyed. Except… ^{14}C which is created by cosmic rays and destroys itself by radioactive decay. Because that are extremely small quantities, that doesn't influence the mass balance of the bulk CO_2 amounts.

Let us have a look at the mass balance over the past 60+ years since the exact CO_2 measurements at Mauna Loa started, together with the South Pole:

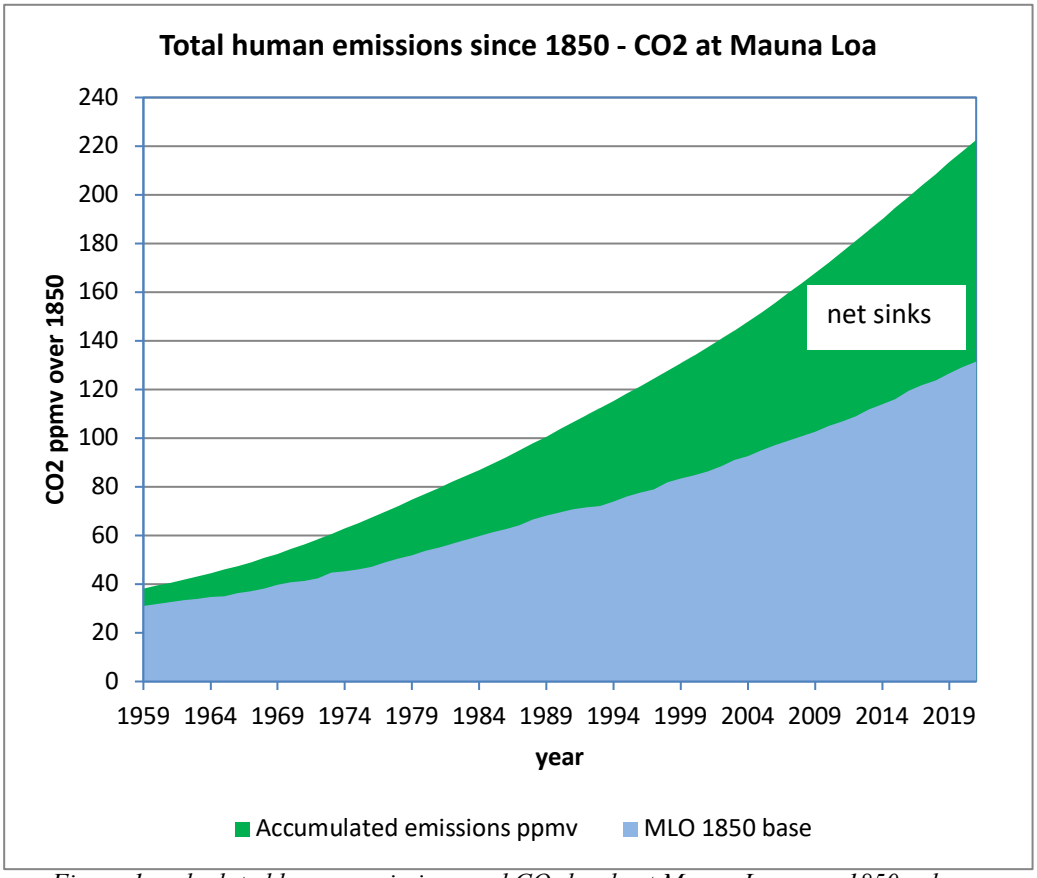

Figure 1: calculated human emissions and CO_2 levels at Mauna Loa over 1850 values. Human emissions of the Global Carbon Project [4] Mauna Loa data of the NOAA Carbon Tracker [5]

The emissions data are from the Global Carbon Project and compiled into one Excel file by Dave Burton [4]. The accuracy of the emission data is quite high, as based on fossil fuels sales (taxes!). Maybe somewhat underestimated, certainly not overestimated. As the Mauna Loa data also are quite accurate (NOAA Carbon Tracker [5]), the difference between both is also quite accurate. Thus even without knowing any natural CO_2 flux on earth, the net result of all natural CO_2 fluxes is exactly known within narrow borders.

The figures don't include land use changes which are more uncertain but simply add to total human emissions, which means that the net sinks in reality are even larger.

Even if one doesn't like the ice core CO_2 data and starts everything in 1960 from zero, accumulated human emissions increased faster than the increase in the atmosphere.

Thus indeed, human emissions do exceed the increase in the atmosphere and the difference must be absorbed somewhere in nature no matter the distribution over the different reservoirs.

If one looks at the derivatives, that is even more interesting:

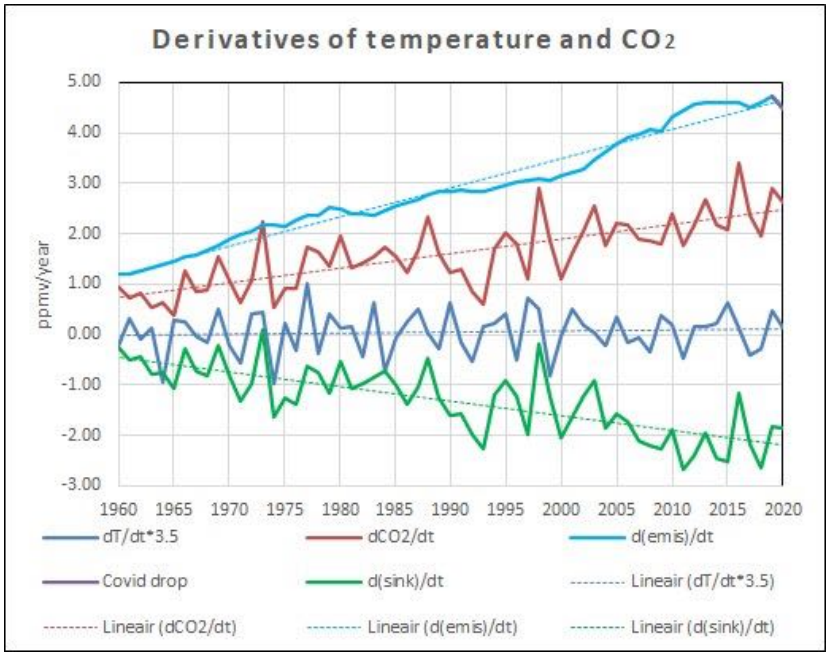

Figure 2: derivatives of human emissions, CO_2 increase, absorption and temperature.
The green line is the simple subtraction of the CO_2 increase in the atmosphere from human emissions and reflects the net sink capacity by nature. The small purple dent is the influence of Covid on human emissions, hardly of interest. Temperature data are enhanced with a factor 3.5 to show about the same amplitude as for CO_2. CO_2 data from the Global Carbon Project [4] and the NOAA Carbon Tracker [5] and T data are from HasCRUT4gl via WfT [6].

Except for a few borderline El Niño years, in all years nature was a *net* sink for CO_2. Obviously, the temperature derivative drives the variability in net sink capacity with a small lag, with as result that there is a (delayed) correlation between temperature rate of change changes and CO_2 rate of change changes in the atmosphere.

Also obvious is that the temperature derivative is *not* the driver for the CO_2 increase in the atmosphere, as there is hardly a slope in the derivative, only a small offset from zero, which gives a more or less linear increase of temperature in the oceans and atmosphere of about 0.63 K in the period 1958-2020.
Per Henry's law, that gives a change in dynamic equilibrium between ocean surface and atmosphere of less than 10 ppmv CO2 extra in the atmosphere over the full period (see chapter 2.).

On the other hand, human emissions are about twice the increase in the atmosphere and the slope also is twice as steep as for the increase, leading to a slightly quadratic increasing CO_2 level in the atmosphere of about 100 ppmv over the same period. The effect is that the net flux from atmosphere into the oceans increased over the full period and that the temperature increase only played a role in reducing the net CO2 flux from atmosphere into the ocean surface with less than 10%.

This alone is already sufficient to exclude any *net* contribution from natural sources, even if an individual CO_2 input like from all volcanoes on this world doubled or tripled in some year. The sum of all natural fluxes since 1958 was negative (near) all the time.

As long as the increase of CO_2 in the atmosphere is less than human emissions, there is zero net contribution from natural sources and sinks to the increase in the atmosphere.

It doesn't matter how huge the natural inputs and outputs are: these form a cycle and a cycle has zero impact on the amounts of CO_2 in the atmosphere and only the *difference* between all the

natural ins and all natural outs together does change the CO_2 quantity in the atmosphere. That difference is exactly known from two accurately known variables: human emissions and increase in the atmosphere.
Only if the increase in the atmosphere gets larger than from human emissions alone, the increase would be in part caused by natural causes.

The only way that natural fluxes could be the cause of the increase, is when the total natural emissions and total natural sinks exactly followed human emissions in timing and increase: a quadruple increase between 1960 and 2000. Only in that case, human emissions would be overwhelmed by the increased natural cycle. That also would result in a residence time that is ¼ of the current one, which is not observed at all…

Any theory that results in a substantial net addition of CO2 by the natural cycles violates the carbon mass balance and therefore is rejected.

2. The misinterpretations of what the IPCC said.

In formula (4a) and (4b) of Harde (2023) [1] implies that the IPCC assumes a fixed airborne fraction of what remains in the atmosphere from human emissions. As far as I know, the IPCC never said or implied such assumption. The net sink capacity depends of the extra CO_2 in the atmosphere (whatever the source) above equilibrium, not the emissions of one year. The only reason that the increase in the atmosphere is such a fixed ratio to human emissions is that human emissions are linearly increasing each year leading to a slightly quadratic accumulation of human emissions (as mass, not the original molecules!) in the atmosphere and thus of the sink rate. That gives a rather fixed ratio between accumulated human emissions and increase in the atmosphere. See the linear trends in Figure 2.

About the allegations of Harde (2023) [1] in his chapter 3.1.: as already said, the IPCC never said or implied that the increase in the atmosphere is proportional to human emissions. The increase in the atmosphere is a matter of emissions minus absorptions. The net effect depends of the total extra CO_2 pressure (pCO_2) in the atmosphere (whatever the cause: human or natural) above the long-time equilibrium with the oceans surface pCO_2 per Henry's law.
The latter influenced by temperature with a modest change: 12-16 ppmv/K (Takahashi et al, 2002 [7]), or about 13 ppmv increase since the LIA. That is all.

For the current (area weighted) average sea surface temperature, the dynamic equilibrium between oceans and atmosphere would be around 295 ppmv per Henry's law, not 415 ppmv. The 120 µatm (~ppmv) pCO_2 difference between the real pCO_2 in the atmosphere and the oceans pCO_2 is what drives *net* CO_2 from the atmosphere into the oceans, even when that is a dynamic equilibrium where lots of CO_2 are emitted by warm waters in the tropics and absorbed by cool waters near the poles.
See further Feely et al (2001) [8] for the observed net CO_2 uptake by the oceans for the reference year 1995.

About the allegations in chapter 3.2: as far as I know, the IPCC never made a differentiation between natural and human CO_2 for any physical process.
Neither did they assume a constant natural cycle: the graphs provided by the IPCC show an increasing natural cycle, also caused by human emissions, e.g. thanks to more vegetation… See the IPCC carbon cycle graph (2013) [9].

The crux of the matter is in chapter 3.3: the Bern model and other models do *not* assume that the different reservoirs absorb CO_2 in series, they assume that the sinks work in parallel, with the fastest process leading. That is clearly shown by Peter Dietze (1997) [10] on the blog of the late

John Daly and the later discussion between Peter Dietze and Fortunat Joos, inventor of the Bern model, and several others also on the blog of the late John Daly (2001) [11].
The main error of the Bern model is that it assumes a saturation of all reservoirs, which is true only for the ocean surface layer but by far not for vegetation (maximum uptake around 1500 ppmv) and absolutely not for the deep oceans, which are far from saturated, but have a limited exchange rate with the atmosphere via the sinking polar waters.

From reference [8] by Feely e.a.:

"The pCO_2 in surface seawater is known to vary geographically and seasonally over a range between about 150 µatm and 750 µatm, or about 60% below and 100% above the current [note: reference year 1995] *atmospheric pCO_2 level of about 370 µatm."*

As the deep ocean waters are fed with the sinking cold ocean waters near the poles with about 150 µatm pCO2, the deep oceans are and remain by far undersaturated for CO_2, even if they are slightly warmer (4-5ºC) than the sinking polar waters (still less than 200 µatm pCO_2).

A recent paper by Seltzer, Alan, et al (2023) [12] also shows an undersaturation of noble gases in the deep oceans, due to the slow air-ocean gas transfer at the sink places.

Compared to the enormous amount of CO2 and derivatives in the deep oceans (about 37,000 PgC according to the IPCC [9]), the total human contribution since the start of the industrial revolution is about 1% of the total inorganic carbon species in the deep oceans. Once in equilibrium, that would give an increase of only 3 ppmv CO2 in the atmosphere, but that needs a lot of time because of the limited exchange rate between deep oceans and atmosphere...

Where it goes completely wrong is in:

„The direct absorption time of CO_2 is therefore equal to its residence time“

That is absolutely *not* the case. It is the same error that (too) many made in the past and present: the residence time is how fast CO_2 in the atmosphere is *ex*changed with CO_2 from other reservoirs but *that has zero impact on the total amount of CO_2 in the atmosphere.*
The only way extra CO_2 above the dynamic equilibrium can be removed out of the atmosphere is by the difference in total inputs and total outputs and that is a much slower process: about 50 years e-fold time as observed over the past 60+ years.

That needs a lot of explanation and that will be for another paper, as many others, from Segalstad (1998) [13] via Berry (2019) [14] to formula (2.1) in Salby and Harde (2022) [2] all made the same error by confusing the residence time with the relaxation time, the latter is the time needed to remove any excess CO_2 (from whatever cause) above the long-time dynamic equilibrium out of the atmosphere.

Conclusion

Too many misinterpretations of what the IPCC said by Hermann Harde and still promoting alternatives for the human caused CO_2 increase in the atmosphere which violate the carbon mass balance…

Funding:

No funding was received to write this comment.

Debate-Editor:

Olav M. Kvalheim

Acknowledgements:

The author thanks the Debate-Editor for the positive remarks to clarify several items with more background information.

References

[1] Harde, Hermann, *Understanding Increasing Atmospheric CO_2,* Science of Climate Change, Vol. 3.1, pages 46-67 (2023):
https://doi.org/10.53234/SCC202301/23

[2] Salby, M. and Harde, H., *Theory of Increasing Greenhouse Gases*, Science of Climate Change, vol. 2, no. 3, pages 212-238 (2022):
https://doi.org/10.53234/SCC202212/17

[3] Andrews, David, E., *Clear Thinking About Atmospheric CO_2,* Science of Climate Change, Vol. 3.1, pages 33-45 (2023):
https://doi.org/10.53234/SCC202301/20

[4] https://www.globalcarbonproject.org/
Compiled into one Excel file by Dave Burton at:
https://sealevel.info/carbon/global.1751_2021.ems13.xlsx

[5] Carbon tracker at the NOAA website:
https://gml.noaa.gov/dv/iadv/

[6] Global temperatures according to HadCRUT4gl via WfT:
https://www.woodfortrees.org/plot/hadcrut4gl/from:1960/compress:12/derivative:3.5/scale:3.5

[7] Formula of Takahashi to calculate the change in ocean surface pCO_2 with temperature:
$\partial \ln pCO_2/\partial T=0.0423/K$ or around 4%/K, based on ten thousands of sea surface water samples.
Takahashi, Taro, et al, *Global sea–air CO_2 flux based on climatological surface ocean* p*CO_2, and seasonal biological and temperature effects,* Topical Studies on Oceanography, Volume 49, Issues 9-10, 2002, Pages 1601-1622.
https://www.sciencedirect.com/science/article/abs/pii/S0967064502000036

[8] Feely, Richard A.; Sabine, Christopher L.; Takahashi Taro; Wanninkhof, Rick: *Uptake and Storage of Carbon Dioxide in the Ocean: The Global CO_2 Survey,* Oceanography, 14(4), 18–32 (2001).
https://www.pmel.noaa.gov/pubs/outstand/feel2331/exchange.shtml and following pages
Or directly to the graph:
https://www.pmel.noaa.gov/pubs/outstand/feel2331/mean.shtml

[9] https://www.researchgate.net/figure/Simplified-schematic-of-the-global-carbon-cycle-IPCC-2013-Numbers-represent-carbon_fig4_281185559

[10] Dietze, Peter, *Little Warming with new Global Carbon Cycle Model,* on the blog of he late John Daly (1997):
http://www.john-daly.com/carbon.htm

[11] Discussion between Peter Dietze and Fortunat Joos and several others about the Bern model and Dietze's model about the extra CO_2 decay out of he atmosphere on the late John Daly's blog (2001):
http://www.john-daly.com/dietze/cmodcalD.htm

[12] Seltzer, Alan, et al*, Dissolved gases in the deep North Atlantic track ocean ventilation processes,* PNAS Vol 120, No. 11 (2023):
https://www.pnas.org/doi/10.1073/pnas.2217946120

[13] Segalstad, Tom, V,. *Carbon cycle modelling and the residence time of natural and anthropogenic atmospheric CO_2: on the construction of the "Greenhouse Effect Global Warming" dogma,* at pages 13-14. Printed in: Bate, R. (Ed.): "Global Warming: The Continuing Debate", European Science and Environment Forum (ESEF), Cambridge, England (ISBN 0-9527734-2-2), pages 184-219 (1998).
https://www.co2web.info/ESEF3VO2.pdf

[14] Berry, Edwin, X., *Human CO_2 Emissions Have Little Effect on Atmospheric CO_2,* International Journal of Atmospheric and Oceanic Sciences, Volume 3, Issue 1, Pages: 13-26 (2019). https://www.sciencepublishinggroup.com/journal/paperinfo?journalid=298&doi=10.11648/j.ijaos.20190301.13

Correspondence to
harde@hsu-hh.de

Vol. 3.1 (2023)
pp. 114 - 118

Reply to a Comment on:
Understanding Increasing Atmospheric CO_2

Hermann Harde

Helmut-Schmidt-University, Hamburg, Germany

Abstract

This reply refutes all misstatements, that were published by F. Engelbeen as Comment on an article "*Understanding Increasing Atmospheric CO_2*" by Hermann Harde.

Keywords: Carbon cycle; absorption time; anthropogenic emissions; natural emissions

Submitted 24-03-2023, Accepted 29-03-2023. https://doi.org/10.53234/scc202301/28

1. Introduction

All climate experts agree that the basis for calculating changes of the CO_2 concentration in the atmosphere is the balance equation or Conservation Law, which sums up all in- and outfluxes of the atmosphere. However, differences exist in the interpretation, how strongly fluxes from anthropogenic sources can affect this balance and how far natural emissions have to be considered.

In three articles of this journal this has been discussed extensively (see: Harde & Salby 2021; Berry 2021; Schrøder 2022) with the concordant result that mostly nature must be made responsible for the observed CO_2 increase. A critical Comment of Andrews (2023) was refuted by Harde (2023) and Berry (2023), but a further Comment (Engelbeen 2023), that mostly refers to the last clarification of Harde (2023), alleges a number of misstatements, in particular concerning the balance equation, which need to be rejected and corrected by this reply.

2. Some Clarifications on the Balance Equation

Generally, the balance for changes of the atmospheric CO_2 concentration can be expressed as:

$$\frac{dC_{CO_2}}{dt} = e_A + e_N - a_N \tag{1}$$

with dC_{CO2}/dt as the concentration changes per time interval dt, e_A as anthropogenic emission rate, e_N as natural emission rate and a_N as natural absorption rate.

The changes over one year $\delta C_{CO2}/\delta t$ can relatively well be derived from CO_2 measurements at Mauna Loa (CDIAC 2022), and the anthropogenic emissions deduced from the Global Carbon Budget (GCB 2022). Thus, rearranging (1) in the form

$$\frac{\delta C_{CO_2}}{\delta t} - e_A = e_N - a_N, \tag{2}$$

the left-hand side is known within some narrower bounds, and therefore also the difference of natural emissions and absorption, quantities which can only roughly be estimated, is known with the same accuracy.

So far there is no larger discrepancy between experts, also not to Engelbeen's Fig. 1, only that the calculations in Harde & Salby (2021) and Harde (2023) also include Land Use Changes, which were neglected in his Fig. 1. But the further interpretation of the right-hand side of (2) differs significantly with dramatic consequences for the right understanding of the carbon-cycle.

So, in Section 2 of Engelbeen's Comment (2023) we read:

- *Even without knowing any natural CO_2 flux on earth, the net result of all natural CO_2 fluxes is exactly known within narrow borders,* and later*: This alone is already sufficient to exclude any net contribution from natural sources, even if an individual CO_2 input like from all volcanoes on this world doubled or tripled in some year.*
- *As long as the increase of CO_2 in the atmosphere is less than human emissions, there is zero contribution from natural sources and sinks to the increase in the atmosphere.*
- *It doesn't matter how huge the natural inputs and outputs are: these form a cycle and a cycle has zero impact on the amounts of CO_2 in the atmosphere and only the difference between all the natural ins and outs together does change the CO_2 quantity in the atmosphere. That difference is exactly known from two accurately known variables: human emissions and increase in the atmosphere. …. Only if the increase in the atmosphere gets larger than from human emissions alone, the increase would be in part caused by natural causes.*

These are quite strong statements, which have to be considered in some more detail.

Indeed, for a decoupled cycle of natural CO_2 fluxes and an absorption rate, that is exactly compensating any natural variations, independent of the human emissions and therefore independent of the instantaneous atmospheric CO_2 concentration, it is per se sufficient to consider only *the net of all natural CO_2 fluxes, to exclude any net contribution from natural sources*. This is the case:

- for the simple Airborne Fraction Model with an actual anthropogenic emission rate $e_A \approx 5.5$ ppmv/yr, an airborne fraction $AF \approx 46\%$ and an absorption rate $a_N = (1\text{-}AF)\cdot e_A$,
- it also holds for the more advanced Bern-Model (Joss et al. 1996) assuming only anthropogenic emissions as δ-pulses in the form $e_A(t') \cdot R(t-t') \cdot dt'$, with $R(t\text{-}t')$ as the pulse response function, which represents 5 essentially independent decay channels, one even with an infinite absorption time (zero absorption),
- and it holds for several hybrid models, considering only an excess concentration C'_{CO2} above an equilibrium level, e.g., $C^{eq}_{CO2} = 280$ ppmv at 1750, with an absorption rate $a_N = C^{eq}_{CO2}/\tau_{NR} + C'_{CO2}/\tau_A$, where τ_{NR} is the residence or turnover time of CO_2 molecules belonging only to the natural cycle with $\tau_{NR} \approx$ 3-4 yrs, and τ_A is the adjustment time for the excess concentration caused only by anthropogenic emissions with $\tau_A \approx 50$ yrs.

All these categories are distinguished by focussing exclusively on changing anthropogenic emissions, while natural emissions in advance are excluded or are supposed to form a closed cycle. Under these conditions is the right-hand side of (2) not really the net of all natural fluxes, but represents the anthropogenic absorption rate. It is obvious that under such assumptions native emissions cannot have any impact. A conclusion that *there is zero contribution from natural sources and sinks to the increase in the atmosphere*, is no more and no less circular reasoning.

It is also in contradiction to the Equivalence Principle, when additional native emissions can be compensated by 100%, while human emissions, or their equivalent mass units, are only partially absorbed and some fraction remains for ever in the atmosphere or is absorbed significantly slower. And what kind of 'closed' cycle shall this be with a constant net balance for all natural fluxes and continuous uptake of human emissions? Is this stored in a separate native reservoir?

As elaborately discussed in Harde (2023), a realistic absorption rate, which is in agreement with all observations and physical principles, is scaling proportional to the instantaneous CO_2 concentration and does not discriminate between native or anthropogenic emissions. Then, with an additional native emission rate Δe_N and a unitary effective residence or absorption time τ_{eff} for all

molecules, including partial re-emission from extraneous reservoirs[1], (2) becomes:

$$\frac{\delta C_{CO2}}{\delta t} - e_A = e_{N0} + \Delta e_N - \frac{C_{CO2}}{\tau_{eff}}, \tag{3}$$

or as excess concentration $C'_{CO2} = C_{CO2} - C^{eq}_{CO2}$ relative to the quasi-steady state concentration $C^{eq}_{CO2} = 280$ ppmv in 1750 and with $e_{N0} = a_{N0} = C^{eq}_{CO2}/\tau_{eff}$ we get:

$$\frac{\delta C'_{CO2}}{\delta t} - e_A = \Delta e_N - \frac{C'_{CO2}}{\tau_{eff}}. \tag{4}$$

It is evident that with additional emissions, anthropogenic or natural ones, also the absorption rate is increasing to compensate these additional emissions and to adapt to a new equilibrium. But the decisive difference to the previously discussed approaches is that this absorption no longer distinguishes between different sources; the total concentration in (3) and in the same way the excess concentration in (4) are determined by the common emissions, which together are defining a unitary absorption rate for human and native emissions.

In this context it is also important to note that absorption and emission of CO_2 at the surface is not simple mixing like liquids with different alcoholic content, as unfortunately confused by some people (Andrews 2023). CO_2 is mixing in the atmosphere with the other gases, but at the surface it is absorbed, partially even changing its compound in seawater or in the biosphere, and it is again released decades to thousands of years later, strongly dependent on chemical and biological reactions, which on their part are controlled by temperature and humidity.

Therefore, different to the illusion of *clear thinkers* the right-hand side of (4) does not represent only *the net result of all natural fluxes*, but also contains the human uptake. A constant difference doesn't say anything, particularly not when the total emissions and absorption develop largely parallel to each other.

So, for an increasing concentration over time, but less than the anthropogenic emissions e_A, i.e., $0 < \delta C'_{CO2}/\delta t < e_A$, this leads to an inequality for the absorption rate with:

$$\Delta e_N < \frac{C'_{CO2}}{\tau_{eff}} < \Delta e_N + e_A\,. \tag{5}$$

Of course, can this inequality be satisfied for $\Delta e_N = 0$, when $C'_{CO2}/\tau_{eff} < e_A$. With an excess concentration $C'_{CO2} \approx 130$ ppmv and anthropogenic emissions of $e_A \approx 5.5$ ppmv/yr this is the case for a residence time $\tau_{eff} > 24$ yrs. But from observations of the ^{14}C-decay and independently from the seasonal emission-absorption cycles (Harde & Salby, 2021) we know that the absorption time cannot be larger than 10 yrs. This already excludes an assumption of zero native emissions.

So, with $\tau_{eff} \leq 10$ yrs the actual excess absorption rate must be $C'_{CO2}/\tau_{eff} \geq 13$ ppmv/yr. Then, (5) is also satisfied for additional native emissions $\Delta e_N > (C'_{CO2}/\tau_{eff} - e_A) \geq 7.5$ ppmv/yr, and for an actually observed CO_2 increase of $\delta C'_{CO2}/\delta t \approx AF \cdot e_A \approx 2.5$ ppmv$/yr$, from (4) we even derive an emission rate of $\Delta e_N = 10$ ppmv/yr, which is almost twice the anthropogenic emissions.

Whereas τ_{eff} cannot be larger than 10 yrs, it can be significantly shorter. With an estimated total emission $e_T = 106.8$ ppmv/yr as average over the period 2010 – 2019 (see IPCC, AR6 2021, Fig. 5.12) and an average atmospheric concentration of $C_{CO2} = 400$ ppmv, we get an effective absorption time of $\tau_{eff} = C_{CO2}/e_T \approx 3.8$ yrs. With this faster absorption and with the observed increase $\delta C'_{CO2}/\delta t \approx 2.5$ ppmv$/yr$, according to (4), then natural emissions even contribute $\Delta e_N = 31.2$ ppmv/yr to the increase, which is almost 6 times more than the human emissions.

These examples clearly refute Engelbeen's claim that "*there is zero contribution from natural*

[1] Not to complicate the further discussion, here we abstain to distinguish between a direct and effective absorption time. For details, see Harde & Salby (2021) and Harde (2023).

sources and sinks to the increase of CO_2 in the atmosphere, as long as this increase is less than human emissions", and also his statement at the end of Section 2: "*Any theory that results in a substantial net addition of CO_2 by the natural cycles violates the carbon mass balance and therefore is rejected"* is nonsense and misses any scientific basis.

The preceding considerations and examples are in full agreement with the balance equation for atmospheric CO_2 and are exclusively based on fundamental physical relations like the Equivalence Principle. Different to the artificially introduced cycles and time constants, on the one hand for a more or less closed natural cycle, and on the other hand for the adjustment of anthropogenic emissions, we demonstrate that all observations, even the seasonal cycles are exactly reproduced with a unitary time scale, which controls the total balance of emissions and absorption.

3. Interpretation of the IPCC

In Section 3 Engelbeen further claims, the IPCC was misinterpreted. Here some short answers:

- He believes, *IPCC never assumed a fixed airborne fraction of what remains in the atmosphere from human emissions*. Engelbeen should study AR6, Chapter 5.2.1.2 and look to Fig. 5.7.
- He claims: *The IPCC never said or implied that the increase in the atmosphere is proportional to human emissions*. Again, we refer to AR6, Chapter 5.2.1.2, where he can read: "*Based on the airborne fraction (AF), it is concluded with medium confidence that both ocean and land CO_2 sinks have grown consistent with the rising of anthropogenic emissions*". In addition, everyone who looks closer to the Bern-Model (Joos et al. 1996), will see that the absorption is assumed to scale proportional to the δ-pulse emission.
- Engelbeen's considerations about a thermal contribution apparently completely embezzle the much stronger soil emissions, permafrost, volcanos and El Niños (Salby & Harde 2022).
- He questions that *the IPCC ever made a differentiation between natural and human CO_2 for any physical process*. Isn't it a differentiation, when natural fluxes are assumed to form a cycle with a residence time of about 3 yrs, even for additional native emissions, and only anthropogenic emissions or their equivalent mass will stay forever in the atmosphere?
- He claims: "*The Bern model and other models do not assume that the different reservoirs absorb CO_2 in series, they assume that the sinks work in parallel, with the fastest process leading"*. When this would really be true, how does he explain, when the IPCC supposes that the removal of all the human-emitted CO_2 from the atmosphere by natural processes will take a few hundred thousand years, and the Bern Model considers for 18% of anthropogenic emissions an infinite cumulation in the atmosphere? The different exponential decays by far do not represent saturation or a parallel uptake, but stand for different exchange processes from photosynthesis to silicate weathering (AR5, Chapter 6, Box 6.1), apparently working in series. Parallel sinks ad up to a total uptake and can well be described by a single exponential.

And indeed, it goes completely wrong, when so-called climate experts and clear thinkers consider a separate cycle only for natural CO_2 fluxes with a residence time of 3-4 yrs, and have to introduce artificially an additional time scale with an adjustment time of about 50 yrs, only to explain a pure anthropogenic impact and to exclude any natural contribution to the growing CO_2 level. In Section 2 we have already discussed that such an approach violates the Equivalence Principle and is also in contradiction to observations of the ^{14}C-decay, from which we derive an absorption time shorter than 10 yrs. Direct absorption processes can even be as short as one year, as this follows from the faster oscillations on the $^{14}CO_2$ decay (Salby & Harde 2021) and also from cross-correlation analyses of interannual CO_2 and temperature fluctuations (Humlum et al. 2013; Salby 2013).

4. Conclusion

With this reply we firmly reject the false claims, that were published by Engelbeen (2023) as Comment on an article "*Understanding Increasing Atmospheric CO_2*" by H. Harde (2023).

Instead annunciating such comments with untenable and dubious statements Engelbeen and his clear thinkers should reflect their own delusions, which are in contradiction to the Equivalence Principle, in conflict with the observed ^{14}C-decay time, and which cannot explain the seasonal emission-absorption cycles of atmospheric CO_2.

Chief-Editor: Prof. Jan-Erik Solheim; **Debate-Editor**: Prof. Olav Martin Kvalheim

References

Andrews, D. E., 2023: *Clear Thinking about Atmospheric CO_2*, Science of Climate Change, Vol. 3.1, pp. 33 - 45, https://doi.org/10.53234/scc202301/20

AR5 – IPCC's Fifth Assessment Report, 2013: T. F. Stocker et al. (Eds.): *Climate Change 2013: The Physical Science Basis. Contribution of Working Group I*, Cambridge University Press, Cambridge, United Kingdom and New York, NY, USA.

AR6 – IPCC's Sixth Assessment Report, 2021: V. Masson-Delmotte et al.: *Climate Change 2021: The Physical Science Basis. Contribution of Working Group I,* Cambridge University Press.

Berry, E., 2021: *The Impact of Human CO_2 on Atmospheric CO_2,* Science of Climate Change, Vol. 1.2, pp. 213 - 249, https://doi.org/10.53234/scc202112/13

Berry, E., 2023: *Nature Controls the CO_2 Increase,* Science of Climate Change, Vol. 3.1, pp. 68 – 91, https://doi.org/10.53234/scc202301/21.

CDIAC: Carbon Dioxide Information Analysis Center, 2022, https://cdiac.ess-dive.lbl.gov/trends/co2/recent_mauna_loa_co2.html

Engelbeen, F., 2023: *Comment on Understanding Increasing Atmospheric CO_2 by Hermann Harde*, Science of Climate Change, Vol. 3.1, pp. 107-113, https://doi.org/10.53234/scc202301/26

Global Carbon Budget (GCB) 2022: https://www.carbonbrief.org/analysis-global-co2-emissions-from-fossil-fuels-hit-record-high-in-2022/

Harde, H., M. L. Salby, 2021: *What Controls the Atmospheric CO_2 Level?* Science of Climate Change, Vol. 1.1, pp. 54 - 69, https://doi.org/10.53234/scc202106/22.

Harde, H., 2023: *Understanding Increasing Atmospheric CO_2*, Science of Climate Change, Vol. 3.1, pp. 46-67, https://doi.org/10.53234/scc202301/23

Humlum, O., K. Stordahl, and J.-E. Solheim, 2013: *The phase relation between atmospheric carbon dioxide and global temperature*, Global and Planetary Change, vol. 100, pp. 51–69.

Joos, F., M. Bruno, R. Fink, U. Siegenthaler, T. F. Stocker, C. Le Quéré, J. L. Sarmiento, 1996: *An efficient and accurate representation of complex oceanic and biospheric models of anthropogenic carbon uptake*, Tellus B 48, p 397, https://doi.org/10.1034/j.1600-0889.1996.t01-2-00006.x

Salby, M. L., 2013: *Relationship Between Greenhouse Gases and Global Temperature*, Video Presentation, April 18, 2013, Helmut-Schmidt-University Hamburg https://www.youtube.com/watch?v=2ROw_cDKwc0.

Salby, M. L., H. Harde, 2021: *Control of Atmospheric CO_2 - Part I: Relation of Carbon 14 to Removal of CO_2*, Science of Climate Change, Vol. 1.2, pp. 177 - 195, https://doi.org/10.53234/SCC202112/30

Salby, M. L., H. Harde, 2022: *Theory of Increasing Greenhouse Gases*, Science of Climate Change, Vol. 2.3, pp. 212 - 238, https://doi.org/10.53234/scc202212/17.

Schrøder, H., 2022: *Less than half of the increase in atmospheric CO_2 is due to the burning of fossil fuels*, Science of Climate Change, Vol. 2.3, pp 1-19, https://doi.org/10.53234/scc202111/17